Summer 8-19-2016

The Role of Glutaminase and Extracellular Vesicles in Macrophages and Microglia

Beiqing Wu
University of Nebraska Medical Center

The Role of Glutaminase and Extracellular Vesicles in Macrophages and Microglia

By

Beiqing ‘Mercury’ Wu

A DISSERTATION

Presented to the Faculty of

The Graduate College in the University of Nebraska

In Partial Fulfillment of the Requirements

For the Degree of Doctor of Philosophy

Department of

Pharmacology and Experimental Neuroscience

Under the Supervision of Dr. Jialin Zheng

Medical Center

Omaha, Nebraska

June, 2016

The Role of Glutaminase and Extracellular Vesicles in Macrophages and Microglia

Beiqing 'Mercury' Wu, M.D. Ph.D.

University of Nebraska, 2016

Advisor: Jialin Zheng, M.D.

Glutamate serves as a crucial excitatory neurotransmitter that is essential for the proper functioning of the brain. However, excess levels of glutamate are neurotoxic and contribute to the pathogenesis of various neurodegenerative diseases, inducing HIV-1 associated neurocognitive disorders (HAND). Glutaminase 1 (GLS1) is an important mitochondrial enzyme responsible for producing glutamate from glutamine. GLS1 is upregulated during HAND and released from mitochondria to cytosol and extracellular space. However, why and how GLS1 is released remains unknown. In chapter II, we demonstrated that extracellular vesicles (EVs) carry GLS1 as cargos from cytosol to extracellular space during HIV infection and innate immune activation. The GLS-containing EVs induce neurotoxicity through the overproduction of glutamate, implicating the pathogenic role of EVs and GLS1 in HAND.

Regulation of EV remains to be fully elucidated in HAND. Interestingly, when carried as cargo, GLS1 showed a potential effect on the release of EV. Therefore, we hypothesize that the release of EV is dependent on GLS1-mediated glutamine and sphingolipid metabolism. In chapter III, we investigated the involvement of GLS1 in EV release in GLS1-overexpressing HeLa cells, HIV-

1-infected macrophages, and immune-activated microglia through the use of GLS1 inhibitors. In the aforementioned cell types, GLS1 inhibitor significantly decreased the level of EVs, suggesting an important role of GLS1 in EV regulation. In chapter IV, we further investigated the mechanism of GLS1-mediated EV release. We identified that GLS1-mediated EV release is dependent upon the level of glutamine and a-ketoglutarate (a-KG). Because a-KG is an important metabolite of glutamate, these data suggest that a-KG is an essential GLS1 downstream factor that regulates the release of EVs. Biogenesis of EVs requires the sphingolipid ceramide. However, it is unknown whether GLS1-mediated EV release involves ceramide. We have demonstrated that the addition of ceramide rescued the suppression of EV release by GLS1 inhibitors, suggesting that GLS1 mediates EV release through ceramide.

In summary, our data revealed two interesting insights into the biology of EVs. First, GLS-containing EVs is a pathogenic component of neurodegeneration in HAND. Second, the release of EVs is dependent on GLS1-mediated glutamine and sphingolipid metabolism. Studies on both of these aspects in EVs could lead to potential novel therapeutic targets for HAND and other neurodegenerative diseases.

TABLE OF CONTENTS

List of Tables and Figures

Abbreviations

Human immunodeficiency virus (HIV)

HIV-1 associated neurocognitive disorders (HAND)

HIV-1 associated dementia (HAD)

Mild neurocognitive disorders (MND)

Asymptomatic neurocognitive impairment (ANI)

Highly active antiretroviral therapy (HAART)

Blood brain barrier (BBB)

Central nervous system (CNS)

HIV-1 encephalitis (HIVE)

Monocyte-derived Macrophages (MDM)

Mononuclear Phagocytes (MPs)

Antigen presenting cells (APC)

Tumor necrosis factor-α (TNF-α)

Interleukin-1 β (IL-1β)

Glycoprotein 120 (gp120)

HIV *trans* activator of transcription (HIV-Tat)

N-Methyl-D-aspartic acid (NMDA)

Dizocilpine (MK-801)

Glutaminase 1 (GLS1)

Glutaminase 2 (GLS2)

Glutaminase C (GAC)

Kidney-type glutaminase (KGA)

Tricarboxylic acid (TCA)

Interferon α/β (IFN-α/β)

Signal transducer and activator of transcription 1 (STAT1)

Extracellular vesicles (EVs)

Microvesicles (MVs)

Intraluminal vesicles (ILVs)

Multivesicular bodies (MVBs)

Endoplasmic reticulum (ER)

Amyloid precursor protein (APP)

Amyloid β (Aβ)

Superoxide dismutase (SOD)

Endosomal Sorting Complexes Required for Transport (ESCRT)

lipopolysaccharide (LPS)

Cerebrospinal fluid (CSF)

Institutional Animal Care and Use Committee (IACUC)

Institutional Review Board (IRB)

Dulbecco's modified Eagles medium (DMEM)

Macrophage colony stimulating factor (M-CSF)

Multiplicity of infection (MOI)

Rat cortical neuron (RCN)

Transmission electron microscopy (TEM)

Scanning electron microscope (SEM)

Bis-2-(5-phenylacetamido-1,2,4-thiadiazol-2-yl)ethyl sulfide (BPTES)

Reverse phase high performance liquid chromatography (RP-HPLC)

Morris-Water-Maze (MWM)

Sodium dodecyl sulfate-polyacrylamide gel electrophoresis (SDS-PAGE)

Polyvinyldifluoridene (PVDF)

Analysis of variance (ANOVA)

Standard deviation (SD)

Carbenoxolone (CBX)

6-Diazo-5-oxo-L-norleucine (L-DON)

Vesicular glutamate transporter (VGLUT)

Voltage-dependent anion-selective channel (VDAC)

Cytochrome C (cyt c)

Neutral sphingomyelinase (nSMase)

Atazanavir (AZT)

Wide-type (WT)

Contextual fear conditioning (CFC)

Green fluorescent protein (GFP)

Polymerase chain reaction (PCR)

Phosphate-buffered saline (PBS)

Paraformaldehyde (PFA)

Reverse transcription polymerase chain reaction (RT-PCR)

α–ketoglutarate (α–KG)

Peroxisomal membrane protein (PMP70)

ALG-2-interacting protein X (Alix)

Chapter 1

Introduction

1.1 HIV-1 associated neurocognitive disorders

1.1.1 Clinical manifestation

As reported by UNAIDS in 2014 (UNAIDS), approximately 35 million people worldwide are infected with Human Immunodeficiency Virus (HIV), which continues to cause significant morbidities [1]. Among the cases of HIV infection, more than 90% of the global HIV pandemic attributes to HIV-1 infection but not HIV-2 [2].

In addition to immune compromise, HIV infection causes a wide spectrum of HIV-1-associated neurocognitive disorders (HAND), which range from mild cognitive disease to dementia, even under the treatment of successful anti-retroviral therapy [3, 4]. HAND is characterized by cognitive deteriorations, behavioral impairments and motor function loss due to progressive neuronal damage. HAND consists of three major classifications based on guidelines in the measurements of cognitive dysfunction: HIV-1 associated dementia (HAD), mild neurocognitive disorder (MND), and asymptomatic neurocognitive impairment (ANI) [4-6]. Thanks to the effective treatment of highly active antiretroviral therapy (HAART), the prevalence of the most severe form of HAND, HAD has been dramatically reduced [7]. However, the incidence of the moderate and mild forms of HAND remains high and cannot be ignored [7-9]. Recent reports have shown that the increasing resistance to the antiretroviral drug can be caused to the following reasons: the increasing viral mutation, the increasing lifespan of HIV-infected individuals, and the compromised blood-brain barrier (BBB) disturbed by

HAART [10-12]. Mononuclear phagocytes, including macrophages and microglia, are found to be HIV reservoirs [7, 13, 14].

The quality of life for HIV individuals is significantly affected because of the difficulty in obtaining employment due to discrimination/disease burden and a decreased ability to perform complex daily tasks due to HAND. Examples of impairments include finance management and housekeeping, and poor quality of life and poor compliance to medical instructions [4, 15-18]. Despite peripheral control of HIV replication by HAART, 60% - 90% of the individuals have a certain degree of cognitive disease [1, 19].

1.1.2 Pathobiology of HAND

HIV-1 associated dementia is the most severe form of HAND, which is a chronic disease state in progressive HIV-1 infection with HIV encephalopathy or AIDS dementia complex [7, 20]. During HIV-1 infection, HIV virus infects circulating monocyte/macrophages and enters the central nervous system (CNS) within weeks after the initial infection through a ‘Trojan horse’ mechanism, which impairs the cognition including attention, memory, language, problem solving and decision making [1, 20]. The other symptoms of HAND include confusion, forgetfulness, behavioral changes, headaches, gradual weakening and loss of falling in the arms and legs, problems with cognition or movement and pain due to nerve damage (NIH) [21-23].

HAND correlates with HIV-1 encephalitis (HIVE) histologically [24]. Studies with in situ hybridization indicate that productive HIV-1 infections appear

exclusively in perivascular monocyte-derived macrophages (MDM) [25-27]. The post-mortem pathology reports from HAD patient brain sections show progressive infection and infiltration of perivascular MDM, which results in the formation of multinucleated giant cells [26, 27]. Activated perivascular macrophages activate astrocytes and lead to reactive astrogliosis, myelin pallor and white mater diffusion, reduction in synaptic density, increased BBB permeability, and neuronal damage or loss [21, 28].

In the pre-HAART era, approximately 40% reduction in neuronal densities in the frontotemporal cortex [21, 29], and 50%-90% reduction in neuronal densities in the hippocampus were reported [30]. Highly regulated cell death, known as apoptosis, was believed to be the major cause of neuronal loss. Recent observations of samples from HAND patients with treatment of HAART still showed decrease of neuronal loss and further neuronal damage [31-33]. The neuronal damage in the areas of the brain such as basal ganglia, cerebral cortex, and hippocampus in HAND patients' causes significant cognitive impairment [34].

HIV majorly infects brain microglia and macrophages. Infection of astrocytes is restricted because of the lack of CD4 presence on the cells [35-38]. Although neurons are not susceptible to HIV, neurons are largely affected by the HIV-infected neighboring cells in the CNS [39, 40], such as HIV-infected astrocytes, macrophages and microglia, due to the production of viral proteins, cytokines and neurotoxins [41-46]. The elevation of these neurotoxic factors contributes to the damage of synapses, impairment of neuronal function and chronic inflammation. This leads to the disruption of the connections of the

neuronal network and impaired neurotransmission, and thus causes neurodegeneration [47-51]. Studies show that the viral proteins released by infected macrophages and microglia further infect uninfected cells in the CNS, and release a variety of proinflammatory molecules and neurotoxins, which causes further neuronal damage and leads to more severe form of HAND [52, 53].

1.2 Macrophage and microglia activation

Macrophages and microglia are mature mononuclear phagocytes (MPs) that are both crucial to the innate and adaptive immune responses. MPs engulf pathogens and cellular debris, process them into small peptides of 10-14 amino acids and present them onto the cell surface. Antigens can be presented to appropriate specific T cells receptor, which leads to a high-affinity interaction between antigen presenting cells (APC) and T N-Methyl-D-aspartic acid cells and initiates T cell activation. MPs stimulate the immune response through the production of inflammatory cytokines and chemokines, and further amplifying the immune response [54, 55].

Both macrophages and microglia are believed to be pivotal in the pathogenesis of neurodegenerative disease, particularly HAND. During HAND, MPs infiltrated into the CNS through the BBB. There, MPs acquire enhanced phagocytic capability, secrete proinflammatory cytokines and chemokines, and release cytotoxic factors. All of these events lead to injury to bystander cells including neurons [48, 56]. In the past, there was controversy over whether or not

MPs express neurotrophic factors during brain inflammation or clear pathogens through phagocytosis. Recent studies have shown that MPs do perform both functions, and that these functions account for the pathogenesis of HAND.

During HAND, HIV establishes a latent and persistent infection within MPs, which serves as a viral reservoir and allows HIV to evade immune surveillance. HIV in the CNS primarily exists within the perivascular blood and parenchymal brain macrophages and microglia [41]. Neurons, astrocytes, oligodendrocytes and endothelial cells in the brain are barely infected by HIV [22, 57, 58]. MPs are the major population that produces and releases a variety of neurotoxins into the brain [41-45, 59-62], including platelet activating factor [63-65], arachidonic acid [66], pro-inflammatory cytokines and chemokines [67], quinolinic acid [68, 69], nitric oxide [70] and excess glutamate [71, 72]. MPs have been believed to be immune protective. However, MPs can also be responsible for tissue damage. The mechanism wherein activated MPs during HIV infections can induce neuronal injury remains to be elucidated.

1.3 Excitotoxicity

Chronic neuroinflammation contributes to the major pathogenesis of neurodegenerative diseases including HAND, amyotrophic lateral sclerosis, multiple sclerosis, Parkinson's disease and Alzheimer's disease [48, 49, 51]. Brain inflammation has been suggested to be closely associated with neuronal injury [47, 73]. HIV infection and immune stimulation activate microglia and macrophages, which induce brain inflammation and neuronal damage via

production of a variety of soluble neurotoxic factors [70, 74] including viral proteins, platelet activating factors, proinflammatory cytokines and chemokines, nitric oxide, and excess glutamate [46, 50, 75-77]. In neurodegenerative pathology, the proinflammatory cytokines tumor necrosis factor-α (TNF-α) and interleukin-1β (IL-1β) are released in increasing concentrations, which induces neuronal damage via the excess release of glutamate [78].

Glutamate is one of the most important excitatory neurotransmitters and secondary messengers in the mammalian CNS [79, 80]. Glutamate plays a pivotal role in physiologic function regarding neural development, synaptic plasticity, learning and memory [81, 82]. Glutamate is packaged into presynaptic vesicles, which are recruited and docked to the release sites onto the dense electron active zones of presynaptic neurons [83]. After glutamate-containing vesicles are exocytosed into the synaptic cleft from the presynaptic nerve terminals with the intracellular calcium influxes, glutamate binds to glutamate receptors on the postsynaptic neurons [84-86]. The binding alters membrane potential of the postsynaptic neurons and thus the downstream signal transduction cascades.

There are three major downstream pathways of glutamate. First, glutamate is taken up by postsynaptic neurons for neuronal signal transmission. Second, glutamate can be taken up by presynaptic neurons through glutamate transporters. Third, the extra amount of glutamate in the synaptic cleft will be taken up by neighboring astrocytes through glutamate transporters at a sodium-dependent mechanism [87-89].

Studies also show that glutamate can potentially lead to extensive neuronal damage and excitotoxicity at excess level via the overactivation of glutamate receptors, which are N-Methyl-D-Aspartate (NMDA) receptors on neurons [90]. Neurotoxic viral proteins, such as HIV-1 coat protein glycoprotein 120 (Gp120) and HIV trans-acting protein Tat, can induce modification of the kinetics of NMDA receptors located on postsynaptic neurons through the stimulation of the release of arachidonic acid from infected glial cells [91]. The increasing production of extracellular glutamate contributes to the overactivation of NMDA receptors and the calcium overload within neurons [92, 93]. Calcium has long been understood as one of the most important secondary messengers in neural signal transduction. When dysregulated, calcium leads to oxidative stress including increasing production of free radicals, disruption of redox balance, mitochondrial dysfunction, caspase activation and cell death [94]. It has been reported that memantine, a moderate-affinity glutamate receptor antagonist, can reverse HIV viral protein-induced calcium overload in neurons and apoptosis. The inhibition of NMDA receptor, dizocilpine (MK-801), reverses the excitotoxicity in neurons induced by glutamate, which confirms the importance of glutamate in excitotoxicity [95, 96].

Furthermore, during HIV infection, the ability of astrocytes to absorb the extra amounts of glutamate in the extracellular space is impaired due to the dysfunction of the glutamate transporters, which exacerbates the excess levels of glutamate and further induces excitotoxicity [97-101].

In summary, elevation in extracellular glutamate levels has been proven to be associated with the pathogenic processes of various CNS disorders and neurodegenerative diseases including HAND [72, 102-104].

1.4 Glutaminase 1

Glutaminase is a phosphate-activated amidohydrolase, which deaminases glutamine into glutamate in the mammalian CNS [105]. Two major types of glutaminase have been identified in mammals, kidney-type glutaminase and liver-type glutaminase. Kidney-type glutaminase, also known as glutaminase 1 (GLS1) is the predominant enzyme to utilize glutamine to produce glutamate. GLS1 is a hetero-tetramer, located in the inner membrane of mitochondria. GLS1 is found abundantly expressed in a variety of cells in CNS. Liver-type glutaminase, or glutaminase 2 (GLS2) is expressed at lower levels in the brain [106].

GLS1 and GLS2 are encoded by separate genes on different chromosomes. The human *Gls1* gene is located on chromosome 2 and has two major isoforms attributed to tissue-specific alternative splicing [107, 108]. In a twist of confusing nomenclature, one of the isoforms of GLS1 is named kidney-type glutaminase (KGA), while the other isoform is known as glutaminase C (GAC). These two splice variants of GLS1, are found abundantly in mammalian brain tissues [109]. KGA and GAC transcribe exons 1-14 in the N-terminal and share the same functional region of KGA from 230 to 550 AA. KGA and GAC have a unique C-terminal, respectively, where KGA transcribes exons 16-19 and

GAC transcribes exon 15 [109]. When glutamine is catalyzed by glutaminase into glutamate, glutamate is subsequently further catalyzed by glutamate dehydrogenase into α-ketoglutarate. Subsequently, α-ketoglutarate enters the tricarboxylic acid (TCA) cycle to manage the energy generation [110]. Therefore, the important metabolism of glutamine through GLS1 is critical to the generation of the neurotransmitter, glutamate, and the brain bioenergetics via the TCA cycles.

In the physiological conditions, GLS1 is found most abundantly in neurons and less so intense in astrocytes, microglia, and macrophages in the CNS. However, when microglia and macrophages are activated, the level of GLS1 is altered, which leads to the abnormal glutamate-glutamine cycle in the CNS.

1.5 The pathological role of Glutaminase 1 in HAND

Although the exact mechanisms of how HIV infection induces HAND remains to be elucidated, the role of GLS1 has been reported to be crucial in the pathogenesis of HAND. In the past decade, our lab has helped to determine the neurotoxic profile of brain macrophages and microglia in cooperation with other researchers. We have been devoted to discovering novel molecular mechanisms and biochemical tools to understand the pathogenesis and a potential target for treating HAND.

Our group has identified that HIV-1 infected human macrophages and microglia express high levels of GLS1 that contribute to the production of excess extracellular glutamate, which leads to neurotoxicity through overstimulation of

NMDA receptors. Notably, HIV-infected macrophages and microglia show upregulated GLS1 that produces increasing levels of glutamate dependent on glutamine, which indicates that the increasing level of GLS1 can augment the neuroinflammation and neurotoxicity [53, 72]. We have also reported that HIV-1-infected macrophages and microglia are the major sources of increased extracellular glutamate and that they are significantly more neurotoxic than the uninfected macrophages and microglia [53, 111, 112]. The major upregulated isoform of GLS1 in HIV-1-infected macrophages and microglia is GAC, both at the RNA and protein levels, not KGA. Using siRNA to target GLS1 in HIV-1-infected macrophages and microglia significantly reduces the production of glutamate and the associated toxicity in neurons. Removing the glutamine, antagonizing the NMDA receptor, or blocking GLS1 activity by pharmacological GLS1 inhibitors effectively reversed the excess generation of glutamate and neurotoxic effects from HIV-1-infected macrophages and microglia [53]. In the samples of postmortem HAND patients', increasing levels of glutamate and upregulated GLS1 are found in vivo, which also proves the importance of GLS1 in the pathogenic process and disease progressions of HAND.

Mitochondrial oxidative stress is caused by the infection of HIV-1, which mediates the release of GLS1 from the inner membrane of mitochondria to cytosol through the permeability transition pore [111]. Interestingly, we also detected the release of GLS1 in the extracellular media. However, the mechanism of release of GLS1 from cytosol to extracellular media remains unknown.

The expression of GLS1 is usually most abundant in neurons. However, little has been known about the role of GLS1 in mediating the excitotoxicity in neurons associated with HAND until recently. In our laboratory, we reported that treatment of IL-1β and TNF-α, the two proinflammatory cytokines typically elevated during neurodegenerative conditions, on neurons induces cell apoptosis through substantially increased intracellular and extracellular glutamate levels [78]. The glutamate produced from these neurons under inflammation induces toxicity in other neurons. Furthermore, IL-1β and TNF-α upregulates the expression of the GLS isoform KGA expression in human neurons and increases the release of KGA from the mitochondria into the cytosol. TNF-α also triggers the release of GLS1 into the extracellular space. We also found that Interferon α/β (IFN-α/β), generated from HIV-1-infected macrophage/microglia, activates Signal transducer and activator of transcription 1 (STAT1) to bind with glutaminase promoters and regulate GLS1 expressions [113]. The neurotoxicity is reversed by the inhibition of GLS1 activity with pharmacological inhibitors or by the blockage of NMDA receptors with antagonists.

Taken together, these results indicate the critical role of dysregulated GLS1 in neurons, macrophages, and microglia in the pathogenesis of brain inflammation and HAND.

1.6 Extracellular vesicles

Extracellular vesicles (EVs) have been implicated in various neurodegenerative diseases and neuroinflammation including Alzheimer's

disease, Parkinson's disease, prion disease, Huntington's disease, multiple sclerosis, and HAND. EVs are vesicles ranging from 30 nm to 1000 nm that are shed from various cell types including neurons, astrocytes, macrophages, microglia, oligodendrocytes and blood endothelial cells in the CNS. EVs are released under normal and pathological conditions. EVs are composed of microvesicles (MVs) and exosomes, in which MVs range from 100 nm to 1000 nm while exosomes range from 30 nm to 100 nm. Biologically, MVs are believed to be derived from the plasma membrane, while exosomes are thought to be derived from the inward budding of the late endosomes. After budding, they are held within multivesicular bodies, which fuse with the plasma membrane. Both MVs and exosomes were once considered as a mechanism for discarding cellular debris or material. However, attention has been drawn to the role of EVs in the importance of intercellular communication and signal transduction. Evidence has shown that EVs can carry, nucleic acids, mRNAs, and other noncoding RNAs, proteins, cytokines and lipids among cells. Since differentiating exosomes and MVs is still a big challenge, the entire population of secreted and released MVs and exosomes in the extracellular milieu are all identified as EVs. Due to the various intracellular origins and formation of EVs, the detailed functional role of EVs under normal and disease conditions warrants further investigation.

The biogenesis of EVs including microvesicles and exosomes is still under investigation. Exosomes are believed to originate in the endocytic pathway, where proteins are internalized, and are either recycled back to the plasma

membrane or sorted for degradation [114, 115]. After internalization, early endosomes are formed and mature into late endosomes with an inward budding of their membrane and accumulation of intraluminal vesicles (ILVs) to form multivesicular bodies (MVBs). MVBs either fuse with lysosomes for degradation of their contents, or fuse with the plasma membrane to release the exosomes to the extracellular milieu via exocytosis [116-118]. However, it remains to be elucidated how pathway selection is determined. The biogenesis of microvesicles also needs further investigation.

As a mixture group of proteins, lipids and other cytosolic molecules is sorted into exosomes and microvesicles, the specific contents of EVs can vary depending on the type of cells, the condition of the cells, and the microenvironment niche the cells are in. There has been increasing interest in EVs and studies have focused on building the databases of the contents of EVs from different physiologic environments, which is continuously updated in Exocarta, Vesiclepedia and EVpedia [119-121]. In these database, different proteins, lipids, mRNAs, and miRNAs are identified in EVs from different cells types and organisms by proteomics, mass spectrometry and microarray. Studies show that EVs contain proteins from endosomes, plasma membrane, and cytosol that are involved in MVB biogenesis, membrane associated proteins, transmembrane proteins, cytoskeletal proteins, signal transduction proteins, chaperones and metabolic enzyme, but few from nuclei, Golgi, endoplasmic reticulum (ER) and mitochondria [119, 122, 123]. Among these proteins, there is an overlap of important proteins between microvesicles and exosomes, which

makes it a challenge to find individual specific markers. EVs are also enriched in lipid composition such as ceramide, cholesterol, sphingomyelin, and phosphatidylserine, which provides a tool and a recipe for artificial liposome formulation to mimic the EVs [124]. However, due to the complexity and variability of EVs, there are still limitations to overcome in liposomes synthesis. Additionally, miRNAs of 20-22 nucleotides have been associated with EVs. These miRNAs target the 3' untranslated region of specific mRNAs to inhibit their translation, which affects the proliferation, differentiation, survival and function of the cells [125]. Despite the variety of cellular contents in the EVs, questions remain as to mechanisms of cargo incorporation into EVs are, and how they are altered dependent on the cell source and the physiological or pathological condition and microenvironment of the cells [126, 127].

EVs were believed to be a pathway to degrade unwanted cellular contents, however, the recent hypotheses focus more on their role in cargo delivery, and intercellular signaling, especially during immune responses [128, 129]. While more light has been shed on the role of EVs in several cancers; however, further investigation is needed on their role in the CNS system.

Recent studies have indicated the importance of EVs in translational research, since it is know that EVs can be detected in biological fluids, such as blood, plasma, urine, and CSF [130-132]. It has been suggested that EVs have been used as biomarkers for various diseases. The contents in the EVs detected from CSF-samples reflect brain physiology, including amyloid precursor protein (APP) and amyloid β (Aβ) in Alzheimer's disease, α-synuclein in

Parkinson's disease, PrPsc in prion disease, and Superoxide dismutase (SOD) in amyotrophic lateral sclerosis.

1.7 Mechanism of extracellular vesicle release

The mechanisms of detailed differentiation of EVs is still understudied. There are a few major hypotheses about the EV release. One of these is called Endosomal Sorting Complexes Required for Transport (ESCRT) machinery, which involves the ESCRT complexes and their associated proteins [133]. One of the alternative mechanisms is the ESCRT-independent pathway. This lipid-driven mechanism of EV release depends on the synthesis of ceramide from sphingomyelin by neutral sphingomyelinase [134]. Another hypothesis is the RhoA-dependent pathway, which has been suggested in EVs studies in cancer research [135].

Despite the recent studies of the extracellular vesicles, very little is known about the mechanisms of EV release in macrophages and microglia. The role of GLS1 in the regulation of EVs remains to be further explored.

1.8 Conclusion

Regarding the need to better understand HAND pathogenesis, we have learned that EVs contribute to the neuronal damage associated with overproduction of glutamate and excitotoxicity. The critical role of EV as the specific molecular cargo carriers and their place in intercellular communication cannot be ignored. Previous reports from the lab have shown the importance of

GLS1 and glutamate in HAND, and further investigation revealed the role of EVs in the release of GLS1 and the potential neurotoxic role of EVs during HIV-1 infection and immune activation. In this case, we discovered a GLS1 inhibitor, and we are in the process of developing new inhibitors to rescue the GLS1-mediated neurotoxicity, which can be a novel therapeutic strategy.

With the heated discussion about EVs, their contents, biogenesis, delivery and functions still require further investigations. During our study, we discovered an interesting phenomenon in that the inhibition of GLS1 could disrupt the formation or release of EVs to the extracellular space. This provides us with a new perspective on the important role of GLS1 in the biogenesis of EVs. This evidence can also be applied to the fields outside of neuroscience study, such as cancer research due to the important role of GLS1 in both fields. This observation can shed light on the correlation of glutamine metabolism and other pathways including sphingolipid biogenesis in EV release, which also indicates the importance of developing a new therapeutic strategy against EVs and GLS1.

1.9 Figures

Figure 1.1

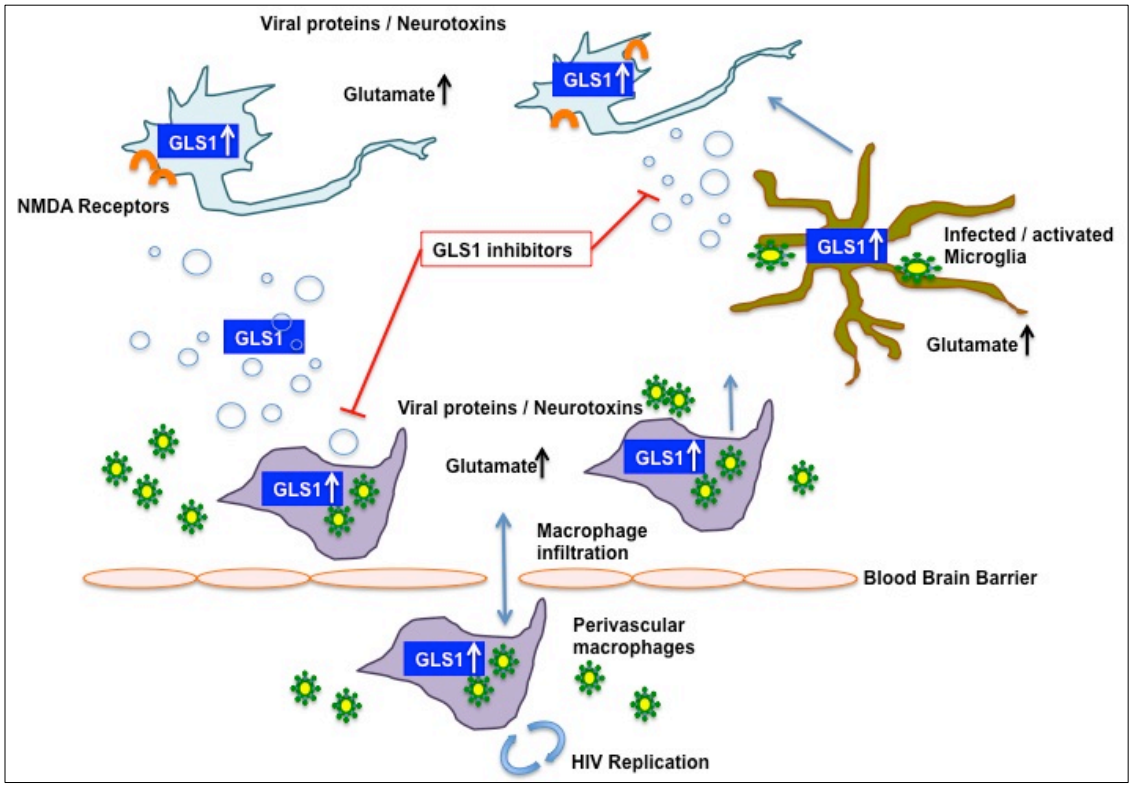

Figure 1.1 proposed model for the pathogenic role dysregulated GLS1 and EVs in HAND.

Chapter 2

HIV infection and immune activation induce neurotoxicity through GLS1-containing extracellular vesicles

2.1 Abstract

HIV-1-infected and/or immune-activated microglia and macrophages are pivotal in the pathogenesis of HIV-1-associated neurocognitive disorders (HAND). Glutaminase, a metabolic enzyme that facilitates glutamate generation, is upregulated and may play a pathogenic role in HAND. Our previous studies have demonstrated that glutaminase is released to the extracellular fluid during HIV-1 infection and neuroinflammation. However, key molecular mechanisms that regulate glutaminase release remain unknown. Recent advances in understanding intercellular trafficking have identified extracellular vesicles (EVs) as a novel means of shedding cellular contents. We posit that during HIV-1 infection and immune activation, microvesicles may mediate glutaminase release, generating excessive and neurotoxic levels of glutamate.

EVs isolated through differential centrifugation from cell-free supernatants of monocyte-derived macrophages (MDM) and BV2 microglia cell lines were first confirmed in electron microscopy and immunoblotting. As expected, we found an elevated number of EVs, glutaminase immunoreactivities, as well as glutaminase enzyme activity in the supernatants of HIV-1 infected MDM and lipopolysaccharide (LPS)-activated microglia when compared with controls. The elevated glutaminase was blocked by GW4869, a neutral sphingomyelinase inhibitor known to inhibit EV release, suggesting a critical role of EVs in mediating glutaminase release. More importantly, EVs from HIV-1-infected MDM and LPS-activated microglia induced significant neuronal injury in rat cortical neuron cultures. The EV neurotoxicity was blocked by a glutaminase inhibitor or

GW4869, suggesting that the neurotoxic potential of HIV-1-infected MDM and LPS-activated microglia is dependent on the glutaminase-containing EVs.

These findings support EVs as a potential pathway/mechanism of excessive glutamate generation and neurotoxicity in HAND and therefore EVs may serve as a novel therapeutic target.

2.2 Introduction

HIV-1-associated neurocognitive disorders (HAND) are currently prevalent in spite of major advances in combination anti-retroviral therapy. Therefore, novel therapeutic targets are required to be developed to treat the disease [5, 9, 71, 136]. The HIV-1-infected and immune-activated mononuclear phagocytes (MPs, including macrophages and microglia) are critical to HAND pathogenesis, producing a variety of inflammatory and neurotoxic factors, including excess levels of the excitatory neurotransmitter glutamate [137, 138]. Glutamate is a major mediator of excitatory synaptic transmission and has a vital role in mediating learning and memory [139-141]. Early studies reported that the concentrations of glutamate in the plasma and cerebrospinal fluid were significantly higher in HIV-1-infected patients than in uninfected controls [142-145]. Studies also showed that excessive levels of extracellular glutamate induce excitotoxicity and augment neuroinflammation and neuronal injury, which may play a role in the pathogenesis of HAND [74, 108, 146-149].

Glutaminase (GLS), a resident mitochondrial enzyme, is specialized in the de novo synthesis of the neurotransmitter glutamate [42, 105, 150-152]. Two major types of GLS exist in mammals, which include “kidney-type” GLS (GLS1) and “liver-type” GLS (GLS2) transcribed from different genes. GLS has also been found to be abundant in the brain tissue [108]. In the human brain, GLS1 has two allozymes: kidney-type glutaminase (KGA) [153] and glutaminase C (GAC) [154]. The allozymes are generated through tissue-specific alternative splicing from the same gene and have the identical core GLS1 enzyme domain but different 3’

tails [109]. Our previous studies suggested that GAC and KGA are differentially upregulated in HAND brain samples, HIV-1-infected MPs and inflammatory neurons [53, 72, 78, 112, 137]. Increased extracellular levels of glutamate from activated MPs could cause excitotoxicity to neurons through NMDA receptor activation [53, 112]. Therefore, regulation of GLS1 isoforms is of importance to HAND research. A key molecular event associated with the elevation of glutamate is the release of GLS1 [72, 78, 112]. Although several early observations of GLS1 release were linked with cell death, more recent data from our lab suggested that mitochondrial stress could lead to membrane destabilization and relocation of GLS1 from the mitochondrial matrix to the cytosol through the permeability transition pore [111]. Because the further release of GLS1 into extracellular supernatants contributes to excess glutamate production, it is imperative to understand the molecular mechanism of cellular GLS1 release.

Recent evidence indicates that extracellular vesicles (EVs), cellular secretory vesicles, are shed from the plasma membrane and range from 100 nm to 1 μm in diameter [155]. Interestingly, EVs are abundant in the central nervous system (CNS) and are derived from multiple brain cell types, including neurons, microglia, oligodendrocytes, and astrocytes [156]. Therefore, there is a growing appreciation of the important role of EVs in regulating the brain microenvironment [157, 158]. CNS-derived EVs may contribute to neuroinflammation through secretion of signaling molecules, nucleic acids, lipids, and proteins, and may participate in inter- and intra-cellular communication [155, 159-164]. The release

of EVs is increased upon neural cancer progression, neuroinflammation, and acute neurological disorders [165-167]. EVs could serve as a useful biomarker for CNS diseases including ischemic stroke, multiple sclerosis, glioblastoma, and other neurological and neurodegenerative disorders. However, the role of EVs in the pathogenesis of neurodegenerative disorders, especially HAND, remains to be elucidated. In our current study, we identified EVs as a primary mechanism of GLS1 release, which subsequently mediates excess glutamate generation and neurotoxicity from HIV-1-infected macrophages and immune-activated microglia. The investigation of the function of GLS1-containing EVs is important for understanding a potentially pathological event in HAND, and it may provide possible therapeutic targets and a unique biomarker.

2.3 Materials and methods

Culture, HIV-1 infection and LPS activation of macrophages and microglia

Human peripheral blood-derived mononuclear cells were isolated through leukopheresis from healthy donors. Human macrophages were differentiated in Dulbecco's Modified Eagle's Media (DMEM) (Sigma Chemical Co., St. Louis, MO) with 10% human serum, 50 μg/ml gentamycin, 10 μg/ml ciprofloxacin (Sigma), and 1,000 U/ml recombinant human macrophage colony-stimulating factor (MCSF) for 7 days. The HIV-1_{ADA} strain was used to infect the macrophages and microglia at a multiplicity of infection (MOI) of 0.1 and 0.5, respectively. The HIV-1_{ADA} strain was originally isolated from the PBMCs of an HIV-infected patient with Kaposi's sarcoma [168, 169]. MDM was infected with HIV-1_{ADA} at a multiplicity of infection (MOI) of 0.05 virus/target cell. For mock-infection, MDM was incubated with the same volume of medium without the virus. After 24 hours, the culture medium was changed to remove any remnant virus. Seven days after HIV-1-infection, the culture medium was changed to glutamine-free neurobasal medium for 24 h and supernatants were collected for subsequent RT-HPLC or Western blot analysis. BV2 cell lines were obtained from ATCC, and both cell lines were grown in DMEM with 10% fetal bovine serum and antibiotics. Lipopolysaccharide (LPS) (50 ng/ml) (Sigma) was used to immune activate BV2 cells for 24 h and supernatants were collected for HPLC and Western blot analysis.

Rat cortical neuron cultures

Cerebral cortices were dissected from Sprague-Dawley rat (Charles River Laboratories International Inc., Wilmington, MA) between embryonic days 15 and 17 and triturated with a pipet to generate cell suspension. The cell suspension was passed through a 70-μm nylon membrane (Becton Dickinson Labware, Franklin Lakes, NJ) and then plated at a density of 40,000 cells/well in 96-well plates pre-coated with 5 μg/ml poly-D-lysine. The cells were then cultured at 37 °C in a 5% CO_2 atmosphere for 7 days in neurobasal medium containing B27 supplement (Life Technologies), 0.5 mM glutamine, 100 U/ml penicillin and 100 μg/ml streptomycin.

Ethics statement

Primary rat cortical neuron (RCN) were prepared in accordance with ethical guidelines for care and use of laboratory animals set forth by the National Institutes of Health (NIH), with Institutional Animal Care and Use Committee (IACUC) #: 04-097-01; Monocytes were used in full compliance with the University of Nebraska Medical Center and NIH ethical guidelines, with the Institutional Review Board (IRB) #: 162-93-FB. We have the informed written consent from all participants involved in this study.

Isolation of EVs

EVs were isolated from the supernatants of HIV-1-infected macrophages and LPS-activated microglia through differential centrifugations with or without neutral sphingomyelinases inhibitor GW4869 (Sigma) at different dosages, 2, 5

and 10 μM. Briefly, the supernatants were first centrifuged at 300 X g for 10 min to remove free cells, at 3,000 X g for 20 min to remove cellular debris and then 10,000 X g for 30 min to remove free organelles. Lastly, EVs were collected by ultracentrifugation at 100,000 X g for 2 h at 4°C. To prepare EVs for Western blot, the EVs pellets were lysed in M-PER mammalian protein extraction reagent (Thermo Scientific, Pittsburgh, PA). For negative staining, EVs were fixed in 2% glutaraldehyde and 2% paraformaldehyde. For glutaminase activity assay and neurotoxicity, the EVs were resuspended in 1 ml of glutamine-free neurobasal medium.

Negative staining and electron microscopy

EVs were negatively stained with onscreen measurements. Briefly, EVs were fixed and then spread on the silicon monoxide and nitro-cellular film coated copper grid. The droplets of EVs were removed with filter paper, air-dried at room temperature and then subjected to transmission electron microscopy (TEM) (FEI Tecnai G2 Spirit TWIN). For the scanning electron microscope (SEM) (FEI Quanta 200), cells were fixed in 2% glutaraldehyde and 2% paraformaldehyde and point dried, mounted and coated with gold/palladium. The investigator in the EM core facility was blinded for image acquisition and quantification.

Neurotoxicity assays

Resuspended EVs were added to neuronal cultures for 48 h with or without 10 μM of bis-2-(5-phenylacetamido-1,2,4-thiadiazol-2-yl)ethyl sulfide (BPTES) (a

generous gift presented by Dr. Tsukamoto from Colorado State University) and cell viability was assessed by MTT assays in 96-well plates. MTT (Sigma) was added to the cultures to a final concentration of 125 μg/ml. The plates were incubated for 30 minutes at 37 °C with 5% CO_2 and the medium was aspirated. The insoluble formazan was solubilized in DMSO, and the concentrations were determined by optical density at 490 nm with an EL_X808 densitometer (Bio-Tek Instruments, Winooski, and VT). MAP2 ELISA was performed on primary RCN cultures as previously described. Briefly, fixed neurons were blocked with 3% normal goat serum in phosphate buffered saline and incubated for 2 hours with antibodies against microtubule associated protein 2 (MAP-2) (Millipore-Chemicon International, Atlanta, GA), followed by the anti-mouse biotinylated antibody (Vector Laboratories, Burlingame, CA) for 1 hour. Avidin/biotin complex solution was added for 30 minutes, and then color was developed using TMB substrate (Sigma Chemical Co., St. Louis, MO) and terminated with 1 M sulfuric acid (Sigma Chemical Co., St, Louis, MO). The absorbance was read at 450 nm using a microplate reader (Bio-Rad Laboratories, Hercules, CA). For morphological data that demonstrated neuronal damage after exposed to the supernatant of HIV-1-infected macrophages or immune-activated microglia, MAP2 immunostaining was examined by a Nikon Eclipse TE2000E fluorescent microscope and photographed by a digital camera (CoolSNAP EZ, Photometrics). All obtained images were imported into Image-ProPlus, version 7.0 (Media Cybernetics, Sliver Spring, MD) for quantifying levels of MAP2 staining. The assessors were blinded during image acquisition or quantification.

Western blot

Protein concentrations were determined by Bradford protein assay. SDS PAGE separated proteins from whole cell and EV lysates. After electrophoretically transferred to polyvinyldifluoridene membranes (Millipore, Billerica, MA and Bio-Rad, Hercules, CA). Membranes were incubated overnight at 4 °C with polyclonal antibodies for GAC (Dr.N.Curthoys, Colorado State University, Fort Collins, CO), Alix (Santa Cruz Biotechnology, CA) and flotillin-2 (Cell Signaling Technology, Danvers, MA), followed by horseradish peroxidase-linked secondary anti-rabbit or anti-mouse secondary antibodies (Cell signaling Technology). Antigen-antibody complexes were visualized by Pierce ECL Western Blotting Substrate. For quantification of the data, films were scanned with a CanonScan 9950F scanner and images were analyzed using the public domain NIH image program (developed at the U.S. National Institutes of Health and available on the internet at http://rsb.info.nih.gov/nih-image/).

Analysis of glutamate and glutamine by RP-HPLC

Glutamate levels were analyzed by reverse phase high performance liquid chromatography (RP-HPLC) using an Agilent 1200 liquid chromatograph and fluorescence detector as previously described [53] with a few modifications. The experiments utilized 4.6 × 75 mm, 3.5 μm ZORBAX Eclipse AAA analytical columns (Agilent). A gradient elution program was optimized for glutamate measurement with a flow rate 0.75 ml/min.

Statistical analysis

Data are expressed as means ± SD unless otherwise specified. Statistical analysis was performed using Analysis of variance (ANOVA), followed by the Tukey-post-test for paired observations. Significance was determined by a p value < 0.05. All experiments were performed with cells from at least three donors to account for any donor-specific differences. Assays were performed at least three times in triplicate or quadruplicate within each assay.

2.4 Results

HIV-1 infection and immune activation increase EV release from macrophages and microglia

Our previous studies have demonstrated that GLS1 is released to the extracellular fluid during HIV-1 infection and neuroinflammation [72, 78, 112]. However, key molecular mechanisms that regulate GLS1 release remain unknown. The recent discovery of EVs during HIV-1 infection in macrophages and dendritic cells offers an exciting possibility that GLS1 may be released through EV mechanism [155, 170]. We used scanning electron microscopy (SEM) to identify EVs that were in the process of budding from macrophages (Fig. 2.1A, B). To quantitatively evaluate EV release, two different techniques for EV detection were used. First, EVs were isolated from cultured monocyte-derived macrophages (MDM) supernatants by differential centrifugation. To reflect the changes of EVs from the same number of cells, EVs were isolated from normalized volumes of supernatants based on the protein concentrations in the whole cell lysates. Cells, nuclei, debris and subcellular organelles were removed from the supernatant after serial centrifugation. The EV pellet was collected and resuspended for negative staining under transmission electron microscopy (TEM). Images of EVs from ten random fields were captured. The numbers of EVs per field under TEM was significantly higher in HIV-1-infected macrophages than EVs from mock-infected macrophages, suggesting that HIV-1 infection leads to increased release of EVs in MDM (Fig. 2.1C-E). Second, EVs isolated from infected human macrophages were subjected to Western blots for specific EV

markers, including ALG-2 interacting protein (Alix) and flotillin-2. Consistent with TEM data, Western blot analysis revealed increased levels of Alix and flotillin-2 in EV lysates from HIV-1-infected cells, compared with those from uninfected cultures (Fig. 2.1F, G). Western blot also showed intact levels of voltage-dependent anion channels (VDAC) from whole cell lysates. Absence of VDAC from EV lysates was confirmed to exclude contamination of mitochondria in isolated EVs (Fig. 2.1H).

Similarly, when murine microglia cell line BV2 was treated with lipopolysaccharide (LPS) for immune activation, the EV number was significantly higher in the LPS-treated EV2 compared with the untreated group (Fig. 2.2A-C). The increased release of EVs from LPS-treated EV2 cells was further confirmed by Western blot detecting EV markers, Alix and flotillin-2 (Fig. 2.2D, E). Because EVs were isolated from normalized volumes of supernatants based on their corresponding whole cell protein concentrations, a higher number of EVs in TEM and increased immunoreactivities of EV markers in Western blots from HIV-1-infected macrophages and LPS-stimulated microglia suggest that HIV-1 infection and immune activation both increase EV release from the cultures.

EVs mediate GLS1 release in HIV-1-infected MDM and immune-activated microglia

To determine whether EVs are the main mechanism for GLS1 release in HIV-1-infected MDM and immune-activated microglia, we treated the cultures with GW4869, a neutral sphingomyelinases (nSMase) inhibitor, for 24 hours prior

to EVs isolation. GW4869 is known to disrupt in the biogenesis of EVs by inhibiting the generation of ceramide [134, 171]. Because GW4869 was dissolved in DMSO, we used DMSO as a solvent control for GW4869 and used the same amount of DMSO in each dose of the GW4869 treatment. EV markers, Alix and flotillin-2, were both increased in the EVs isolated from HIV-1-infected MDM (Fig. 2.3A-C). Pretreatment with GW4869 for 24 hours reduced the levels of Alix and flotillin-2 in the EVs isolated from HIV-1-infected MDM, indicating the increased EV release in HIV-1-infected MDM could be blocked by GW4869 (Fig. 2.3A-C). The protein levels of GAC, a GLS1 isoform previously identified to have neurotoxic potential, were also increased in EVs after HIV-1 infection and diminished after GW4869 treatment, indicating that EVs carried GAC as cargo and that HIV-1 increases GAC release through EVs (Fig. 2.3A, D). Supernatants were collected from the mock-infected, HIV-1-infected with or without GW4869 and subjected to RT activity assay. The results indicated that after seven days of HIV-1 infection, the treatment of GW4869 with different concentration did not affection the HIV-1 virus replication, indicating GW4869 is inhibiting the release of EV through a mechanism other than lowering HIV-1 infection (Fig. 2.3E).

Consistent with HIV-1 infection, LPS activation of microglia line BV2 cells also lead to increased EV secretion (Fig. 2.4A-C). After treatment with increasing concentrations of GW4869, the increase of Alix and Flotillin-2 in the EVs isolated from LPS-activated microglia was blocked, suggesting that immune activation also increases EV release in microglia (Fig. 2.4A-C). Importantly, GAC protein levels were also increased in EVs after LPS activation and diminished after

GW4869 treatment, confirming that immune activation also increases GAC release through EVs (Fig. 2.4A, D).

EVs isolated from HIV-1-infected MDM and immune-activated microglia mediate extracellular glutamate production through GLS1

The identification of EVs in mediating GAC release raises the question of the functional relevance of GAC to EVs. HIV-1 infection is known to increase extracellular levels of glutamate in human macrophages [71]. We treated cell-free HIV-1-infected supernatants with 5 mM glutamine, the reaction substrate for GLS1 enzyme, in the presence of 6-Diazo-5-oxo-L-norleucine (L-DON), a GLS inhibitor. The levels of glutamate production, as determined by RT-HPLC, increased after HIV-1 infection, which was dependent on glutamine (Fig. 2.5A). Furthermore, the elevation of glutamate was blocked by L-DON, indicating that the released GLS1 promotes glutamate generation in the extracellular fluid of HIV-1-infected MDM (Fig. 2.5A). More importantly, EV pellets extracted from both mock- and HIV-1-infected MDM were directly tested for GLS1 activity by HPLC. EVs were incubated with neurobasal media with or without glutamine for two days. Interestingly, the levels of glutamate generated in EVs from HIV-1-infected cultures elevated significantly compared with mock-infected control (Fig. 2.5B). Low-speed pellets were collected after 10,000 g centrifugation, which may contain subcellular organelles and debris. Interestingly, blockage of GLS1 activity by L-DON was only observed in the EVs but not in the low-speed pellets from HIV-1-infected MDM, suggesting that EVs are the specific compartments for

GLS1 release and responsible for excess glutamate production (Fig. 2.5B). To further investigate how EVs facilitate glutamine hydrolysis through the GLS1, we determined the level of vesicular glutamate transporter (VGLUT) in the EV lysates from HIV-1 infected MDM through Western blots (Fig. 2.5C, D). VGLUT levels increased after HIV-1 infection and decreased after GW4869 treatment, consistent with the overall EV levels. These results indicate VGLUT is a component of EVs and suggest that glutamate transporters on the EV lipid bilayer may facilitate the transportation of glutamate. Consistent with HIV-1-infected MDM, EVs isolated from the supernatant of LPS-stimulated microglia significantly increased glutamate generation, which could be blocked by L-DON (Fig. 2.6A). Taken together, these data suggest that GLS1 released through EVs in HIV-1-infected MDM and immune-activated microglia maintains enzyme activity and promotes glutamate generation.

GLS1-containing EVs induce neurotoxicity

To investigate the functional significance of GLS1-containing EVs from HIV-1-infected MDM and immune-activated microglia, EVs were collected and re-suspended in the neuronal culture medium. The volumes of culture medium used to re-suspend EVs were adjusted based on the whole cell protein concentration in the same culture. Rat cortical neurons (RCN) treated with 1 µl, 10 µl or 100 µl per well of EVs from mock-infected MDM didn't show significant neurotoxicity (Fig. 2.7A, B). However EVs extracted from HIV-1-infected MDM had significantly lower viabilities (Fig. 2.7C) and higher neurotoxicity (Fig. 2.7E) compared with

those treated with EVs from mock-infected cells. However, the EV-induced toxicity was rescued at the presence of BPTES, a GLS1 inhibitor, when 100 µl of EVs were incubated with RCN (Fig. 2.7D, F). When RCN was treated with 100 ng/ml of soluble receptor for TNF, the toxicity induced by EVs from HIV-1-infected MDM was not rescued, which suggests the toxicity is not affected through TNF-α (Fig. 2.7G). Interestingly, the toxicity was rescued by the application of MK801, an uncompetitive agonist of N-Methyl-D-Aspartate (NMDA) receptor, indicating the toxicity of GLS1-containing EVs was through the excitotoxicity via glutamate (Fig. 2.7H).

Similarly, EVs from control BV2 cells didn't show any neurotoxicity (Fig. 2.8A), but neurotoxicity was observed in neurons treated with EVs isolated from LPS-activated microglia in a volume-dependent manner (Fig. 2.8B). This toxicity was blocked by BPTES (Fig. 2.8C). Interestingly, RCN didn't demonstrate toxicity when treated with EV free supernatants collected after EV isolation (Fig. 2.8D), indicating the toxicity was majorly induced via EVs. These data suggest that the GLS1-containing EVs induce neurotoxicity through the GLS1 activity in the EVs.

HIV-1-infected MDM induce neurotoxicity through GLS1-containing EVs

To determine whether HIV-1-infected MDM induce neurotoxicity through GLS1-containing EVs, we obtained supernatants from HIV-1-infected macrophages that were pre-treated with 2, 5 or 10 µM of GW4869 and used the supernatants to treat RCN for neurotoxicity. Similar to prior experiments, we used DMSO as a solvent control for GW4869 and used the same amount of DMSO in

each dose of the GW4869 treatment. Neurotoxicity was determined through quantifications of neuronal antigen MAP2 with either MAP2 ELISA (Fig. 2.9A) or MAP2 immunostaining (Fig. 2.9B-H). The HIV-1-infected MDM-induced neurotoxicity was blocked by increasing concentrations of GW4869 (Fig. 2.9), indicating that supernatants from HIV-1-infected MDM induce neurotoxicity through EVs. Next, we isolated EVs from mock-infected and HIV-1-infected MDM and investigated the direct neurotoxicity of EVs. Interestingly, EVs isolated from HIV-1-infected MDM manifested higher levels of neurotoxicity as determined by MAP2 ELISA (Fig. 2.10A) or MAP2 immunostaining (Fig. 2.10C-I), when compared with EVs from mock-infected control. However, the EV-free supernatants did not show any toxicity from the indication of MAP2 ELISA (Fig. 2.10B). Treatment of GW4869 prior to EV isolation rescued EV-induced neurotoxicity at a dose dependent manner, suggesting a direct neurotoxic role of EVs from HIV-1-infected MDM. Together, these data strongly suggest that HIV-1-infected macrophages induce neurotoxicity through EVs.

2.5 Discussion

Our previous reports have described the release of GLS1 into extracellular space during neuroinflammation or HIV-1 infection. However, key molecular mechanisms that regulate GLS1 release remain unknown. Our current study presents two important new findings regarding the GLS1 release. First, EVs contain GLS1, which is a key enzyme for generating glutamate in the brain, and GLS1 is released into the extracellular fluid primarily via EVs in HIV-1-infected cells and immune-activated microglia. Second, HIV-1 infection and LPS activation increase the magnitude of EV release from macrophages and microglia. Interestingly, increased release of GLS1-containing EVs also induces excitotoxicity in RCN. The toxic effect of EVs was reversed by glutaminase inhibitors and EV inhibitors. These observations suggest that EVs may contribute to excess glutamate production in macrophages in the context of HIV-1 neurotoxicity.

The physiological relevance of this observation is significant, where elevated endogenous levels of GLS1 have been reported in the post-mortem brain tissues of HIV-1-associated dementia patients [53, 113]. Furthermore, it has been demonstrated that both of the upregulated GLS1 isoforms, KGA and GAC, are released from the inner membrane of mitochondria into the cytosol through the permeability transition pore [72, 111]. However, it is the extracellular glutamate that causes neurotoxicity, and the mechanisms by which cytosolic GLS1 is released into the cell supernatant have not been previously established. The current study provides strong evidence that GLS1-containing EVs are the

main mechanism for the release of GLS1 from the macrophage and microglia cytosol into the extracellular compartment, where the extracellular glutamate subsequently induces neurotoxicity. It is unclear how GLS1 hydrolyzes extracellular glutamine inside EVs. We have detected vesicular glutamate transporter in the EV lysates from HIV-1 infected MDM (Fig. 2.5), suggesting that EVs may transport glutamate across its lipid bilayer through glutamate transporters.

Our studies were designed to rigorously establish the purity and characterization of the isolated microvesicles. To confirm complete separation of EVs from mitochondria, the absence of the mitochondrial marker protein voltage-dependent anion-selective channel (VDAC) and cytochrome C was confirmed through Western blots. Secondly, to characterize the EVs, both scanning and transmission electron microscopies were used, which showed vesicles ranging in size from 50 nm to 500 nm. Western blot could not detect the presence of GLS1 in exosomes collected from commercially available exosome kits, suggesting that GLS1 is selectively packed into the larger form of EVs rather than into smaller exosomes. Furthermore, because the EV-free supernatants and the pellets that contained cellular debris had minimum GLS1 activities and GLS1 was found predominantly in the isolated EVs fraction, we concluded that EVs are the primary instigator in facilitating GLS1 release in HIV-1-infected macrophages and LPS-activated microglia.

Chronic activation of the immune system is a hallmark of progressive HIV infection yet its etiology remains obscure. Circulating microbial products such as

LPS, possibly derived from the gastrointestinal tract, was significantly increased in chronically HIV-infected individuals and may be a cause of HIV-related systemic immune activation [172]. In our report, when LPS was used to treat BV2 microglia cell line, high levels of GLS1 were found in the supernatants leading to neurotoxicity. These results support the pathogenic effect of the immune activation in the CNS during HIV-1 infection. The discovery that GLS1 upregulation induces GLS1 release via EVs may have a broader implication to other neurological diseases, where excitotoxicity and GLS1 are involved. Because EVs are abundantly expressed in the CNS, it is tempting to speculate whether qualitative or quantitative changes of EVs contribute more broadly to neurological diseases. In addition, the regulation of EVs could be exploited as a novel therapeutic target.

In the current study, we also utilized an EV inhibitor, GW4869, to block the release of the EVs. Both GLS1 and EV markers were decreased in a dose-dependent manner by GW4869, suggesting that GLS1 release is through EVs. GW4869 is an inhibitor for nSMase2, which is responsible for the production of ceramide. Ceramide has been found enriched in EVs and involved in the formation of vesicles. Our results point to a possible mechanism of EVs release in the microglia and macrophages through the endosomal sorting complex required for transport (ESCRT) machinery or a ceramide-dependent pathway [134, 171]. These interesting possibilities remain the subject of future investigation. Furthermore, we have demonstrated that the neurotoxicity by HIV-1-infected MDM was abolished by pre-treatment with GW4869, which indicates

that GLS1-containing EVs are the neurotoxic factors in HIV-1-infected macrophages and immune-activated microglia. Therefore, inhibiting the release of EVs might become a potential therapeutic approach for the treatment of HAND patients.

Three aspects of the studies merit further investigation. First, how is cytosolic GLS1 loaded into EVs for extracellular secretion from macrophages? Second, how are GLS1-containing EVs formed? Third, what mediates the release of GLS1-containing EVs from the plasma membrane? Autophagosomes, inflammasomes or mitochondria-derived vesicles may provide possible mechanisms for these events to occur. It is possible that HIV-1 infection and immune activation of macrophages and microglia directly lead to the release of GLS1-containing EVs, however, other possibilities also need to be explored.

2.6 Conclusion

In summary, our studies address important questions regarding the cellular mechanisms of GLS1 release, implicating a critical role of EVs. This newfound knowledge of neurotoxic GLS1-containing EVs has potentially important clinical implications for neurologic diseases such as HAND. Developing inhibitors of EV formation and release or inhibitors of GLS1 might yield effective new therapies for reducing glutamate-induced neurotoxicity in HIV-1-infected and immune-activated individuals.

2.7 Figures

Figure 2.1

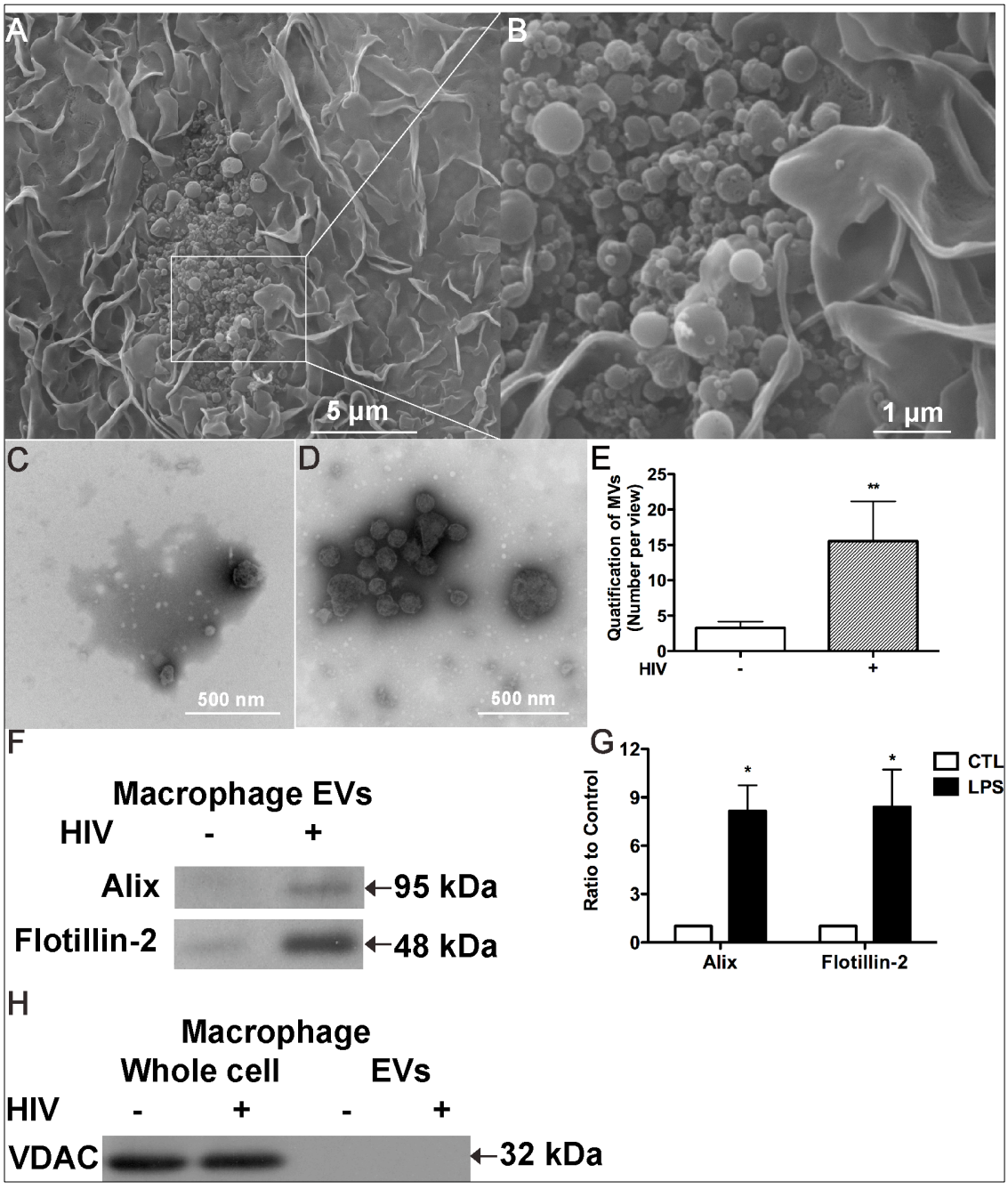

Figure 2.1 HIV-1 infection increases EVs release from macrophages.

(A) MDM was fixed at 7th day post HIV-1 infection and subsequently subjected to SEM for EV detection. Magnification, 6000 X. **(B)** High-magnification image of the corresponding small box area in panel A was shown. Magnification, 24000 X. **(C-E)** eVs were isolated through differential centrifugation from normalized volumes of cultural supernatants and observed under TEM using negative staining. Representative TEM images of EVs from mock-infected MDM (C), HIV-1 infected MDM (D) were shown. **(E)** EVs numbers in C and D were quantified by manually counting from a total of 10 random vision fields. Results are representative of TEM images and quantification results are means ± SD of EV numbers from 10 fields of TEM images. ** denotes $p < 0.01$ in comparison to controls. **(F)** EVs were isolated from normalized volumes of supernatants in mock-infected and HIV-1-infected MDM cultures. The levels of Alix and flotillin-2 in EVs were determined by Western blot. **(G)** Densitometric quantifications of the Alix and flotillin-2 protein levels were presented as fold change relative to the untreated controls. **(H)** The level of mitochondrial marker, voltage-dependent anion channels (VDAC) was detected in both whole cell and EV lysates to exclude contamination in EVs.

Figure 2.2

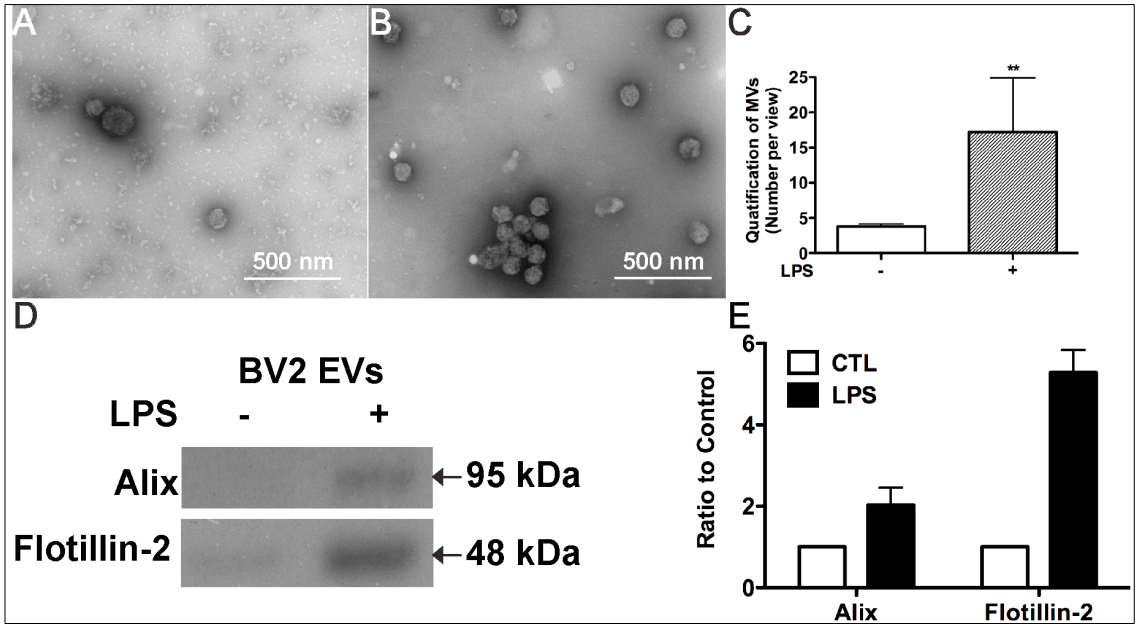
A
500 nm
B
500 nm
C
Quatification of MVs (Number per view)
25
20
15
10
5
0
**
LPS
-
+
D
BV2 EVs
LPS
-
+
Alix
95 kDa
Flotillin-2
48 kDa
E
Ratio to Control
6
4
2
0
CTL
LPS
Alix
Flotillin-2

Figure 2.2 Immune activation increases EVs release from microglia.

(A-B) EVs were isolated through differential centrifugation from normalized volumes of cultural supernatants and observed under TEM using negative staining. Representative TEM images of EVs from untreated microglia (A), and LPS-stimulated microglia (B) were shown. **(C)** EVs numbers in C, D and E, F were quantified by manually counting from a total of 10 random vision fields. Results are representative of TEM images and quantification results are means ± SD of EV numbers from 10 fields of TEM images. ** denotes $p < 0.01$ in comparison to controls. **(D)** EVs were isolated from normalized volumes of supernatants in untreated and LPS-stimulated microglia cultures. The levels of Alix and flotillin-2 in EVs were determined by Western blot. **(E)** Densitometric quantifications of the Alix and flotillin-2 protein levels were presented as fold change relative to the untreated controls.

Figure 2.3

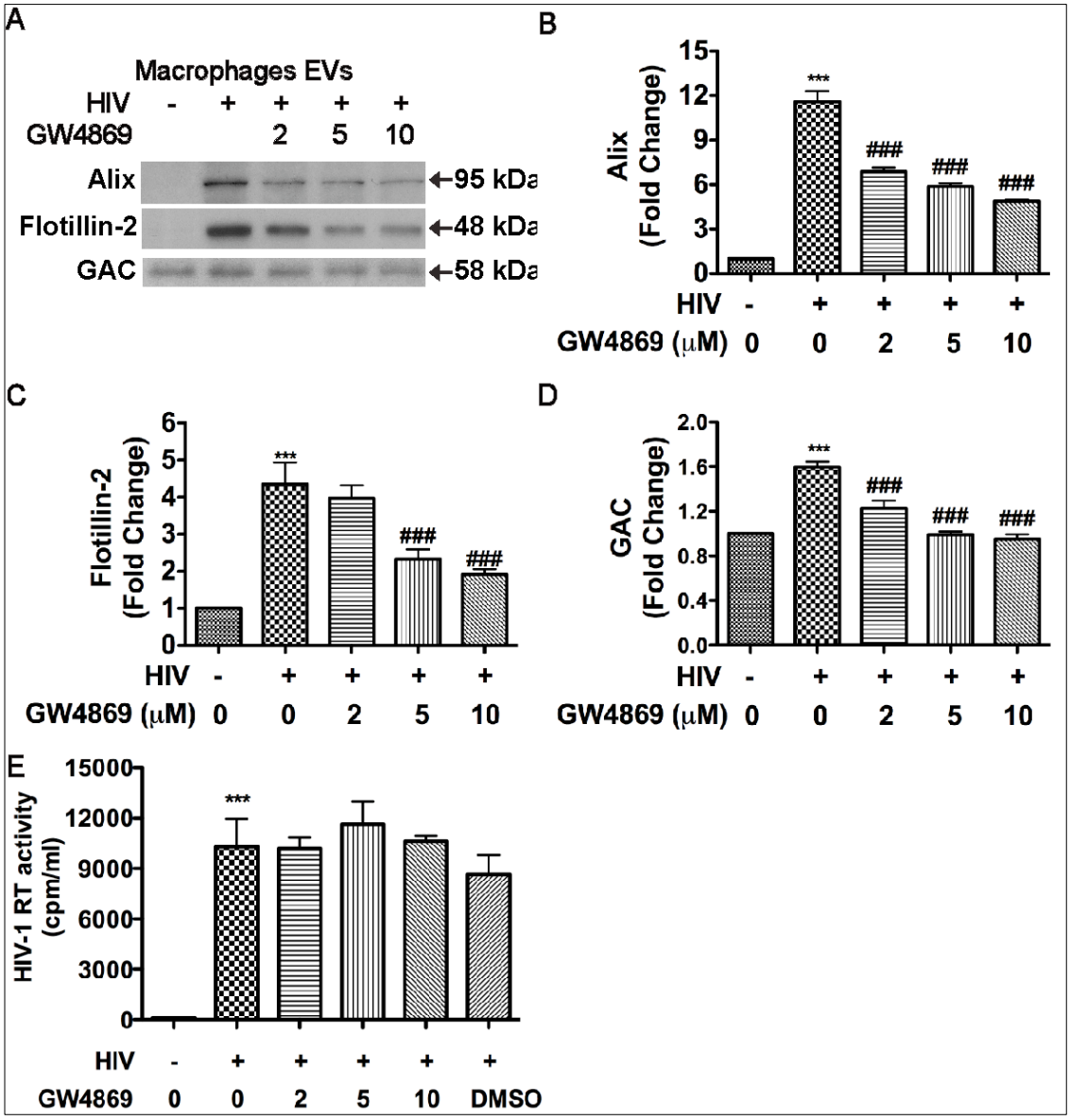
A
Macrophages EVs
HIV - + + + +
GW4869 2 5 10
Alix
Flotillin-2
GAC
←95 kDa
←48 kDa
←58 kDa
B
Alix (Fold Change)
15
12
9
6
3
0
***
###
HIV - + + + +
GW4869 (μM) 0 0 2 5 10
C
Flotillin-2 (Fold Change)
6
5
4
3
2
1
0
***
###
HIV - + + + +
GW4869 (μM) 0 0 2 5 10
D
GAC (Fold Change)
2.0
1.6
1.2
0.8
0.4
0.0
***
###
HIV - + + + +
GW4869 (μM) 0 0 2 5 10
E
HIV-1 RT activity (cpm/ml)
15000
12000
9000
6000
3000
0
***
HIV - + + + + +
GW4869 0 0 2 5 10 DMSO

Figure 2.3 EVs mediate GLS1 release in HIV-1-infected MDM.

(A) At 7 days post-infection, mock-infected and HIV-1 infected MDM were treated with GW4869 for 24 hours in serum-free media. EVs were isolated from the supernatants and EV protein lysates were prepared. The levels of Alix, flotillin-2, and GAC were determined by Western blots. **(B-D)** Densitometric quantifications of the Alix (B), flotillin-2 (C), and GAC (D) protein levels were presented as fold change relative to the mock-infected controls. **(E)** Supernatants were collected and subjected to RT activity assay. DMSO was used as solvent control for GW4869. Western blot results shown are representative of three independent experiments. Quantification results shown are means ± SD of experiments performed in triplicate (n = 3 donors). ** and *** denotes $p < 0.01$ and 0.001 in comparison to mock-infected or untreated control; #, ## and ### denote $p < 0.05$, 0.01 and 0.001 in comparison to HIV-infected or immune-activated groups, respectively.

Figure 2.4

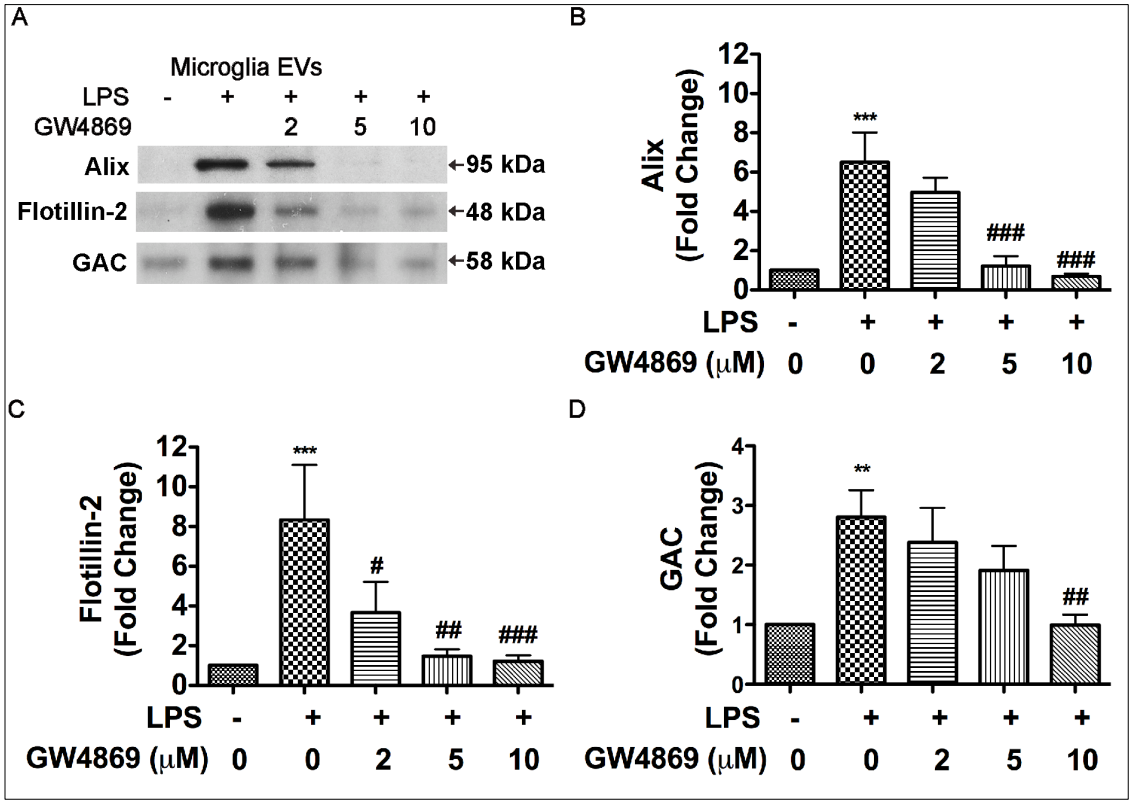
A
Microglia EVs
LPS - + + + +
GW4869 2 5 10
Alix
Flotillin-2
GAC
←95 kDa
←48 kDa
←58 kDa
B
Alix (Fold Change)
***
###
###
LPS - + + + +
GW4869 (μM) 0 0 2 5 10
C
Flotillin-2 (Fold Change)
***
#
##
###
LPS - + + + +
GW4869 (μM) 0 0 2 5 10
D
GAC (Fold Change)
**
##
LPS - + + + +
GW4869 (μM) 0 0 2 5 10

Figure 2.4 EVs mediate GLS1 release in immune-activated microglia.

(A) EVs were isolated from the supernatants of control and LPS-treated microglia in the presence and absence of GW4869. EV lysates were subjected to Alix, flotillin-2, and GAC detection through Western blots. Results shown are representative of three independent experiments. **(B, C, D)** Densitometric quantifications of the Alix (B), flotillin-2 (C), and GAC (D) protein levels were presented as fold change relative to the untreated controls. DMSO was used as solvent control for GW4869. Western blot results shown are representative of three independent experiments. Quantification results shown are means ± SD of experiments performed in triplicate (n = 3 donors). ** and *** denotes $p < 0.01$ and 0.001 in comparison to mock-infected or untreated control; #, ## and ### denote $p < 0.05$, 0.01 and 0.001 in comparison to HIV-infected or immune-activated groups, respectively.

Figure 2.5

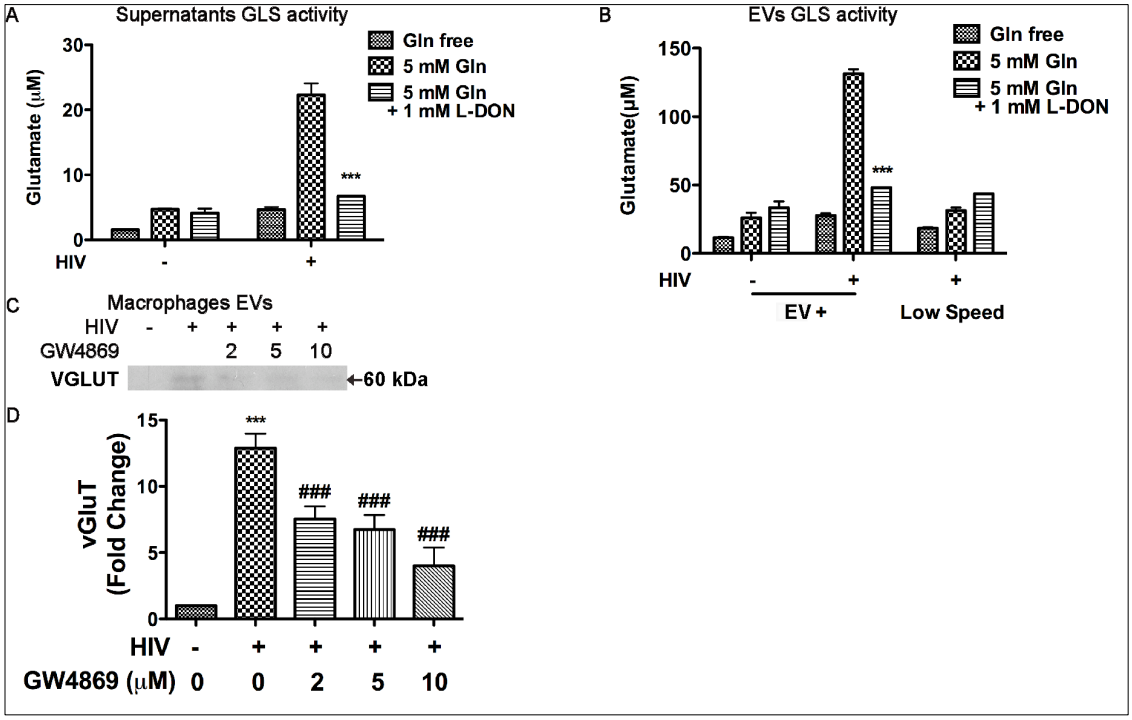
A
Supernatants GLS activity
Gln free
5 mM Gln
5 mM Gln
+ 1 mM L-DON
Glutamate (μM)
30
20
10
0
***
HIV
-
+
B
EVs GLS activity
Gln free
5 mM Gln
5 mM Gln
+ 1 mM L-DON
Glutamate(μM)
150
100
50
0
***
HIV
-
+
+
EV +
Low Speed
C
Macrophages EVs
HIV - + + + +
GW4869 2 5 10
VGLUT
60 kDa
D
vGluT
(Fold Change)
15
10
5
0
***
###
###
###
HIV - + + + +
GW4869 (μM) 0 0 2 5 10

Figure 2.5. EVs isolated from HIV-1-infected MDM mediate extracellular glutamate production through GLS1.

(A) Cell-free supernatants from mock-infected and HIV-1-infected macrophages were incubated with or without glutamine and 1 mM L-DON ex vivo for two days. The resulting glutamate levels were determined by RP-HPLC. *** denotes $p < 0.001$ in comparison to the 5 mM glutamine group in HIV-1-infected samples. **(B)** EVs were isolated from cell-free supernatants from mock-infected and HIV-1-infected MDM and incubated with or without glutamine and 1 mM L-DON ex vivo for two days. Glutamate generation in EVs or low speed (LS) pellets was determined by RP-HPLC. Low-speed pellets were collected after 10,000 g centrifugation, which contained subcellular organelles and debris. **(C)** At 7 days post-infection, mock-infected and HIV-1 infected MDM were treated with GW4869 for 24 hours in serum-free media. EVs were isolated from the supernatants and EV protein lysates were prepared. The levels of vGluT were determined by Western blots. **(E)** Densitometric quantifications of vGluT protein levels were presented as fold change relative to the mock-infected controls. Western blot results shown are representative of three independent experiments. Quantification results shown are means ± SD of experiments performed in triplicate (n = 3 donors). *** denotes $p < 0.001$ in comparison to 5 mM glutamine group in HIV-1-infected samples or mock-infected control; ### denotes $p < 0.001$ in comparison to HIV-infected.

Figure 2.6

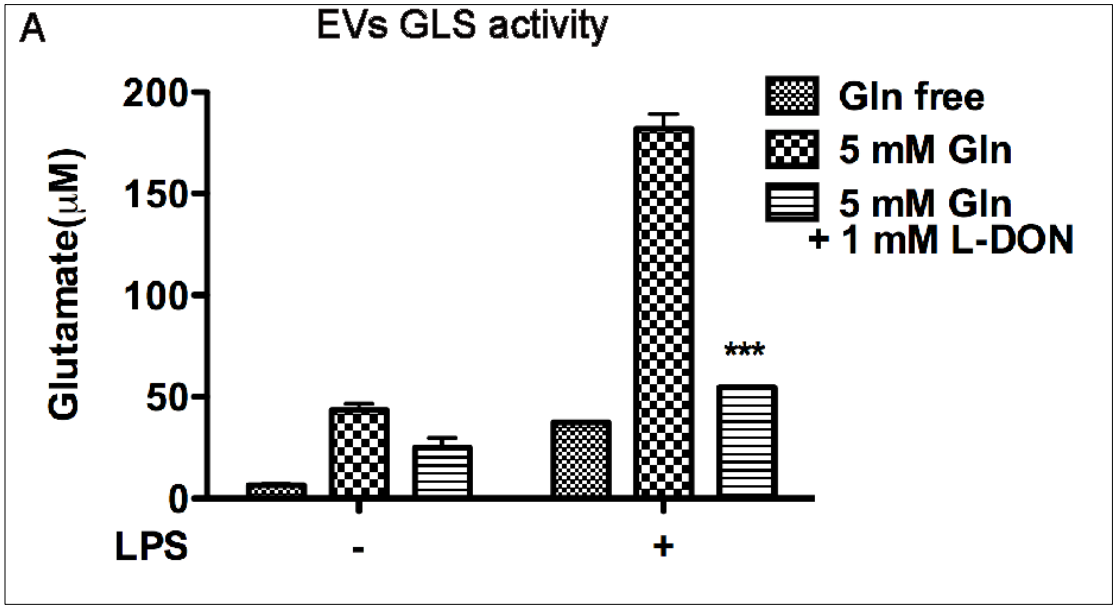
A
EVs GLS activity
Glutamate(μM)
200
150
100
50
0
LPS
-
+
***
Gln free
5 mM Gln
5 mM Gln
+ 1 mM L-DON

Figure 2.6 EVs isolated from immune-activated microglia mediate extracellular glutamate production through GLS1.

(A) EVs were isolated from cell-free supernatants from untreated and LPS-activated microglia and incubated with or without glutamine and 1 mM L-DON ex vivo for two days. Glutamate generation in EVs was determined by RP-HPLC. *** denotes $p < 0.001$ in comparison to 5 mM glutamine group in LPS-activated samples. Results are means ± SD of triplicate samples and are representative of three independent experiments. *** denotes $p < 0.001$ in comparison to 5 mM glutamine group in LPS-treated samples.

Figure 2.7

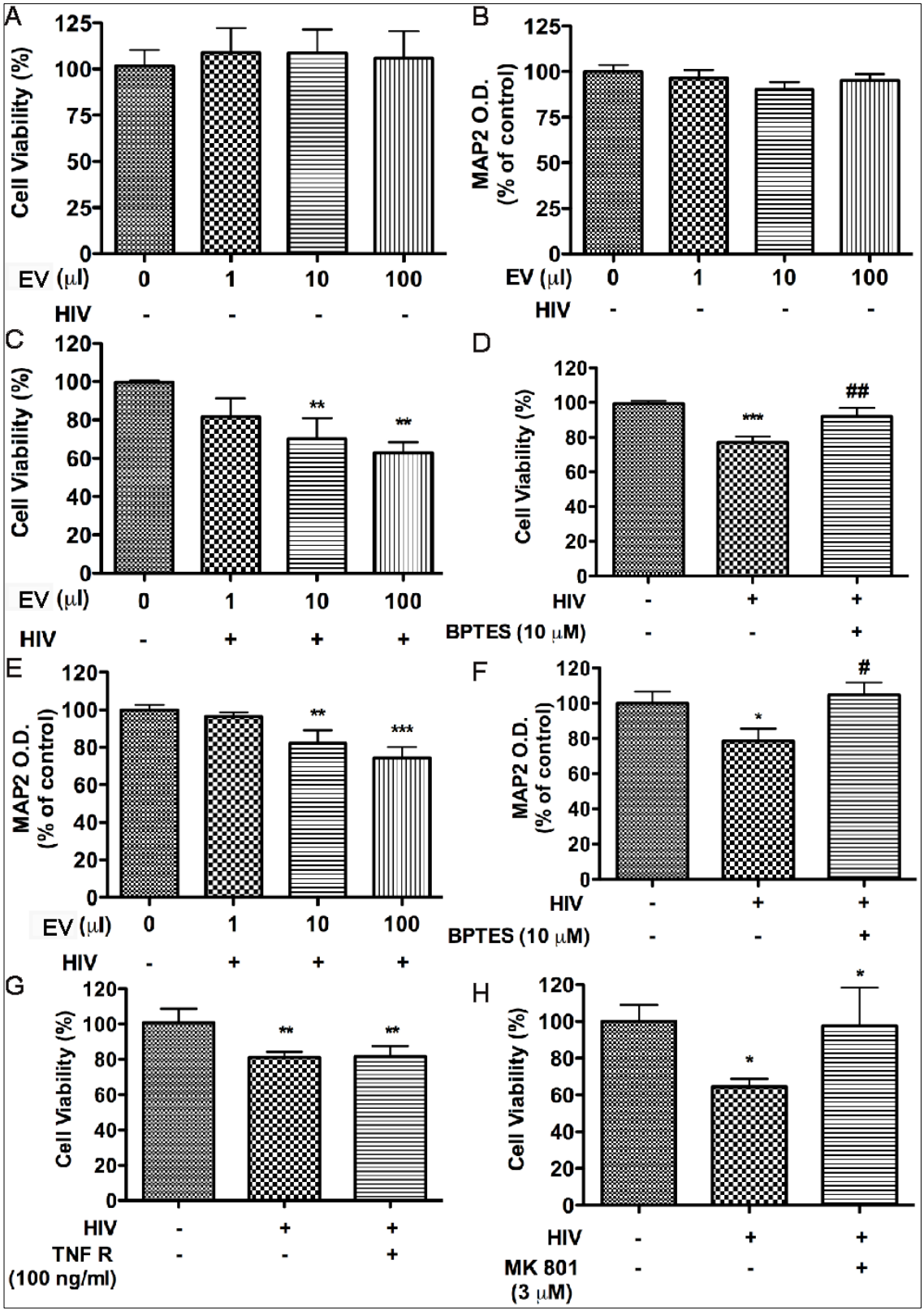
A
Cell Viability (%)
125
100
75
50
25
0
EV (μl) 0 1 10 100
HIV - - - -
B
MAP2 O.D. (% of control)
125
100
75
50
25
0
EV (μl) 0 1 10 100
HIV - - - -
C
Cell Viability (%)
120
100
80
60
40
20
0
**
**
EV (μl) 0 1 10 100
HIV - + + +
D
Cell Viability (%)
120
100
80
60
40
20
0
***
##
HIV - + +
BPTES (10 μM) - - +
E
MAP2 O.D. (% of control)
120
100
80
60
40
20
0
**
***
EV (μl) 0 1 10 100
HIV - + + +
F
MAP2 O.D. (% of control)
120
100
80
60
40
20
0
*
#
HIV - + +
BPTES (10 μM) - - +
G
Cell Viability (%)
120
100
80
60
40
20
0
**
**
HIV - + +
TNF R (100 ng/ml) - - +
H
Cell Viability (%)
120
100
80
60
40
20
0
*
*
HIV - + +
MK 801 (3 μM) - - +

Fig 2.7. GLS1-containing EVs from HIV-1-infected MDM induce neurotoxicity.

EVs were isolated from both mock-infected and HIV-1-infected MDM at 7 days post-infection. EVs were resuspended in neuron medium. Different volume of 0, 1, 10 and 100 µl of EVs from mock-infected (A, B) and HIV-1-infected (C) MDM were added to the RCN and incubated for 24 hours. 100 µl of EVs from mock-infected and HIV-1-infected MDM were added in RCN with or without 10 µM of BPTES, a GLS1 inhibitor, neutralizing TNF-α antibody or MK801 for 24 hours (C, F, G, H). Neurotoxic potentials of EVs were determined by MTT (C, D) and MAP2 ELISA assays (E, F). *, ** and *** denote $p < 0.05$, 0.01 and 0.001 in comparison to controls, respectively; #, ## and ### denote $p < 0.05$, 0.01 and 0.001 in comparison to HIV-infected group, respectively. Results are expressed as means ± SD of triplicate samples and are representative of three independent experiments.

Figure 2.8

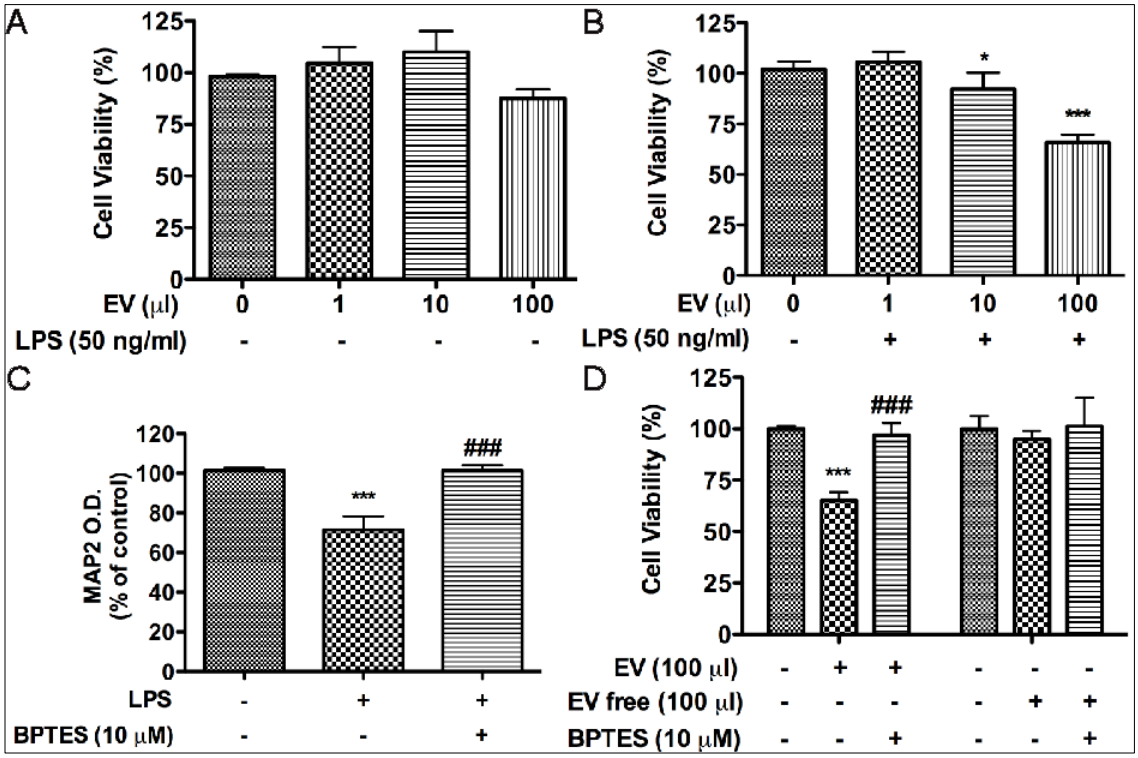
A
Cell Viability (%)
125
100
75
50
25
0
EV (μl) 0 1 10 100
LPS (50 ng/ml) - - - -
B
Cell Viability (%)
125
100
75
50
25
0
*
***
EV (μl) 0 1 10 100
LPS (50 ng/ml) - + + +
C
MAP2 O.D. (% of control)
120
100
80
60
40
20
0
***
###
LPS - + +
BPTES (10 μM) - - +
D
Cell Viability (%)
125
100
75
50
25
0
***
###
EV (100 μl) - + + - - -
EV free (100 μl) - - - - + +
BPTES (10 μM) - - + - - +

Fig 2.8. GLS1-containing EVs from immune activated microglia induce neurotoxicity.

(A-D) EVs were isolated from BV2 microglia cells treated with LPS overnight. EVs were resuspended in neuron medium. Different volume of 0, 1, 10 and 100 µl of EVs from control BV2 cells without LPS treatment (A) and LPS-treated (B) BV2 were added to the RCN and incubated for 24 hours. 100 µl of EVs were added in RCN with or without 10 µM of BPTES, a GLS1 inhibitor, for 24 hours (C). EV free supernatants after differential centrifugation were also collected and 100 µl of supernatants were added to RCN with or without 10 µM of BPTES for 24 hours. Neurotoxic potentials of EVs were determined by MTT (A, B, D) and MAP2 ELISA assays (C). * and *** denote $p < 0.05$ and 0.001 in comparison to controls, respectively; ### denotes $p < 0.001$ in comparison to LPS-treated group, respectively. Results are expressed as means ± SD of triplicate samples and are representative of three independent experiments.

Figure 2.9

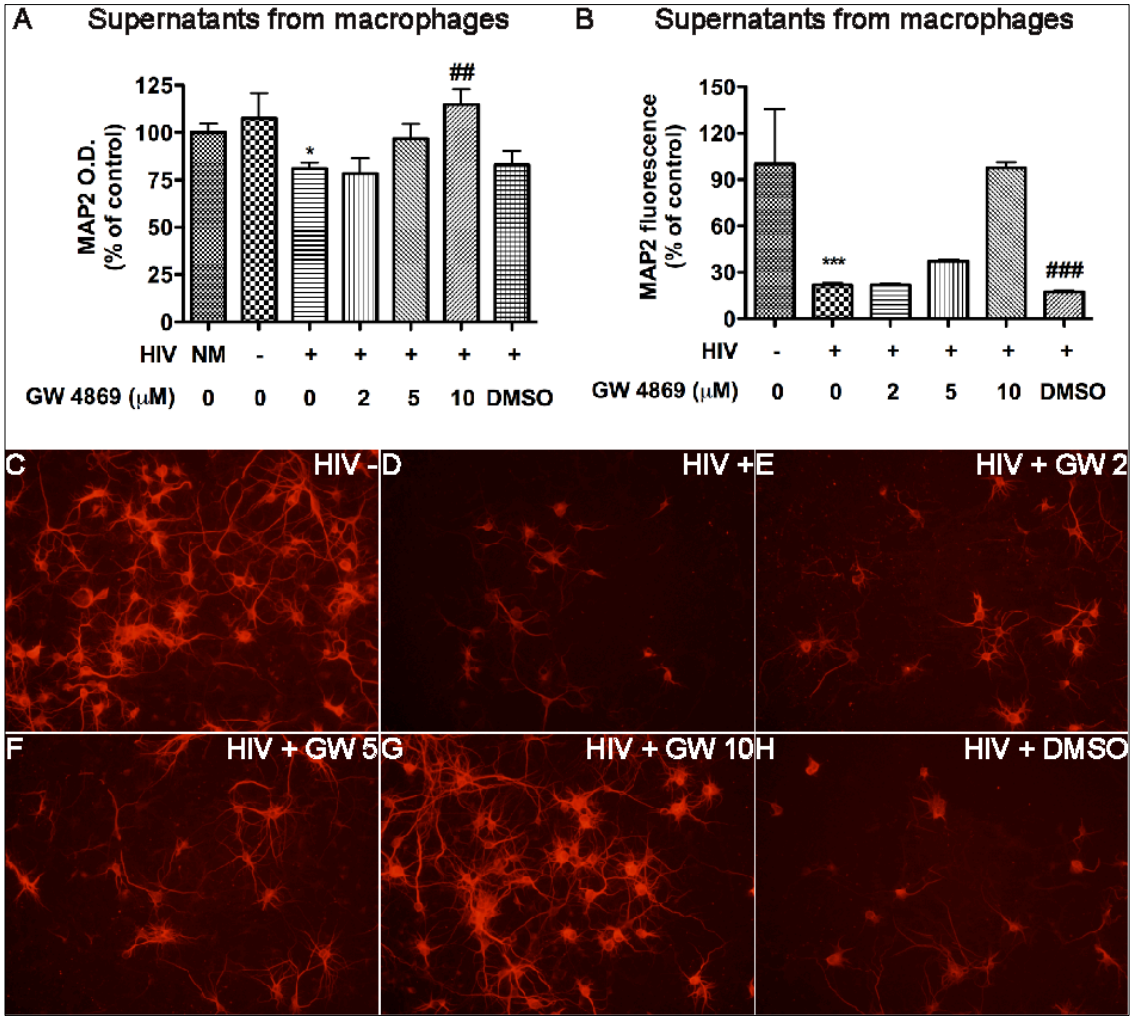
A
Supernatants from macrophages
MAP2 O.D. (% of control)
125
100
75
50
25
0
*
##
HIV NM - + + + + +
GW 4869 (μM) 0 0 0 2 5 10 DMSO
B
Supernatants from macrophages
MAP2 fluorescence (% of control)
150
120
90
60
30
0
***
###
HIV - + + + + +
GW 4869 (μM) 0 0 2 5 10 DMSO
C HIV -
D HIV +
E HIV + GW 2
F HIV + GW 5
G HIV + GW 10
H HIV + DMSO

Fig 2.9. HIV-1-infected macrophages induce neurotoxicity through GLS1-containing EVs.

At 7 days post-infection, mock-infected and HIV-1 infected macrophages were treated with GW4869 at different dosages for 24 hours. Cell-free supernatants and EVs were collected and added to RCN cultures for neurotoxicity. DMSO was used as solvent control for GW4869. **(A, B)** Neurotoxic potentials of the supernatants were determined by MAP2 ELISA assay (A) and quantification of MAP2 fluorescence in immunostaining (B). **(C-H)** Neurotoxic potentials of supernatants with EVs were determined by MAP2 immunostaining followed by quantification of the intensity of MAP2 fluorescence after EVs treatment (B). * and *** denote $p < 0.05$ and 0.001 in comparison to mock-treated control, respectively ; ## and ### denote $p < 0.01$ and 0.001 in comparison to DMSO-pretreated HIV-infected group, respectively. Results are expressed as means ± SD of triplicate samples and are representative of three independent experiments. Results are representative of 20 fluorescent images from three independent experiments.

Figure 2.10

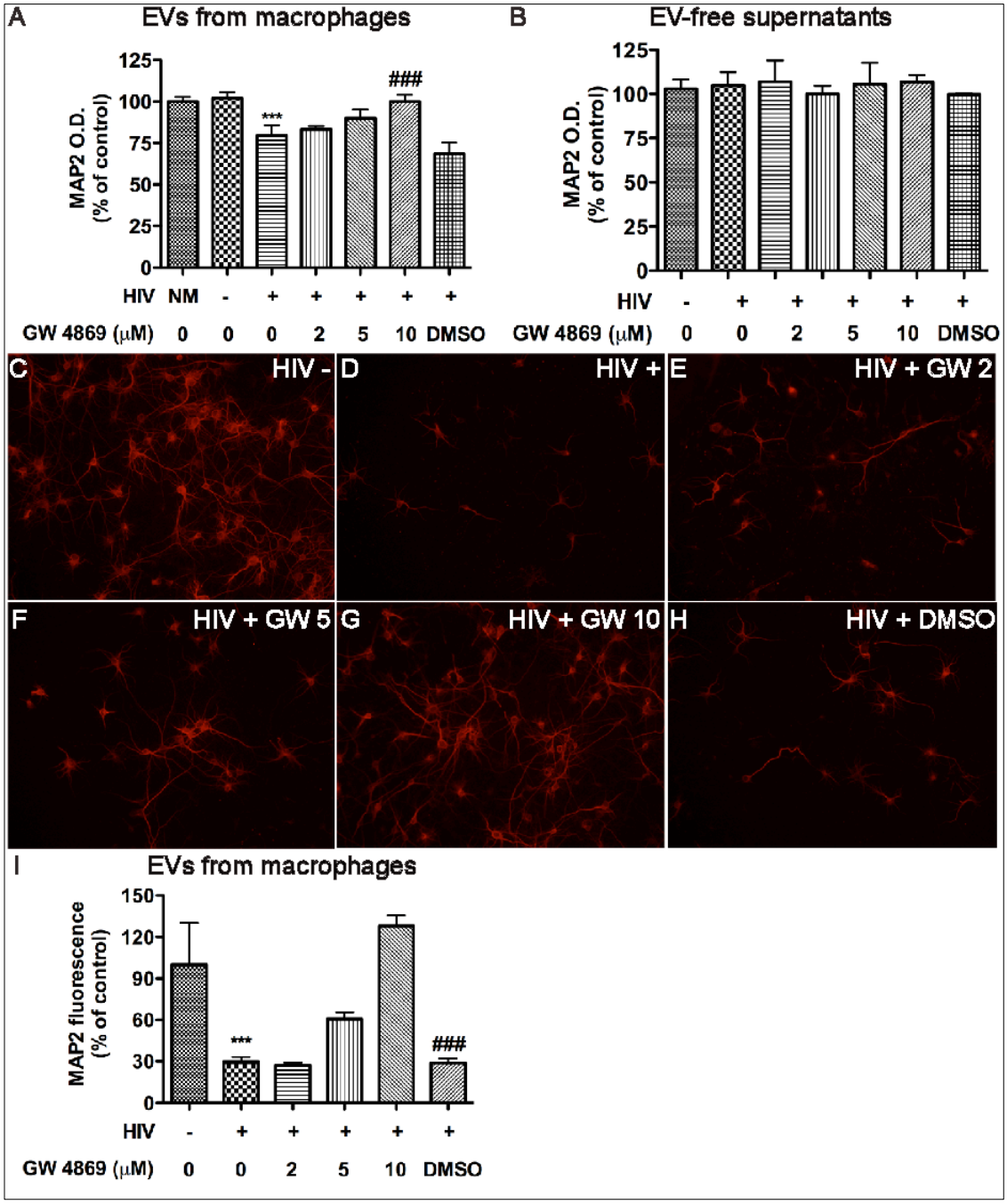
A
EVs from macrophages
MAP2 O.D. (% of control)
125
100
75
50
25
0
***
###
HIV NM - + + + + +
GW 4869 (μM) 0 0 0 2 5 10 DMSO
B
EV-free supernatants
MAP2 O.D. (% of control)
125
100
75
50
25
0
HIV - + + + + +
GW 4869 (μM) 0 0 2 5 10 DMSO
C HIV -
D HIV +
E HIV + GW 2
F HIV + GW 5
G HIV + GW 10
H HIV + DMSO
I
EVs from macrophages
MAP2 fluorescence (% of control)
150
120
90
60
30
0
***
###
HIV - + + + + +
GW 4869 (μM) 0 0 2 5 10 DMSO

Figure 2.10. HIV-1-infected macrophages induce neurotoxicity through GLS1-containing EVs.

At 7 days post-infection, mock-infected and HIV-1 infected macrophages were treated with GW4869 at different dosages for 24 hours. Cell-free supernatants and EVs were collected and added to RCN cultures for neurotoxicity. DMSO was used as solvent control for GW4869. **(A, B)** Neurotoxic potentials of EV (A) and EV free supernatants (B) were determined by MAP2 ELISA assay. **(C-I)** Neurotoxic potentials of EVs were determined MAP2 immunostaining (C-H) followed by quantification of the intensity of MAP2 fluorescence after EVs treatment (I). * and *** denote $p < 0.05$ and 0.001 in comparison to mock-treated control, respectively ; ## and ### denote $p < 0.01$ and 0.001 in comparison to DMSO-pretreated HIV-infected group, respectively. Results are expressed as means ± SD of triplicate samples and are representative of three independent experiments. Results are representative of 20 fluorescent images from three independent experiments.

Chapter 3

GLS1 are involved in the release of extracellular vesicles in activated macrophages and microglia

Abstract

Extracellular vesicles (EVs) are important in the intercellular communication in the central nervous system. Their release is increased during neuroinflammation and neurological disorders. Our previous data demonstrated an increased release of EVs from HIV-1-infected macrophages, and that these EVs have neurotoxic effects. However, the mechanism of elevation of EV release in those HIV-1-infected cells remains unknown. In our current study, we investigated glutaminase 1 (GLS1), which is a mitochondrial enzyme critical for glutamine metabolism. GLS1 is upregulated in HIV-1-infected macrophages and microglia. We propose that HIV-1 infection increases GLS1, leading to a metabolic status that favors the EVs generation and release. This new understanding of the metabolic control of EV release in HIV-1-infected cells will shed light on HIV-1 pathobiology and neurological complications.

Cultures of human primary microglia and monocyte-derived macrophages culture system and macrophage-tropic HIV-1_{ADA} were used to study the regulation of EVs during HIV-1 infection. EVs were isolated through differential centrifugations. A gene overexpression system, delivered via adenovirus vector, was utilized to overexpress GLS1 in the cell culture to mimic the upregulation of GLS1 during HIV-1 infection. A brain-specific GLS1 transgenic mouse line was created to model GLS1 elevation in vivo. BPTES was used to specifically inhibit GLS1 activity. Transmission electron microscopy and Western blot were used to quantify the EVs released from cells and brain tissues. Glutamate and glutamine

levels were determined by reverse phase high-performance liquid chromatography.

An elevated number of EVs was found in the supernatants of HIV-1-infected macrophages and microglia when compared with controls. Overexpression of GLS1 in macrophages and microglia cultures lead to increased release of EVs. Conversely, blocking the GLS1 activity by BPTES significantly reduced EV release and glutamate generation in HIV-1-infected macrophages and microglia, suggesting a critical role of GLS1 in EV release. Interestingly, we detected an elevated release of EVs in the brain tissues of GLS1 transgenic mice, suggesting that GLS1 is also important for EV release in vivo.

GLS1 is essential for EVs release in HIV-1-infected macrophages and microglia. Therefore, blocking EV release through GLS1 inhibitors may serve as a novel therapeutic strategy against the HIV-1 pathobiology and neurological complications.

3.1 Introduction

Glutaminase 1 (GLS1) is a metabolic enzyme located on the inner membrane of mitochondria, which deaminases glutamine into glutamate. GLS1 is known to be associated with cancer cell research and CNS disease [53, 173, 174]. GLS1 is the predominant glutamine-utilizing enzyme in the CNS, where GLS2 is expressed at a lower level [175].

In the past decade, our lab has focused on understanding the role of GLS1 in the brain using molecular and chemical tools. We have reported that GLS1 plays a role in microglia and macrophages and later in neurons during brain inflammation and injury [53, 112]. During HIV-1 infection and immune activation, glutamate level is excessively increased due to the upregulation of GLS1 [53, 72, 112, 149]. The elevated glutamate levels have been associated with the neuronal injury and excitotoxicity in various CNS disorders [102, 176, 177]. Interestingly, the upregulation of GAC in the postmortem brain tissue of HAND patients was identified [53, 112]. Recently, we also reported that extracellular vesicles (EVs) contain GLS1 from HIV-1infected macrophages and immune-activated microglia. We also reported that these EVs induce toxicity in neurons [178].

EVs are secretary vesicles derived from either cell membranes or multivesicular bodies that range from 50 nm up to 500 nm. In physiological conditions, EVs facilitate the cell-to-cell interactions between neurons and glial cells through the transfer of the neurotransmitter cargos. EVs have lipid bilayers, which protect their cargos from degradation via proteases and RNases [135, 155,

160]. However, in response to stress, such as DNA damage, hypoxia, exposure to viruses or bacteria, the release of EVs increases and the contents within the EVs alter as well. As EVs can be detected in a variety of biological fluids such as plasma and cerebral spinal fluid (CSF), they are prime candidates for biomarkers of diseases [167].

EVs have been detected at an elevated level in the cerebral spinal fluid in patients with mild to severe AD, PD, prion disease and ALS [163, 179]. More importantly, protein markers of EVs are present in neuritic plaques in AD brains. This evidence suggests that EVs play a potential role in the pathogenesis of neurodegenerative diseases and neuroinflammation. Moreover, the defective metabolism of sphingolipids in the brain has been associated with EV release. Studies have reported that sphingolipids are increased in different regions of AD brains and may promote Aβ biogenesis [180]. Studies have shown that the neutral sphingomyelinase (nSMase) inhibitor, GW4869 significantly reduces the release of EVs and its neurotoxicity in HAND and AD [178, 180]. However, upon all evidence, it remains unclear what the mechanism of EV regulation is.

Aside from *in vitro* models, our lab has developed a new mouse line to overexpress GAC in the mouse brain to mimic the pathogenesis during HAND, which is competitive with the other available murine models for HAND, including HIV-1 glycoprotein 120 (gp120) transgenic mouse, the HIV-1 encephalitic (HIVE) mouse, HIV-Tat transgenic mouse and the humanized mouse [181], [182-184]. However, none of these HAND models was able to demonstrate the role of GLS1 in the pathogenesis of HAND. The successful generation of the GAC-

overexpressing mice demonstrates an increase of brain inflammation, neuronal damage and learning and memory deficits. This mouse model also provides a strong *in vivo* tool to study the role of GLS1 in EV regulation.

3.2 Materials and Methods

Culture, HIV-1 and LPS infection of macrophages and microglia

Human peripheral blood-derived mononuclear cells were isolated through leukopheresis from healthy donors. Human macrophages were differentiated in Dulbecco's Modified Eagle's Media (DMEM) (Sigma Chemical Co., St. Louis, MO) with 10% human serum, 50 µg/ml gentamycin, 10 µg/ml ciprofloxacin (Sigma), and 1,000 U/ml recombinant human macrophage colony-stimulating factor (MCSF) for 7 days. Human fetal microglial cells were obtained from fetal brain tissue-derived microglia-astrocytes mixed cultures as previously described [185]. The HIV-1_{ADA} strain was used to infect the macrophages and microglia at a multiplicity of infection (MOI) of 0.1 and 0.5, respectively. After 24 hours, culture medium was changed to remove any remnant virus. Seven days after HIV-1-infection, culture medium was changed to glutamine-free neurobasal medium for 24 h and supernatants were collected for subsequent HPLC or Western blot analysis. HeLa and BV_2 cell lines were obtained from ATCC, and both cell lines were grown in DMEM with 10% fetal bovine serum and antibiotics. Lipopolysaccharide (LPS) was used to immune activate BV_2 cells for 24 h and supernatants were collected for HPLC and Western blot analysis. Bis-2-(5-phenylacetamido-1,2,4-thiadiazol-2-yl)ethyl sulfide (BPTES) (a generous gift presented by Dr. Tsukamoto from John Hopkins and later ordered from Millipore) at a concentration of 10 μM were added to HIV-1-infected macrophages or LPS-treated microglia prior to EV isolation. All experiments involving human cell

samples are approved by Institutional Review Board of University of Nebraska Medical Center.

GAC-overexpressing mice

Mouse *Gac* gene was selected and cloned from a C57 mouse cDNA library. The *Gac* gene was then inserted into the pCAG-Loxp-STOP-Loxp-IRES-LacZ plasmid at restriction enzyme site Xhol. The plasmid was constructed and sequenced specially for forwardly inserted *Gac.* The linearized plasmid was selected and microinjected into the fertilized eggs for the further implantation into a pseudopregnant female to create CAG-loxp-GAC mouse in the Mouse Genome Engineering Core Facility of UNMC. The stability of the constructed plasmid was examined through visualizing the GFP expression in the CAG-lloxp-GAC mice brains. Four weeks old *nestin* promoter-driven *cre* transgenic mice (Nestin-Cre mouse) line was purchased from Jackson laboratory (Bar Harbor, ME), where the *cre* activity is only restricted to CNS. The CAG-loxp-GAC mice were then mated with Nestin-Cre mice. Nestin-GAC mice were produced and the absence of GFP was examined to ensure the success of the generation of GAC-overexpressing mice. Similarly, Thy-1 promoter-driven *cre* transgenic mice were used to mate with the CAG-loxp-GAC mice to generate Thy-1-GAC mice. DNA was extracted from embryonic tissue or adult mouse tail tissue with phenol/chloroform. DNA was then purified using isopropanol and ethanol. PCR reactions were conducted to genotype all transgenic mice. All mice were housed and bred in the Comparative Medicine facilities of the University of Nebraska

Medical Center. All procedures were conducted according to protocols approved by the Institutional Animal Care and Use Committee of the University of Nebraska Medical Center.

Morris Water Maze (MWM) test

The training phase and probe phase are the two major parts in MWM test. Mice were introduced into a 91 cm circular water tank, which was equally divided into four quadrants. Visual cues were placed around the pool to direct mice to the submerged 10 cm circular platform. A variety of parameters were recorded to evaluate the movement of the mice. For each trial, the mouse was given 60 seconds to find the submerged platform before guided to the platform. Each mouse completed four trials per day during a 5-day training phase. On the 6th day, the probe test was conducted. The platform was removed and each mouse was given 60 seconds to swim in the tank. The parameters were videotaped and analyzed by Ethovision XT (Noldus, Netherlands).

Contextual Fear Conditioning (CFC) test

Contextual fear conditioning test was performed following standard protocols in the light- and sound-attenuated chambers for mouse (Coulbourn Tru Scan Activity Monitoring System for mouse). On the 1st day of the test, mice were allowed to habituate in the clean chamber for 300 seconds without any stimulation. On the 2nd day, the chamber was scented with 0.1% acetic acid and the mice were given two electric shocks at 170 s and 290 s via automated Tru

Scan Stimulus. On the 3rd day, the chamber was scented with 0.1% acetic acid without shock stimulus. Mice in the chamber were recorded for 180 s. Mouse behavior was evaluated under ambient illumination (room light) and was recorded by a SAMSUNG digital videocamera above the chamber. The behavior recorded was analyzed by Ethovision XT by assessing the time of freezing.

Preparation of adenovirus overexpressing glutaminase

KGA and GAC were cloned into a Shuttle Vector and Replication-defective adenovirus vectors expressing human KGA and GAC were generated by the RAPAd® Adenoviral Expression System (Cell Biolabs, Inc. San Diego, CA 92126) following the manufacturer's instruction. Adenoviral constructs were amplified in a 293AD cell line (Cell Biolabs, Inc) and purified by ultracentrifugation through a CsCl gradient. Quantification of the adenoviral infectious unit was performed using Adeno-X™ Rapid Titer Kit (Clontech Laboratories, Inc. Mountain View, CA 94043). HeLa cells, BV_2 cells, or primary human microglia were infected at a multiplicity of infection of 50. Cells were used for experiments 2 days after infection.

Isolation of EVs from cells

EVs were isolated from the supernatants of GLS1-overexpressing cells, HIV-1-infected macrophages and LPS-activated microglia through differential centrifugations. Briefly, the supernatants were first centrifuged at 300 X g for 10 min to remove free cells, at 3,000 X g for 20 min to remove cellular debris and

then 10,000 X g for 30 min to remove free organelles. Lastly, EVs were collected by ultracentrifugation at 100,000 X g for 2 h at 4°C. To prepare EVs for Western blotting, the EV pellets were lysed in M-PER mammalian protein extraction reagent (Thermo Scientific, Pittsburgh, PA). For negative staining, EVs were fixed in 2% glutaraldehyde and 2% paraformaldehyde. For glutaminase activity assay and neurotoxicity, the EVs were resuspended in 1 ml of glutamine-free neurobasal medium.

Isolation of MVs from mice brain

EV isolations from the brains were carried out as described previously with modifications according to the protocol [186]. Fresh and previously frozen mice hemibrains were harvested and dissected finely. Brain samples were then treated with 20 units/ml papain (Worthington) in Hibernate E solution (BrainBits, Springfield, IL) for 15 minutes at 37 °C. The same volume of cold Hibernate E solution was added to the brains samples to stop the reaction of papain. The brain tissue was then gently homogenized and filtered through a 40-μm mesh filter (BD Biosciences), followed by a centrifugation at 300 X g for 10 min and, 3000 X g for 20 min at 4 °C to get rid of cells, membranes and debris. After the supernatants were filtered through 0.45 μm filter (Thermo Scientific), they were subjected to 10, 000 X g for 30 min at 4 °C to eliminate organelles contaminations. The supernatants were further centrifuged at 100, 000 X g for 70 min at 4 °C to pellet EVs. The pellets were then resuspended in filtered PBS, or MPER lysate solution for Nanosight or Western blot. All the samples were

ultracentrifuged in ultraclear polycarbonate tubes (Beckman Coulter) that have a volume of 13.2 ml. A Beckman Coulter ultracentrifuge (Beckman Coulter OptimaL-90K ultracentrifuge; Beckman Coulter, Fullerton, CA, USA) was used with a rotor type 41 wi.

Negative staining and electron microscopy

EVs were fixed and then spread on the silicon monoxide and nitro-cellular film coated copper grid. The droplets were removed with filter paper, air-dried at room temperature and then subjected to transmission electron microscopy (TEM). For scanning electron microscope (SEM), cells were fixed in 2% glutaraldehyde and 2% paraformaldehyde and point dried, mounted and coated with gold/palladium.

Nano-particle tracking analysis

NanoSight NS 300 (Malvern) equipped with an sCMOS camera was utilized to analyze the size distribution and concentration of EVs. NanoSight utilizes Nanoparticle Tracking Analysis (NTA), which is a combination of light scattering and Brownian motion to measure the concentration and size distribution of particles in the EV supernatants. After the whole process of EV isolation, the pellets were first resuspended in 100 μl of filtered PBS and then diluted by 100 times. The conditions of the measurements include a temperature of 25 °C, viscosity of 1 cP, 25 seconds per capture frame and a measurement time of 60 s. All the conditions were kept the same among all the samples. The results

indicate the mean sizes and concentration of at least three individual measurements.

Toxicity/MTT/MTS assays

GLS1 inhibitors were added to HIV-1-infected macrophage or LPS-activated microglia cultures and cell viability was assessed by MTT assays in 24-well or 96-well plates. MTT (Sigma) was added to the cultures to a final concentration of 125 μg/ml. The plates were incubated for 30 minutes at 37 °C with 5% CO2 and the medium was aspirated. The insoluble formazan was solubilized in DMSO, and the concentrations were determined by optical density at 490 nm with an ELX808 densitometer (Bio-Tek Instruments, Winooski, and VT). Alternatively, Celltiter aqueous one solution cell proliferation assay, which contains a novel tetrazolium compound [3-(4,5-dimethylthiazol-2-yl)-5-(3-carboxymethoxyphenyl)-2-(4-sulfophenyl)-2H-tetrazolium (MTS) (Promega) was utilized to assess cell viability according to the manufacturer instruction. Briefly, 20 μl of reagent was added into a 100 μl of culture medium, and then incubated the plates in a humidified, 5% CO2 and 37 °C atmosphere for 1 hour. The absorbance was determined at 490 nm.

Western blot

Protein concentrations were determined by Bradford protein assay. SDS PAGE separated proteins from whole cell and EVs lysates. After electrophoretically transferred to polyvinyldifluoridene membranes (Millipore,

Billerica, MA and Bio-Rad, Hercules, CA). Membranes were incubated overnight at 4 °C with polyclonal antibodies for KGA and GAC (Dr.N.Curthoys, Colorado State University, Fort Collins, CO), tissue transglutaminase (tTG) (Lab Vision/Thermo, Fremont, CA), flotillin-2 (Cell Signaling Technology, Danvers, MA) and β-actin (Sigma-Aldrich, St. Louis, MO), followed by horseradish peroxidase-linked secondary anti-rabbit or anti-mouse secondary antibodies (Cell signaling Technology). Antigen-antibody complexes were visualized by Pierce ECL Western Blotting Substrate. For quantification of the data, films were scanned with a CanonScan 9950F scanner and images were analyzed using the public domain NIH image program (developed at the U.S. National Institutes of Health and available on the internet at http://rsb.info.nih.gov/nih-image/).

Glutaminase activity assay

Highly concentrated whole cell lysates were collected from flasks and subjected to GLS activity assay using a two-step assay [187, 188]. Briefly, protein concentrations in the lysates were tested by using BCA Protein Assay Kit (Pierce). All samples were normalized to same concentration. In the first step, fifty milligrams of protein was added to 100 μL of initial assay mix. The mix contains 50 mM glutamine, 0.15 M phosphate, 0.2 mM EDTA, and 50 mM tris-acetate. The PH value of the mix was adjusted to 8.6 and incubated at 37 °C for 30 min. 10 μL of 3 N hydrochloric acid (HCl) was added to inactivate the glutaminase activity and stop the reaction. In the second step, 1 mL of the second reaction mix was added, which contained 0.4 mg of purified bovine liver

glutamate dehydrogenase (Sigma-Aldrich, St. Louis, MO, USA), 0.08 M Tris-acetate at pH 9.4, 0.2 M hydrazine, 0.25 mM ADP (adenosine 5'-diphosphate sodium salt), and 2 mM NAD (β-nicotinamide adenine dinucleotide hydrate). The samples were mixed and incubated for 30 min at room temperature. 100 µL of reaction was used for measurement and absorbance was determined at a wavelength of 340 nm, glutamate concentration was determined using a standard curve of 10, 5, 2.5, 1.25, 0.625, and 0.0 mM glutamate, along with negative controls.

Analysis of extracellular glutamate and glutamine by RP-HPLC

Glutamate levels were analyzed by RP-HPLC using an Agilent 1200 liquid chromatograph and fluorescence detector as previously described [14] with a few modifications. The experiments utilized 4.6 × 75 mm, 3.5 μm ZORBAX Eclipse AAA analytical columns (Agilent). A gradient elution program was optimized for glutamate measurement with a flow rate 0.75 ml/min.

Analyses of intracellular glutamate concentrations

The intracellular glutamate levels in whole brain lysates of mice and whole cell lysates were determined by Amplex Red Glutamic acid/Glutamate Oxidase Assay Kit (Invitrogen) based on the manufacturer's instruction. Brain tissue lysates and whole cell lysates were diluted to the same protein concentration before the assay.

Statistical analysis

Data are expressed as means ± SD unless otherwise specified. Statistical analysis was performed using one way ANOVA, followed by the Tukey-post-test for paired observations or two way ANOVA using Bonferroni post-tests to compare replicate means. Significance was determined by a p value < 0.05. All experiments were performed with cells from at least three donors to account for any donor-specific differences. Assays were performed at least three times in triplicate or quadruplicate within each assay.

3.3 Results

GLS1 overexpression increases EVs release in vitro.

The molecular mechanism(s) for EV release in HIV-1-infected macrophages remain unclear. Our previous reports showed that GLS1 was upregulated and caused increased glutamate production in HIV-1-infected macrophages [112]. To further study the mechanism of GLS1 and EV release, we constructed adenovirus vectors that overexpressed KGA or GAC to mimic the upregulation of these isoforms during HIV-1 infection. The extracellular levels of glutamate increased significantly in both KGA- and GAC-overexpressing HeLa cells at the multiplicities of infection (MOI) of 200 compared with uninfected or vector-treated cells (Fig. 3.1A). An MOI of 200 was then used for the following GLS1-overexpression experiments. The overexpression of KGA and GAC were confirmed by Western blot (Fig. 3.1B). GLS1 enzyme activity assay confirmed increased KGA and GAC activity in concentrated protein lysates from KGA- and GAC-overexpressing HeLa cells, suggesting that the overexpressed KGA and GAC were functional (Fig. 3.1C). Furthermore, protein lysates were utilized to test the intracellular glutamate. The level of glutamate was increased after KGA- and GAC-overexpression compared with GFP and control group (Fig. 3.1D). Consistently, supernatants were collected from each group and cell debris was removed. Samples were subjected to RP-HPLC after acid and base treatment to determine the extracellular level of glutamate. Both KGA and GAC overexpression showed increased glutamate in the supernatants (Fig. 3.1E).

Next, we looked at GLS1 activities in the extracellular fluid of the KGA- and GAC-overexpressing HeLa cells. Previously, we reported that GLS1 was released from the inner membrane of mitochondria in the cytosol in HIV-1-infected macrophages [111]. However, whether elevation of GLS1 levels induces GLS1 translocation or release remains unclear till we proved that GLS1 activity was previously detected in the EVs [178]. Consistently, using KGA and GAC overexpression, cell-free supernatants showed increased glutamate production after addition of glutamine. Furthermore, GLS1 inhibitor, L-DON, blocked the excess generation of glutamate in the overexpression supernatants, indicating that GLS1 activity was present in the extracellular supernatants from KGA- and GAC-overexpressing HeLa cells (Fig. 3.2A). To confirm that glutaminase is released from cytosol to extracellular space via EVs in GLS1 overexpression, EVs were collected from cell-free supernatants and tested for glutaminase activity. EVs that were isolated from KGA- or GAC-overexpressing HeLa cells generated significantly higher levels of GLS1 when incubated with glutamine (Fig. 3.2B). When L-DON was added to the enzyme reactions, the generation of glutamate was blocked, suggesting that KGA- and GAC-overexpression induced EVs release that contain high levels of GLS1 activities (Fig. 3.2B). Due to the limited protein extracted from EVs, extracellular glutamate level was measured using RP-HPLC to test the levels of GLS1 activities instead of the traditional GLS1 activity enzyme assay. Furthermore, proteins from EVs showed increasing EV markers, tTG and flotillin-2 in KGA- and GAC-overexpressing HeLa cells with elevated expression of KGA and GAC in the lysates of MVs (Fig. 3.2C-E).

However, the level of EV markers in the whole cell lysates did not change (Fig. 3.2C-E). Together, these data suggest that elevation of GLS1 is sufficient to induce the extracellular release of GLS1-containing EVs.

Inhibition of GLS1 activity reduces EVs release in HeLa cells.

When treated with EGF, HeLa cells release more EVs to the extracellular fluid [189]. Moreover, EGF has been reported to increase the activity of GLS1. Therefore, the increase of GLS1 activity by EGF triggers the EVs from HeLa cells indicated that the alteration of GLS1 could be a potential mechanism of EVs release. To investigate the effect of the GLS1 inhibitors on GLS1 level in whole cells, and to further explore the impact of GLS1 inhibitor on EV release, both 10 μM BPTES, 30 μM carbenoxolone (CBX) or 100 μM L-DON were treated 24 hr prior to EV isolation. EVs were collected through differential centrifugation and lysed for Western blot. To compare the amount of EV released, the concentration of whole cell lysates was measure to normalize to the volume of EVs according to the concentration of whole cells. The level of EV markers, flotillin-2 and CD9, were decreased under Western blot, indicating a potential inhibition of EV release by the GLS1 inhibitors compared with the endogenous levels of GLS1 in HeLa cells (Fig. 3.3 E-G). This evidence suggests that blocking GLS1 significantly reduces the release of EVs in HeLa cells.

Inhibition of GLS1 activity reduces EV release in HIV-1-infected macrophages and immune-activated microglia.

In HIV-1-infected macrophages or immune-activated microglia, GLS1 expression is upregulated and EV release is increased [178]. To further investigate whether GLS1 inhibitor can affect the level of EV release in macrophages, human macrophages were infected with HIV-1 virus with 10 μM BPTES prior to harvest or 5 μM Atazanavir (AZT) on the second day of infection. Whole cell lysates were collected to detect the expression level of the GLS1 isoform, GAC. The treatment of AZT, which inhibits the HIV-1 viral replication, significantly decreased the level of GAC that was upregulated during HIV-1 infection. The addition of BPTES in HIV-1-infected macrophages didn't reduce the protein level of GAC (Fig 3.4A, B). Interestingly, when BPTES was added one day after HIV-1 infection, or one day prior to EV isolation, EV lysates showed a decreased level of EV markers, Flotillin-2 and tTG from HIV-1-infected macrophages. However, when BPTES was added immediately after the HIV-1 infection, the result of EV release was not affected, indicating BPTES affect the EV release in a short-term manner (Fig 3.4C-F).

To test the effect of GLS1 inhibitors on microglia, we used a murine microglial cell line, BV2 and human microglia cells. When GLS1 inhibitors, 10 μM BPTES, or 10 μM CB839 were added to BV2 cells 4 hours prior to LPS treatment for overnight, GLS1 inhibitors did not reduce cell viability (Fig. 3.5A). The results from GLS enzyme activity assay showed an increased GLS activity in the LPS-activated BV2 cells but a decreased GLS activity with the treatment of BPTES and CB839 (Fig 3.5B). The inhibition of the GLS activity in LPS-stimulated BV2 cells is stronger in the group treated with CB839 than the group treated with

BPTES. Both whole cell lysates and EV lysates were collected and subjected to Western blot. The ratio of GAC to β–actin showed no significant change. However, EV markers in the EV lysates showed an increase trend after LPS treatment and a decrease trend after the treatment of BPTES and CB839 (Fig 3.5C-G). When the EVs were isolated, PBS priorly filtered through 0.22 μm PVDF filter was used to resuspend EV pellets and 10 μl EV was added to 990 μl PBS. One hundred times diluted EVs were then subjected to nanoparticle tracking analysis. LPS treatment group showed an increased EV particle concentration from BV2 cells. Interestingly, the treatment of BPTES and CB839 both reduce the EV concentrations, which is consistent to the results in Western blot (Fig 3.5B).

To further verify this effect in human microglia, EVs were isolated from LPS-treated human microglia with or without BPTES. Both EV markers, Flotillin-2 and CD9 showed an increased level of EV release after LPS treatment but a decrease after 10 μM BPTES treatment (Fig 3.6A-C).

Consistently, these results indicated that GLS1 inhibitors block the release of EVs in HIV-1-infected macrophages and LPS-treated microglia.

Brain-specific GLS1 overexpression increases EVs release in vivo.

To further investigate the release of EVs in vivo, Nestin-GAC and wild type (WT) were generated by crossing Nestin-Cre mice and CAG-loxp-GAC mice and PCR reactions were performed to confirm the genotypes of the mice (Fig. 3.7A). To first confirm the changes in behaviors that are related to the learning and

memory functions, Nestin-GAC mice of 8 weeks old and control littermates were first subjected to Morris-Water-Maze (MWM) test and Cued-Contextual Fear Conditioning (CFC) test. During MWM test, Nestin-GAC mice tended to spend more time and travel a longer distance to reach the target platform and the speed of swimming didn't change compared with WT control from training phase to probe test. Overall, the Nestin-GAC mice had fewer crossings over the platform area when the platform was removed on the probe test day than WT control (Fig 3.7B). Interestingly, in the CFC test, Nestin-GAC mice showed less freezing in the percentage compared with WT control on the probe test day (Fig 3.7C). These results indicate that Nestin-GAC mice have impaired learning and memory related to hippocampal and cortical functions. After the behavioral tests, groups of mice were sacrificed, half of the brain of each mouse was subjected to EV isolation, and the other half was lysed to extract total proteins. The proteins from the kidney of both Nestin-GAC mice and the WT control mice were also collected as controls. The protein levels of GAC in the brain from Nestin-GAC mice were significantly higher than that from control littermates (Fig 3.7D, E). Intracellular glutamate levels were higher in Nestin-GAC brain lysates but the same in the kidney, indicating GAC overexpression is only limited to the mouse brain (Fig 3.7F). Furthermore, proteins were extracted from different regions of the brains of Nestin-GAC mice and WT control. The levels of intracellular glutamate were consistently higher in the hippocampus, cortex, midbrain and cerebellum (Fig 3.7G). Altogether, these results confirmed the GAC overexpression in the Nestin-

GAC mouse brain and demonstrated significant learning and memory deficits that are similar to the HAND model.

EVs were isolated and purified from hemibrains of both WT and Nestin-GAC mice through the specifically developed/modified protocol [186]. The expression levels of EV markers, Alix and Flotillin-2 were both increased using Western blot from Nestin-GAC mice compared with WT mice (Fig. 3.8A-C). Similarly, EVs extracted from Thy1-GAC mice, which is another breed of GAC overexpressing mouse model, were also increased compared with WT control using negative staining by TEM (Fig.3.8D-F). Excitingly, these data indicate that the brain-specific GAC overexpression increases EVs release *in vivo*.

3.5 Discussion

Chronic neuroinflammation is a hallmark in the pathogenesis of neurodegenerative diseases including HAND, Alzheimer's disease, Parkinson's disease, multiple sclerosis and amyotrophic lateral sclerosis [48, 49, 51, 86]. HIV-infected or immune activated macrophages and microglia play a pivotal role in brain inflammation and neuronal injury through the release of various soluble neurotoxic factors including glutamate [49, 71, 74, 78, 190].

We have previously reported that the upregulation of GLS1 in activated macrophages and microglia significantly induce neurotoxicity through the excess production of glutamate [53, 72, 112]. It is also reported that the mitochondrial GLS1 was translocated from the inner membrane of mitochondria to the cytosol upon the oxidative stress induced by HIV-infection or immune activation. Furthermore, the release of GLS1 from cytosol to extracellular milieu was proven to be dependent on EVs, which induce excitotoxicity in neurons [178]. However, a remaining key question is how the EVs are formed, released and regulated. The study in this chapter presents two major findings regarding EV release. First, the upregulation of GLS1 induces increasing release of EVs in HIV-1-infected and immune-activated macrophages and microglia. Second, the increasing release of EVs in GAC-overexpressing mice is associated with the learning impairment and neuronal injury. These observations suggest that GLS1 could be a key component in the regulation of EV release, which could be essential in the mechanism study of EVs.

The pathogenic role of GLS1 in neurodegeneration has been closely associated with clinical implications. Dysregulation of GLS1 has been reported not only in the pathogenesis of HAND, but also in cancer proliferation and metastasis. The increasing release of GLS1 could be crucial in causing the prolonged brain inflammation, increased neuronal injury and worsening disease progression in HAND. GLS1 is a key enzyme in the glutamine metabolism, where glutamate is produced and functions in glutamate signaling and synaptic plasticity [191-195]. The dysregulation of GLS1 causing the aberrant release of glutamate is strongly associated with the memory loss and learning deficits due to disrupted functioning of NMDA receptors [194-196]. The impaired glutamate transporter in the neighboring astrocytes to take up extra glutamate during HIV-1 infection further emphasizes the essential pathogenic role of GLS1 [87, 88]. Taken together, the neurotoxic role of GLS1-containing EVs raised more attention to the study.

To further study the role of GLS1, a new adenovirus was constructed to overexpress both GLS1 isoforms to mimic the upregulation of GLS1 during HIV-1 infection or immune activation. Both KGA- and GAC- overexpressing HeLa cells displayed significantly increased GLS1 enzyme activity. Together with the increasing levels of intracellular and extracellular glutamate, the GLS1 overexpression *in vitro* was proven successfully. Due to low protein concentration and low yield of EVs, it is difficult to conduct GLS enzyme activity assay. Instead, EVs were collected from GLN-free supernatants and incubated with or without GLN or GLS1 inhibitor. The glutamate level is measured by RP-HPLC, which can

also provide the indication of GLS1 activity in the EVs. GLS1 activity was detected in both the supernatants and EVs portions from the KGA- and GAC-overexpressing HeLa cells. Furthermore, an increasing level of EV markers, tTG and flotillin-2 were detected using Western blot. The absence of mitochondrial markers, cytochrome c, VDAC, GM130, PMP70, and Calreticulin exclude the contamination of mitochondria, Golgi, peroxisomes, and ER in the EVs after isolation. Interestingly, when HeLa cells were treated with GLS1 inhibitor, BPTES, CBX and CB839, the release of EVs were significantly reduced. Similar results were also observed in the HIV-1-infected macrophages and LPS-treated microglia when GLS1 inhibitors were added. That release of EVs was reversed by the GLS1 inhibitors suggests that the level of GLS1 regulates the release of EVs.

Aside from the evidence *in vitro,* we also generated a novel mouse model to overexpress GAC *in vivo*, which demonstrated upregulated GLS1 and elevated glutamate in the whole brain, hippocampus, cortex, midbrain, and cerebellum. The mice also displayed increased reactive astrogliosis, neuroinflammation and learning and memory deficits. We also found that the release of EVs is consistently increased in two GAC-overexpressing models, Nestin-GAC and Thy1-GAC mice. However, it needs to be further investigated whether GLS1 inhibitors can block the EV release *in vivo* and whether the blocking of EVs in GAC-overexpressing can attenuate the elevated neuroinflammation and neuronal injury.

Further investigation is needed to elucidate the mechanism of how GLS1 is regulating the EVs. It is also unclear whether the level of GLS1 in the EVs affects the regulation of EV release. By inhibiting GLS1 activity, CBX has been a newly discovered GLS1 inhibitor that can reduce the release of EVs (manuscript in preparation). Because the GLS1 is important in the glutamine metabolism and EVs have been reported to be associated with sphingolipids, including ceramide, it is possible that GLS1 is regulating the EV release through both metabolisms and their connection in this regulation.

3.6 Conclusion

In summary, the studies in this chapter address the importance of GLS1 in the regulation of EVs, which implicate a crucial role of GLS1. Our new understanding of how GLS1 regulates the release of EVs *in vitro* and *in vivo* has a potential clinical implication in neurologic diseases such as HAND and neuroinflammation and also cancer research. The effective inhibition of EV release using GLS1 inhibitors sheds lights on developing potential therapeutic targets in GLS1-EVs related diseases.

3.7 Tables and Figures

Figure 3.1

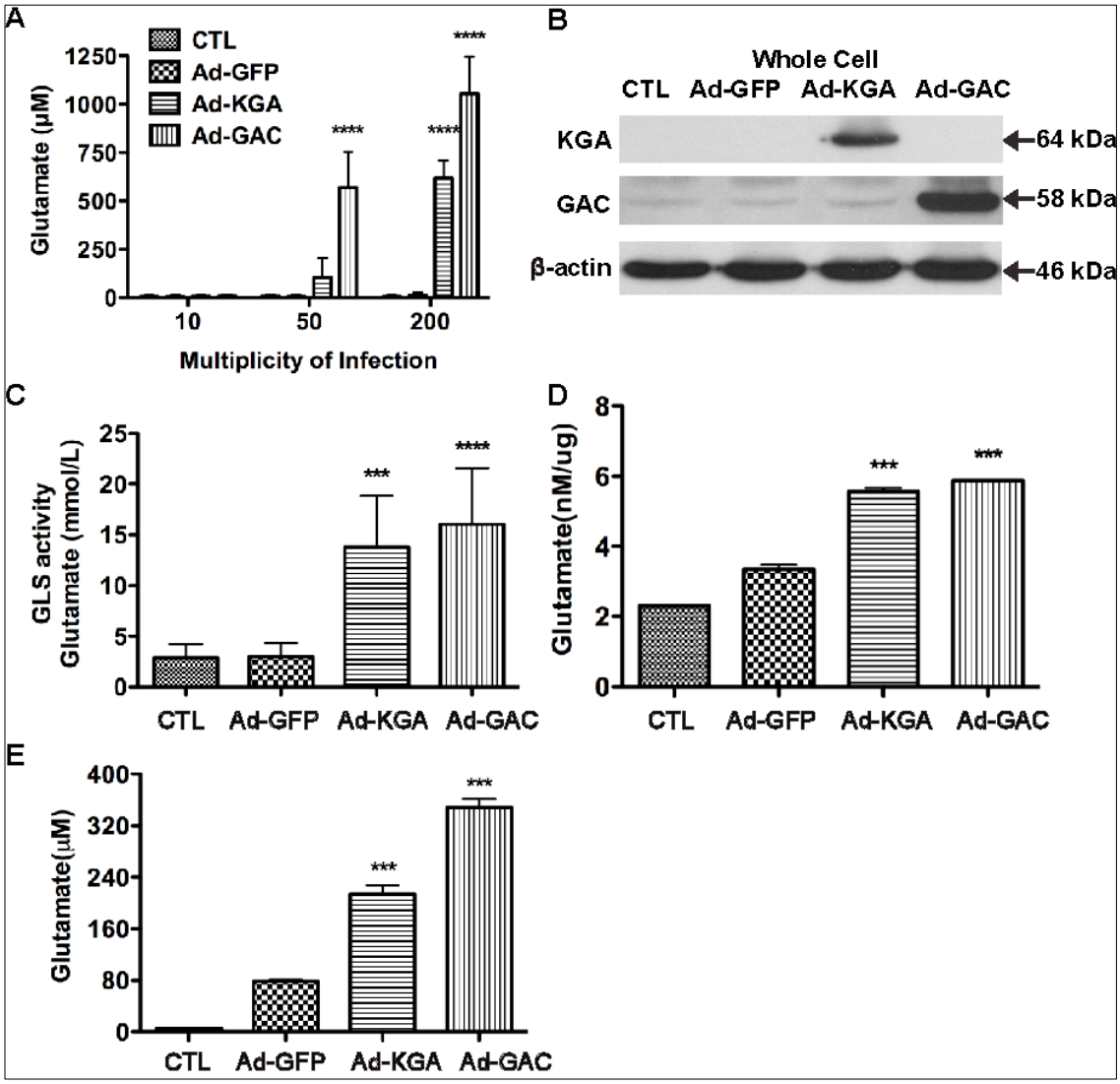

Figure 3.1. Both KGA and GAC are successfully overexpressed by adenovirus *in vitro*.

(A) Cell-free supernatants were collected from adenovirus-infected HeLa cell cultures at the MOI of 10, 50 and 200. RP-HPLC were used to determine the extracellular glutamate level. **(B)** GLS1 was overexpressed through adenovirus vectors that express KGA and GAC isoforms in HeLa cells at a multiplicity of infection (MOI) of 200. Two days after adenovirus infection, proteins lysates were collected from whole cells and the levels of KGA, GAC, tTG and flotillin-2 were determined by Western blot. Actin was used as loading control. **(C)** Protein lysates were collected from KGA- and GAC-overexpressing HeLa cells at the MOI 200. GLS1 activities were determined by the enzyme activity assay. GFP adenovirus Ad-GFP was used as vector control. **(D, E)** Extracellular and intracellular glutamate levels from adenovirus-KGA and -GAC infected HeLa cells with MOI 200 were detected by Amplex Red Glutamic acid/Glutamate oxidase Assay Kit and RT-HPLC, respectively. Quantification results shown are means ± SD of experiments performed in triplicate (n = 3 donors). *** and **** denotes $p < 0.001$and 0.0001, compared with the Ad-GFP group.

Figure 3.2

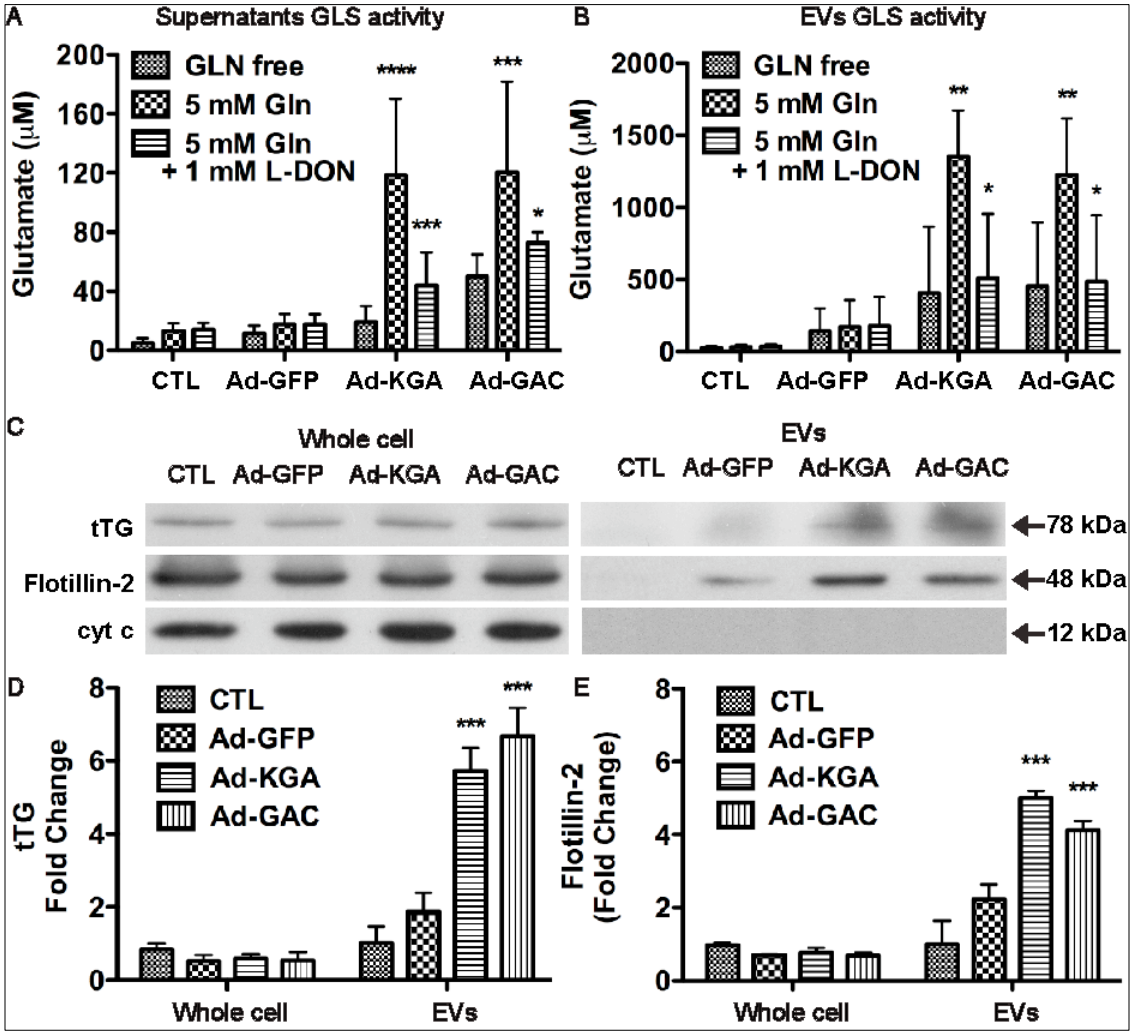
A
Supernatants GLS activity
Glutamate (μM)
200
160
120
80
40
0
GLN free
5 mM Gln
5 mM Gln
+ 1 mM L-DON
****
***
***
*
CTL
Ad-GFP
Ad-KGA
Ad-GAC
B
EVs GLS activity
Glutamate (μM)
2000
1500
1000
500
0
GLN free
5 mM Gln
5 mM Gln
+ 1 mM L-DON
**
*
**
*
CTL
Ad-GFP
Ad-KGA
Ad-GAC
C
Whole cell
CTL Ad-GFP Ad-KGA Ad-GAC
EVs
CTL Ad-GFP Ad-KGA Ad-GAC
tTG
Flotillin-2
cyt c
78 kDa
48 kDa
12 kDa
D
tTG
Fold Change
8
6
4
2
0
CTL
Ad-GFP
Ad-KGA
Ad-GAC
***
***
Whole cell
EVs
E
Flotillin-2
(Fold Change)
8
6
4
2
0
CTL
Ad-GFP
Ad-KGA
Ad-GAC
***
***
Whole cell
EVs

Figure 3.2. KGA and GAC overexpression increase EV release *in vitro*.

(A) Cell-free supernatants from control (CTL), Ad-GFP, Ad-KGA and Ad-GAC infected HeLa cells were incubated with or without 5 mM glutamine (Gln) and 1 mM L-DON *ex vivo* for two days. The glutamate levels were determined by RP-HPLC. **(B)** EVs were isolated from cell-free supernatants from four different groups of HeLa cells and incubated with or without 5 mM glutamine (Gln) and 1 mM L-DON *ex vivo* for two days. Glutamate production from EVs was determined by RP-HPLC. **(C)** Protein lysates were prepared from the whole cell lysates and EVs pellets. The levels of EVs markers, tTG and flotillin-2 were analyzed by Western blot. EVs protein loading was normalized with protein concentrations in whole cell lysates. Mitochondrial marker, cytochrome c, was used as a control to exclude contamination of EV pellets. **(D, E)** Densitometric quantifications of the protein levels in EVs were presented as fold change relative to that in control EV lysate. The protein levels in whole cell lysates were presented as fold change relative to β-actin in whole cells. Western blot results shown are representative of three independent experiments. Quantification results shown are means ± SD of experiments performed in triplicate (n = 3 donors). *, ** and *** denotes $p < 0.05$, 0.01 and 0.001, compared with the Ad-GFP group.

Figure 3.3.

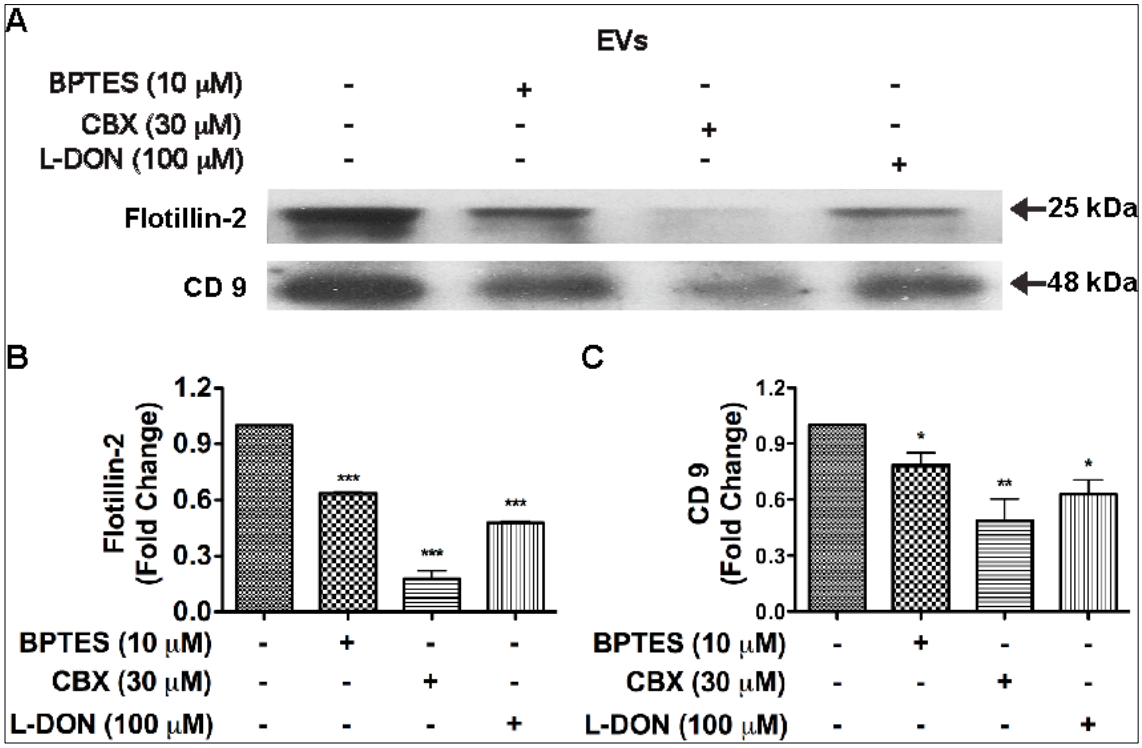
A
EVs
BPTES (10 μM) - + - -
CBX (30 μM) - - + -
L-DON (100 μM) - - - +
Flotillin-2
CD 9
25 kDa
48 kDa
B
Flotillin-2 (Fold Change)
1.2
0.9
0.6
0.3
0.0
***
***
***
BPTES (10 μM) - + - -
CBX (30 μM) - - + -
L-DON (100 μM) - - - +
C
CD 9 (Fold Change)
1.2
0.9
0.6
0.3
0.0
*
**
*
BPTES (10 μM) - + - -
CBX (30 μM) - - + -
L-DON (100 μM) - - - +

Figure 3.3. Inhibition of glutamine metabolism reduces EVs release *in vitro*. **(A)** Hela cells were treated with BPTES and L-DON for 24 hours. Protein lysates were prepared from the EVs pellets in control and GLS1 inhibitor-treated Hela cells. The levels of EVs markers, flotillin-2 and CD9 were analyzed by Western blot. EVs protein loading was normalized with protein concentrations in whole cell lysates. **(B, C)** Densitometric quantifications of the protein Levels were presented as fold change relative to that in control EV lysate. Western blot results shown are representative of three independent experiments. Quantification results shown are means ± SD of experiments performed in triplicate (n = 3 donors). *, ** and *** denotes $p < 0.05$, 0.01 and 0.001, compared with that of the control Hela cells.

Figure 3.4

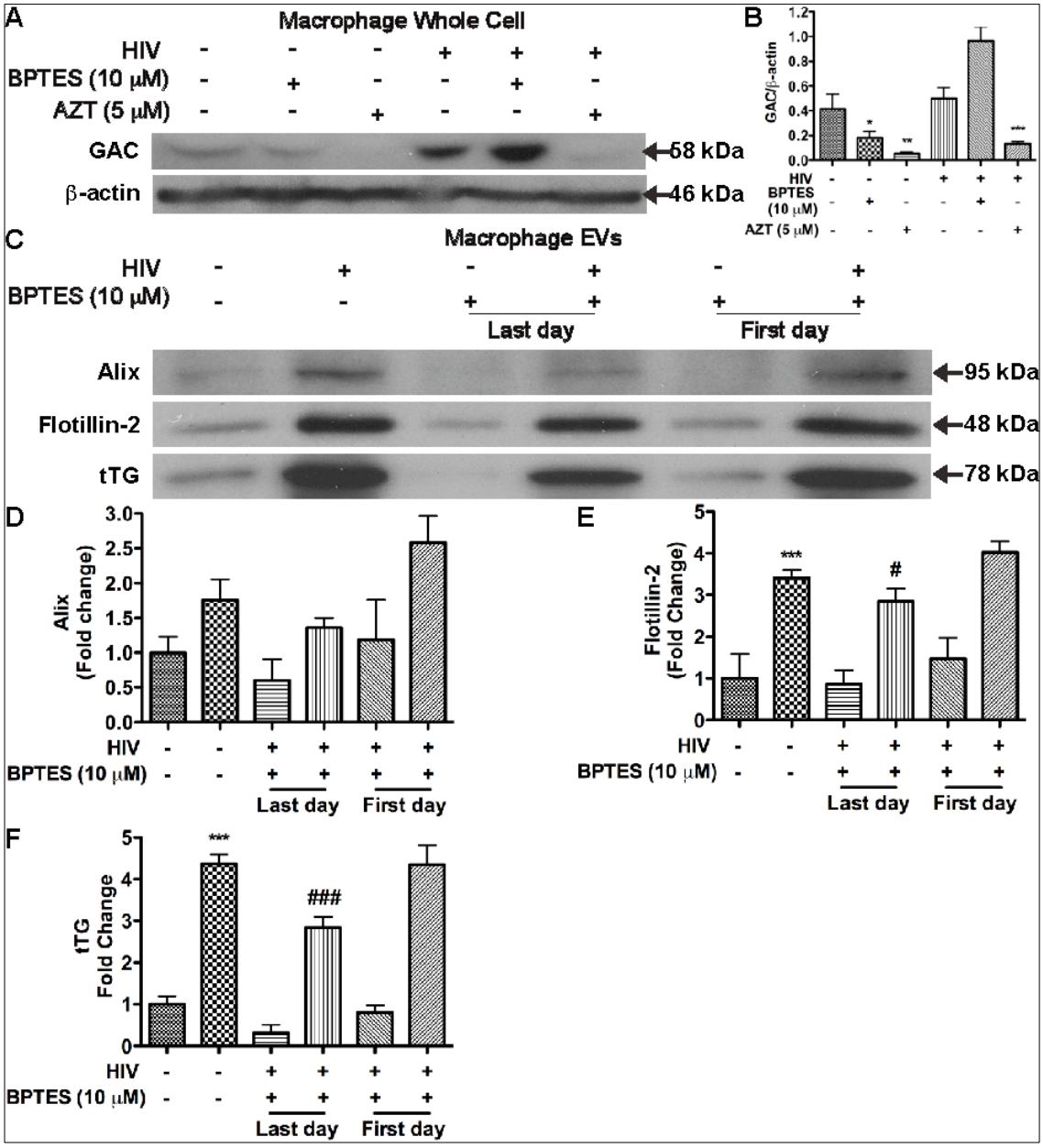
A
Macrophage Whole Cell
HIV
BPTES (10 μM)
AZT (5 μM)
GAC
β-actin
58 kDa
46 kDa
B
GAC/β-actin
C
Macrophage EVs
Last day
First day
Alix
Flotillin-2
tTG
95 kDa
48 kDa
78 kDa
D
Alix (Fold change)
E
Flotillin-2 (Fold Change)
F
tTG Fold Change

Figure 3.4. Inhibition of glutamine metabolism reduces EVs release in HIV-1-infected macrophages. Mock-infected or HIV-1-infected macrophages were treated with 10 μM BPTES 24 h prior to harvest or treated with 10 μM AZT. **(A)** Whole cell lysates were collected and GAC was measured using Western blot. **(B)** Densitometric quantification of the protein level of GAC in whole cell lysates was presented as fold change relative to β–actin. **(C)** EVs were isolated from mock-infected or HIV-1-infected macrophages treated with 10 μM BPTES at the day after infection or one day prior to EV isolation. EVs protein loading was normalized with protein concentrations in whole cell lysates. EV markers, Alix, flotillin-2, and tTG were measured using Western blot. **(D-F)** Densitometric quantifications of the protein levels of in EV markers were presented as fold change relative to that in mock-infected control EV lysates. Western blot results shown are representative of three independent experiments. Quantification results shown are means ± SD of experiments performed in triplicate (n = 3 donors). *, ** and *** denotes $p < 0.05$, 0.01 and 0.001, compared with that of the control microglia cells. # and ### denotes $p < 0.05$ and 0.001 compared with that of the HIV-1-infected macrohphages.

Figure 3.5

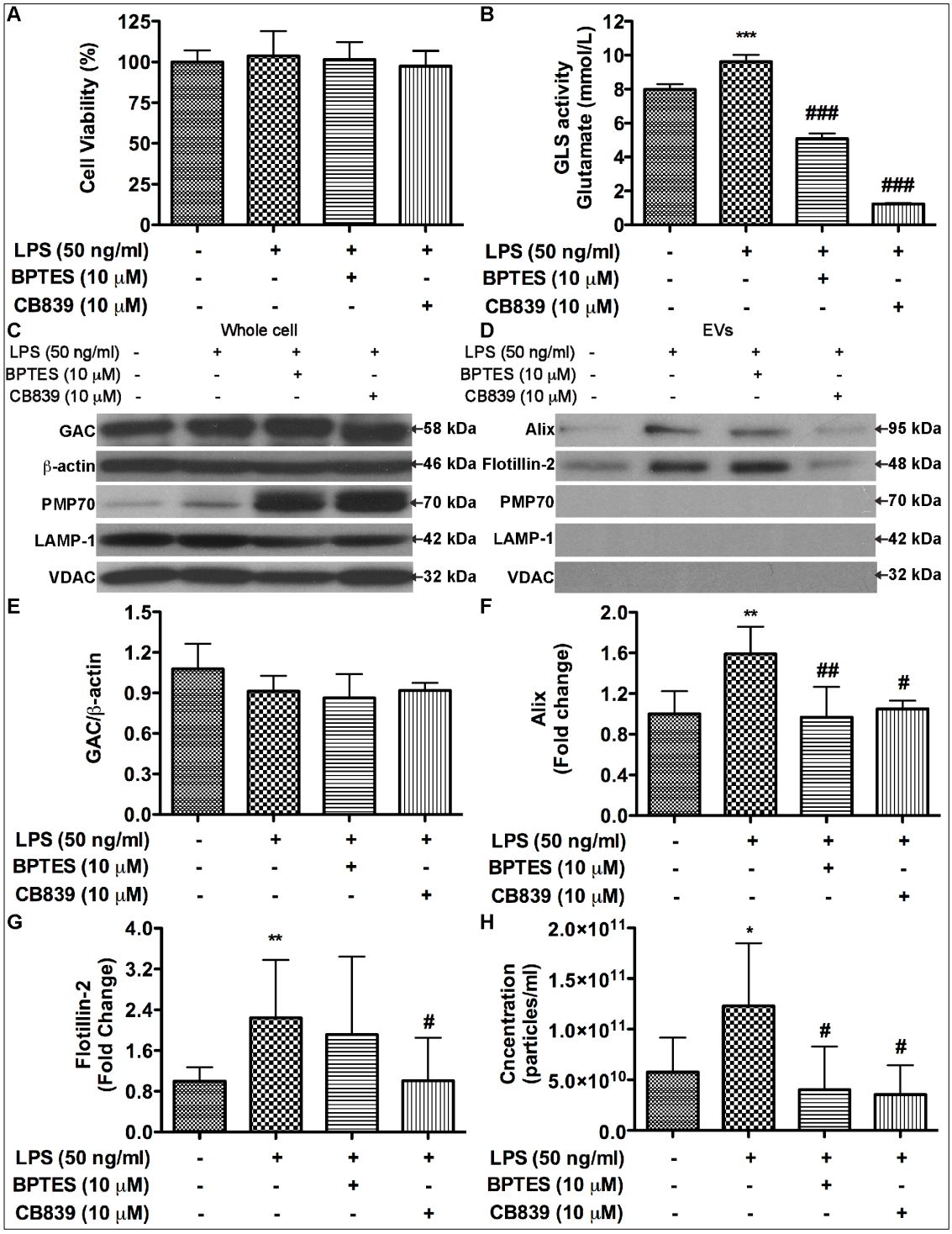
A
Cell Viability (%)
125
100
75
50
25
0
LPS (50 ng/ml) - + + +
BPTES (10 μM) - - + -
CB839 (10 μM) - - - +
B
GLS activity
Glutamate (mmol/L)
12
10
8
6
4
2
0
***
###
###
LPS (50 ng/ml) - + + +
BPTES (10 μM) - - + -
CB839 (10 μM) - - - +
C
Whole cell
LPS (50 ng/ml) - + + +
BPTES (10 μM) - - + -
CB839 (10 μM) - - - +
GAC
β-actin
PMP70
LAMP-1
VDAC
58 kDa
46 kDa
70 kDa
42 kDa
32 kDa
D
EVs
LPS (50 ng/ml) - + + +
BPTES (10 μM) - - + -
CB839 (10 μM) - - - +
Alix
Flotillin-2
PMP70
LAMP-1
VDAC
95 kDa
48 kDa
70 kDa
42 kDa
32 kDa
E
GAC/β-actin
1.5
1.2
0.9
0.6
0.3
0.0
LPS (50 ng/ml) - + + +
BPTES (10 μM) - - + -
CB839 (10 μM) - - - +
F
Alix
(Fold change)
2.0
1.6
1.2
0.8
0.4
0.0
**
##
#
LPS (50 ng/ml) - + + +
BPTES (10 μM) - - + -
CB839 (10 μM) - - - +
G
Flotillin-2
(Fold Change)
4.0
3.2
2.4
1.6
0.8
0.0
**
#
LPS (50 ng/ml) - + + +
BPTES (10 μM) - - + -
CB839 (10 μM) - - - +
H
Cncentration
(particles/ml)
2.0×10^11
1.5×10^11
1.0×10^11
5.0×10^10
0.0
*
#
#
LPS (50 ng/ml) - + + +
BPTES (10 μM) - - + -
CB839 (10 μM) - - - +

Figure 3.5. Inhibition of glutamine metabolism reduces EVs release in immune-activated microglia.

BV2 cells were treated with 10 μM BPTES or 10 μM CB839 4 hours prior to LPS treatment overnight. BV2 cell regular medium was changed to serum-free DMEM medium when GLS1 inhibitors were added. **(A)** Cell viability was measured after overnight treatment using MTS assay. **(B)** Protein lysates were collected from LPS-treated BV2 cells with or without GLS1 inhibitors. GLS1 activities were determined by the enzyme activity assay. **(C, D)** Protein lysates were prepared from whole cell and EV pellets in control, LPS-treated and LPS-treated with GLS1 inhibitor BV2 cells. The levels of GAC in whole cells, EVs markers, Alix and flotillin-2 in EVs were analyzed by Western blot. EVs protein loading was normalized with protein concentrations in whole cell lysates. PMP70, LAMP-1, and VDAC were also measured in the whole cell and EV lysates to exclude contaminations. **(E-G)** Densitometric quantification of the protein level of GAC in whole cell lysates was presented as fold change relative to β–actin. Densitometric quantifications of the protein levels of in EV markers were presented as fold change relative to that in control EV lysates. **(H)** Quantifications of the NanoSight NTA of vesicle concentration for samples from control, LPS-treated, LPS-treated with BPTES and LPS-treated with CB839 groups. Western blot results shown are representative of three independent experiments. Quantification results shown are means ± SD of experiments performed in triplicate (n = 3 donors). * and ** denotes $p < 0.05$ and 0.01, compared with that

of the control BV2 cells. # denotes $p < 0.05$ compared with that of the LPS-treated BV2 cells.

Figure 3.6

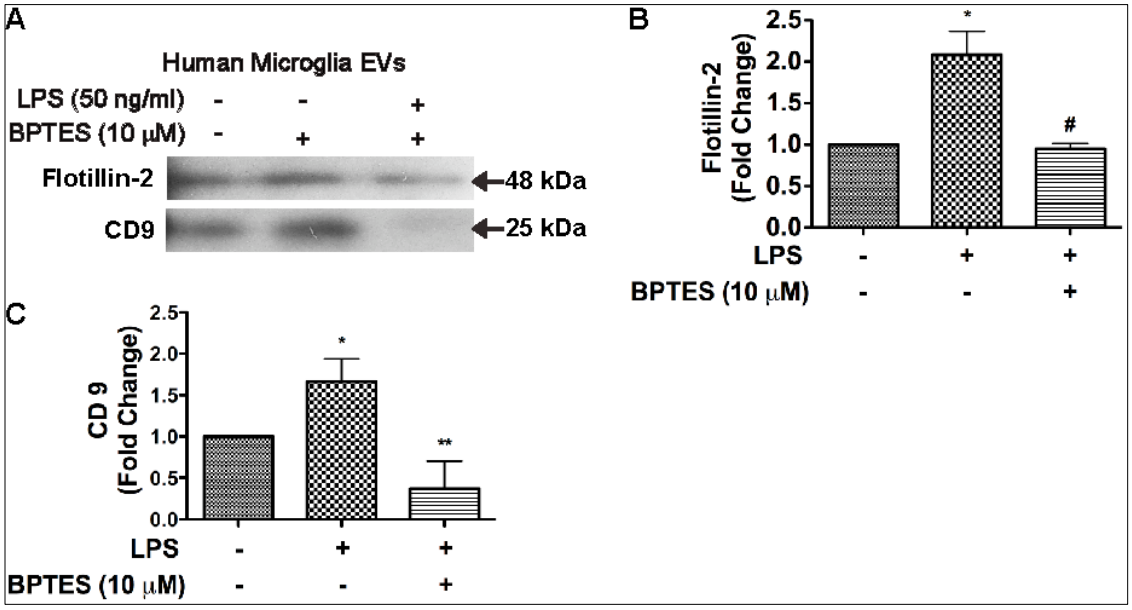
A
Human Microglia EVs
LPS (50 ng/ml) - - +
BPTES (10 μM) - + +
Flotillin-2
48 kDa
CD9
25 kDa
B
Flotillin-2 (Fold Change)
2.5
2.0
1.5
1.0
0.5
0.0
*
#
LPS - + +
BPTES (10 μM) - - +
C
CD 9 (Fold Change)
2.5
2.0
1.5
1.0
0.5
0.0
*
**
LPS - + +
BPTES (10 μM) - - +

Figure 3.6. Inhibition of glutamine metabolism reduces EVs release in immune activated human microglia.

(A) Human microglia were treated with or without 10 μM BPTES 4 h prior to LPS activation. Microglia media was changed to serum-free DMEM medium when BPTES were added. EVs were isolated and normalized depending on whole cell concentrations. EV markers, flotillin-2 and CD9 were measured using Western blot. **(B, C)** Densitometric quantifications of the protein levels of in EV markers were presented as fold change relative to that in mock-infected control EV lysates. Western blot results shown are representative of three independent experiments. Quantification results shown are means ± SD of experiments performed in triplicate (n = 3 donors). *, ** and *** denotes $p < 0.05$, 0.01 and 0.001, compared with that of the control microglia cells. # and ### denotes $p <$ 0.05 and 0.001 compared with that of the LPS-treated microglia cells.

Figure 3.7

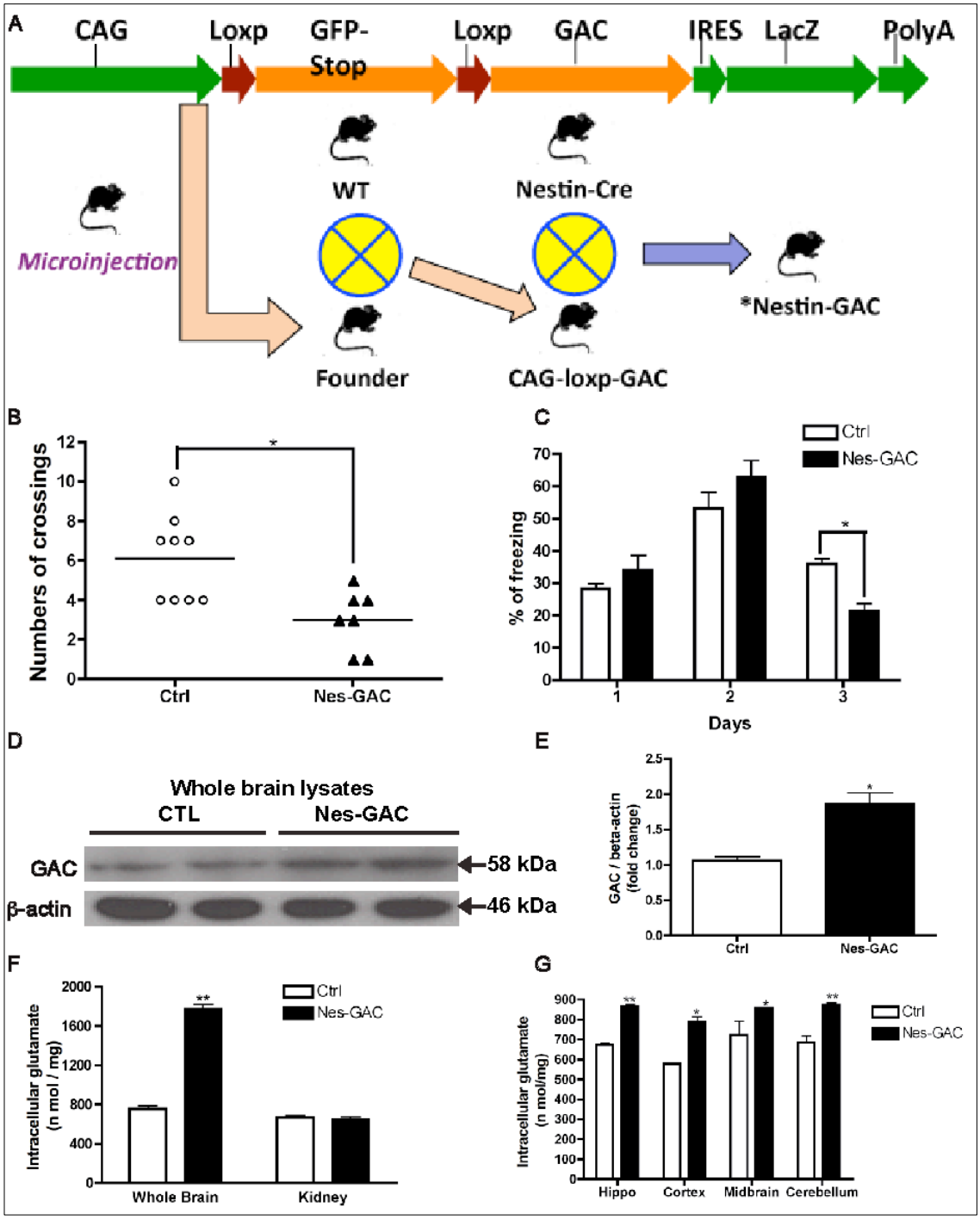
A
CAG
Loxp
GFP-Stop
Loxp
GAC
IRES
LacZ
PolyA
WT
Nestin-Cre
Microinjection
*Nestin-GAC
Founder
CAG-loxp-GAC
B
Numbers of crossings
Ctrl
Nes-GAC
C
Ctrl
Nes-GAC
% of freezing
Days
D
Whole brain lysates
CTL
Nes-GAC
GAC
58 kDa
β-actin
46 kDa
E
GAC / beta-actin (fold change)
Ctrl
Nes-GAC
F
Intracellular glutamate (n mol / mg)
Ctrl
Nes-GAC
Whole Brain
Kidney
G
Intracellular glutamate (n mol/mg)
Ctrl
Nes-GAC
Hippo
Cortex
Midbrain
Cerebellum

Figure 3.7. GAC overexpression is confirmed in Nestin-GAC mouse.

(A) The scheme shows the generation of Nestin-GAC transgenic mouse to specifically overexpress GAC in the CNS. A plasmid vector was engineered to overexpress GAC and then was microinjected into the fertilized egg. The egg was implanted in the uterus of a pseudopregnant female to create CAG-loxp-GAC mouse. CAG-loxp-GAC mice were mated with Nestin-Cre mice to produce Nestin-GAC mice. **(B)** Morris-Water-Maze test was performed to determine the spatial learning and memory of Nestin-GAC mice. After 5 days of the training phase, the probe test was conducted on the 6^{th} day. Nestin-GAC mice spent significantly less time in the target quadrant and had fewer crossings of the target place. **(C) The** Cued-Fear-Conditioning test was used to examine the memory of Nestin-GAC mice. **(D)** Protein lysates were prepared from whole brains and the expression levels of GAC were determined by Western blot. **(E)** Densitometric quantifications of the protein Levels were normalized to β-actin and presented as fold change relative to that in wild-type whole brain lysates. **(F)** Tissue glutamate levels were determined using the Amplex Red Glutamic acid/Glutamate Oxidase Assay Kit. **(G)** Protein lysates from different regions of mice brain were prepared and the expression levels of GAC were determined by Western blot. Quantification data were normalized to β-actin and presented as fold change in WT mice. Data are shown as the means ± SD. * and ** denote $p < 0.05$ and 0.01 compared with WT mice, N = 4 for Nestin-GAC and WT mice.

Figure 3.8

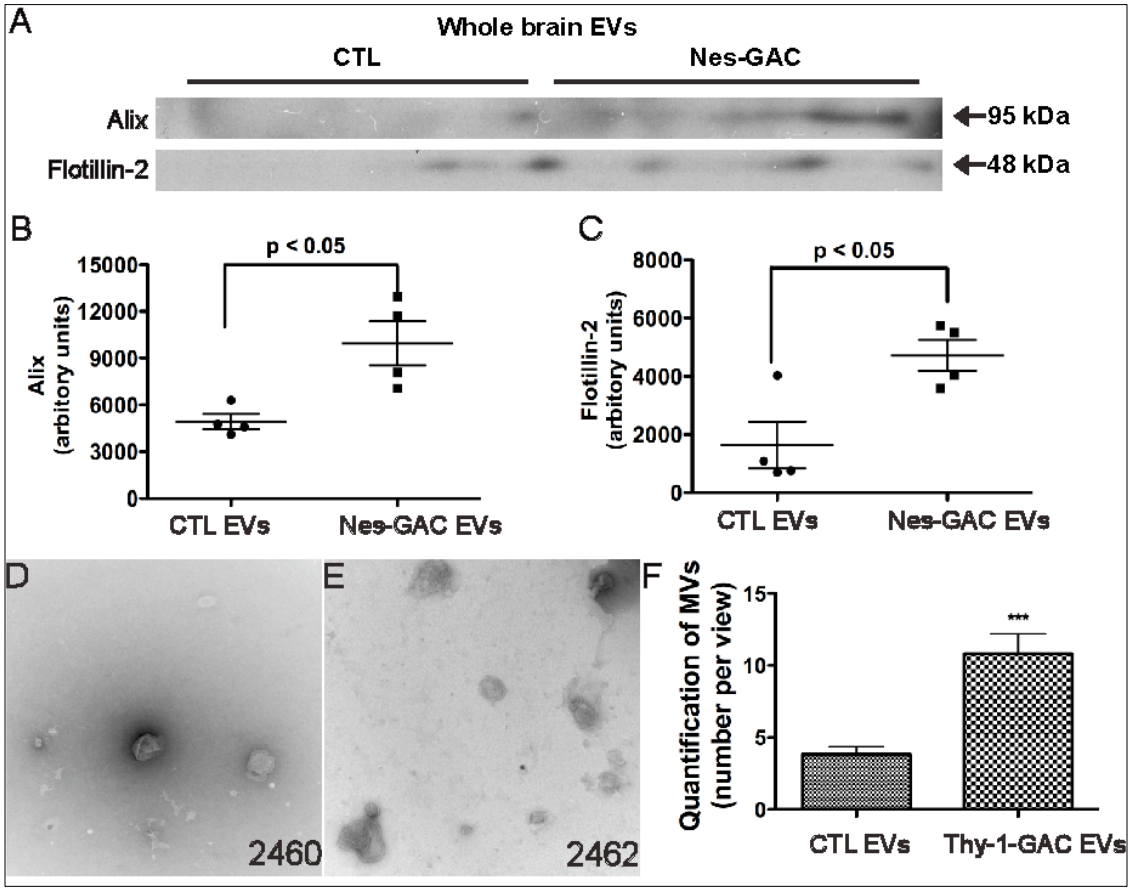
A
Whole brain EVs
CTL
Nes-GAC
Alix
Flotillin-2
95 kDa
48 kDa
B
p < 0.05
Alix (arbitory units)
15000
12000
9000
6000
3000
0
CTL EVs
Nes-GAC EVs
C
p < 0.05
Flotillin-2 (arbitory units)
8000
6000
4000
2000
0
CTL EVs
Nes-GAC EVs
D
2460
E
2462
F
Quantification of MVs (number per view)
15
10
5
0
***
CTL EVs
Thy-1-GAC EVs

Figure 3.8. Brain-specific GLS1 overexpression increases EVs release *in vivo.*

(A) Wild-type and Nestin-GAC mice were sacrificed at 12-16 weeks old. Brains were removed, and for each brain, the right hemibrain was processed for EVs isolation and the left hemibrain was homogenized for brain lysates. Protein lysates were prepared from the EVs pellets in wild type and Nestin-GAC hemibrains. The levels of EVs markers, tTG and flotillin-2 in the EVs lysates were analyzed by Western blot. EVs protein loading was normalized with the weight of their corresponding hemibrains before the EVs isolation. **(B, C)** Densitometric quantifications of the protein Levels were presented as fold changes relative to that in wild-type EV lysate. **(D-F)** Brain tissues from adult Thy1-GAC mice were dissected and EVs were isolated using the same techniques described above. EVs collected from WT (D) and Thy1-GAC (E) were evaluated via negative staining under TEM. Images shown were representative of each group. EVs numbers per vision fields (N = 10) were quantified. *** denotes $p < 0.001$

Chapter 4

Potential mechanism of GLS1 in the regulation of extracellular vesicles in macrophages and microglia

4.1 Abstract

Extracellular vesicles (EVs) are important in the intercellular communication in the central nervous system and their release is increased upon neuroinflammation and neurological disorders. Our previous data demonstrated an increased release of EVs from HIV-1-infected macrophages and immune-activated microglia that is neurotoxic. It also showed this release can be blocked by the inhibition of ceramide production. However, the mechanism of increasing EV release during HIV-1-infected and immune activation remains unknown. In the current study, we investigated glutaminase 1 (GLS1), a mitochondrial enzyme critical for glutamine metabolism, in EV release in HIV-1-infected macrophages and immune-activated microglia. We propose that HIV-1 infection increases GLS1, leading to a metabolic status that favors EV generation and releases through the glutamine and lipid metabolism. This new understanding of metabolic control of EV release in HIV-1-infected macrophages and immune-activated microglia will shed light on HIV-1 pathobiology and neurological complications.

Human primary monocyte-derived macrophages and murine microglia BV2 cell culture system and macrophage-tropic HIV-1_{ADA} and lipopolysaccharide (LPS) were used to study the regulation of EVs during HIV-1 infection and immune activation. EVs were isolated through differential centrifugations. GLS1 inhibitors, BPTES, and CB839 were used to specifically inhibit GLS1 activity. Ceramide and alpha-ketoglutarate were added after the treatment of GLS1 inhibitors to study the change of EV release. Transmission electron microscopy,

Nano-particle tracking analysis and Western blot were used to quantify the EVs released from cells. Glutamate and glutamine levels were determined by reverse phase high-performance liquid chromatography.

An elevated number of EVs was found in the supernatants of HIV-1-infected macrophages and immune-activated microglia when compared with controls. Conversely, blocking the GLS1 activity by BPTES, CB839 and CBX significantly reduced EV release and glutamate generation in HIV-1-infected macrophages and immune-activated microglia, suggesting a critical role of GLS1 in EV release. Consistently, the addition of glutamine substrate increases EV release during HIV-1 infection or immune activation. Interestingly, the inhibited EV release was reversed by the addition of ceramide and alpha-ketoglutarate. Identifying these two factors as critical downstream effectors for GLS1 inhibitors.

In conclusion, these findings support GLS1 as an essential enzyme that regulates through key metabolic intermediate ceramide and α-ketoglutarate during HIV-1-infection and immune activation. Therefore, blocking EV release through GLS1 inhibitors may serve as a novel therapeutic strategy to block the adverse effect of EVs during HIV-1 pathobiology and neurological complications.

4.2 Introduction

EVs have drawn attention by their facilitation of the interactions between neurons and glial cells via their transfer of cargos. EVs are also been significantly altered in response to stress and inflammation. EVs have been reported to be associated with neurodegenerative diseases such as Alzheimer's disease, Parkinson disease, amyotrophic lateral sclerosis, prion disease and HIV-1-associated neurocognitive disorders (HAND). The detection of EVs in various biological fluids such as plasma and cerebral spinal fluid (CSF) provides a potential role for EVs as biomarkers of diseases, including neurological disorders [171, 179, 197-200]. EVs have been detected at an elevated level in the cerebral spinal fluid in patients with mild to severe AD [167]. More importantly, protein markers of EVs are present in neuritic plaques in AD brains [167, 201, 202]. Our study also provided evidence of the increasing release of EVs in HAND models [178]. However, the regulation of EVs formation and release needs to be further elucidated.

GLS1 is a metabolic enzyme that is known to be associated with cancer cell proliferation and transformation [173, 174]. GLS1 is also essential in the glutaminolysis pathway, where it provides an energy source to the proliferating cells and acts as a nitrogen substrate for lipid and protein synthesis [203-205]. During glutaminolysis, glutamine is catalyzed into glutamate and its subsequently intermediate, α-ketoglutarate, which then enters the TCA cycle [110, 206, 207]. Glutamine serves as a nitrogen donor to protein glycosylation via the hexosamine pathway [208, 209], and as a source for the production of

glutathione in the resistance pathway against oxidative stress [205]. Furthermore, glutamine metabolism has also been identified to be important in various CNS diseases, including ALS, MS, and HAND [178, 210, 211]. Our recent reports suggest that GLS1 is upregulated and responsible for the increasing release of glutamate through elevated glutamine metabolism [72, 112]. More interestingly, in our current study, we found that GLS1 is positively regulating the release EVs. However, the mechanism of how GLS1 increases EV release remains unclear. Furthermore, the role of glutamine metabolism in EV release remains understudied.

Recent studies indicate that the formation and secretion of EVs are largely dependent on the proper function of ceramide, which is a type of sphingolipids catalyzed by neutral sphingomyelinase (nSMase) from sphingomyelin. The defective metabolism of sphingolipids in the brain has also been reported to be associated EVs with AD, where increasing EV release is reported as a crucial contributor to the toxicity of amyloid beta and tau phosphorylation [180]. The EV release is also reversed by the inhibition of the nSMase pathway [212, 213]. Studies show that the nSMase inhibitor, GW4869 significantly reduces the release of EVs and its neurotoxicity in HIV-infected or immune-activated macrophages and microglia and in AD model *in vitro* and *in vivo*, indicating the potential involvement of ceramide in the EV biogenesis [178, 180, 214]. However, the correlation between GLS1, glutamine metabolism, ceramide and EV hasn’t been investigated. Therefore, in this chapter, we will

explore the possibilities and discuss the potential mechanism of GLS1 regulation of EV release in response to the glutamine and sphingolipid metabolisms.

4.3 Materials and Methods

Culture, HIV-1 and LPS infection of macrophages and microglia

Human peripheral blood-derived mononuclear cells were isolated through leukopheresis from healthy donors. Human macrophages were differentiated in Dulbecco's Modified Eagle's Media (DMEM) (Sigma Chemical Co., St. Louis, MO) with 10% human serum, 50 µg/ml gentamycin, 10 µg/ml ciprofloxacin (Sigma), and 1,000 U/ml recombinant human macrophage colony-stimulating factor (MCSF) for 7 days. Human fetal microglial cells were obtained from fetal brain tissue-derived microglia-astrocytes mixed cultures as previously described [185]. The HIV-1_{ADA} strain was used to infect the macrophages and microglia at a multiplicity of infection (MOI) of 0.1 and 0.5, respectively. After 24 hours, the culture medium was changed to remove any remnant virus. Seven days after HIV-1-infection, the culture medium was changed to glutamine-free neurobasal medium for 24 h and supernatants were collected for subsequent HPLC or Western blot analysis. HeLa and BV_2 cell lines were obtained from ATCC, and both cell lines were grown in DMEM with 10% fetal bovine serum and antibiotics. Lipopolysaccharide (LPS) was used to immune activate BV_2 cells for 24 h and supernatants were collected for HPLC and Western blot analysis. Bis-2-(5-phenylacetamido-1,2,4-thiadiazol-2-yl)ethyl sulfide (BPTES) (a generous gift presented by Dr. Tsukamoto from John Hopkins and later ordered from Millipore) at a concentration of 10 μM was added to HIV-1-infected macrophages or LPS-treated microglia prior to EV isolation. All experiments involving human cell

samples are approved by Institutional Review Board of University of Nebraska Medical Center.

Isolation of EVs from cells

EVs were isolated from the supernatants of GLS1-overexpressing cells, HIV-1-infected macrophages and LPS-activated microglia through differential centrifugations. Briefly, the supernatants were first centrifuged at 300 X g for 10 min to remove free cells, at 3,000 X g for 20 min to remove cellular debris and then 10,000 X g for 30 min to remove free organelles. Lastly, EVs were collected by ultracentrifugation at 100,000 X g for 2 h at 4°C. To prepare EVs for Western blotting, the EV pellets were lysed in M-PER mammalian protein extraction reagent (Thermo Scientific, Pittsburgh, PA). For negative staining, EVs were fixed in 2% glutaraldehyde and 2% paraformaldehyde. For glutaminase activity assay and neurotoxicity, the EVs were resuspended in 1 ml of glutamine-free neurobasal medium.

Negative staining and electron microscopy

EVs were fixed and then spread on the silicon monoxide and nitro-cellular film coated copper grid. The droplets were removed with filter paper, air-dried at room temperature and then subjected to transmission electron microscopy (TEM). For scanning electron microscope (SEM), cells were fixed in 2% glutaraldehyde and 2% paraformaldehyde and point dried, mounted and coated with gold/palladium.

Nano-particle tracking analysis

A NanoSight NS 300 (Malvern) equipped with an sCMOS camera was utilized to analyze the size distribution and concentration of EVs. NanoSight utlizes Nanoparticle Tracking Analysis (NTA), which is a combination of light scattering and Brownian motion technologyto measure the concentration and size and distribution of particles in the EV supernatants. After the whole process of EV isolation, the pellets were first resuspended in 100 μl of filtered PBS and then diluted by 100 times. The conditions of the measurements include temperature of 25 °C, viscosity of 1 cP, 25 seconds per capture frame and a measurement time of 60 s. All of the conditions were kept the same amongst all of the samples. The results indicate the mean sizes and concentration of at least three individual measurements.

Toxicity/MTT/MTS assays

GLS1 inhibitors were added to HIV-1-infected macrophage or LPS-activated microglia cultures and cell viability was assessed by MTT assays in 24-well or 96-well plates. MTT (Sigma) was added to the cultures for a final concentration of 125 μg/ml. The plates were incubated for 30 minutes at 37 °C with 5% CO2 and the medium was aspirated. The insoluble formazan was solubilized in DMSO, and the concentrations were determined by optical density at 490 nm with an ELX808 densitometer (Bio-Tek Instruments, Winooski, and VT). Alternatively, Celltiter aqueous one solution cell proliferation assay, which

contains a novel tetrazolium compound [3-(4,5-dimethylthiazol-2-yl)-5-(3-carboxymethoxyphenyl)-2-(4-sulfophenyl)-2H-tetrazolium (MTS) (Promega) was utilized to assess cell viability according to the manufacturer instructions. Briefly, 20 µl of reagent was added into a 100 µl of culture medium, and then the plates were incubated the plates in a humidified, 5% CO2 and 37 °C atmosphere for 1 hour. The absorbance was determined at 490 nm.

Western blot

Protein concentrations were determined by Bradford protein assay. SDS PAGE separated proteins from whole cell and EVs lysates. Afterwards they were electrophoretically transferred to polyvinyldifluoridene membranes (Millipore, Billerica, MA and Bio-Rad, Hercules, CA). Membranes were incubated overnight at 4 °C with polyclonal antibodies for KGA and GAC (Dr.N.Curthoys, Colorado State University, Fort Collins, CO), tissue transglutaminase (tTG) (Lab Vision/Thermo, Fremont, CA), flotillin-2 (Cell Signaling Technology, Danvers, MA) and β-actin (Sigma-Aldrich, St. Louis, MO), followed by horseradish peroxidase-linked secondary anti-rabbit or anti-mouse secondary antibodies (Cell signaling Technology). Antigen-antibody complexes were visualized by Pierce ECL Western Blotting Substrate. For quantification of the data, films were scanned with a CanonScan 9950F scanner and images were analyzed using the public domain NIH image program (developed at the U.S. National Institutes of Health and available on the internet at http://rsb.info.nih.gov/nih-image/).

Glutaminase activity assay

Highly concentrated whole cell lysates were collected from flasks and subjected to GLS activity assay using a two-step assay [187, 188]. Briefly, protein concentrations in the lysates were tested by using BCA Protein Assay Kit (Pierce). All samples were normalized to same concentration. In the first step, fifty milligrams of protein was added to 100 μL of initial assay mix. The mix contains 50 mM glutamine, 0.15 M phosphate, 0.2 mM EDTA, and 50 mM tris-acetate. The PH value of the mix was adjusted to 8.6 and incubated at 37 °C for 30 min. 10 μL of 3 N hydrochloric acid (HCl) was added to inactivate the glutaminase activity and stop the reaction. In the second step, 1 mL of the second reaction mix was added, which contained 0.4 mg of purified bovine liver glutamate dehydrogenase (Sigma-Aldrich, St. Louis, MO, USA), 0.08 M Tris-acetate at pH 9.4, 0.2 M hydrazine, 0.25 mM ADP (adenosine 5'-diphosphate sodium salt), and 2 mM NAD (β-nicotinamide adenine dinucleotide hydrate). The samples were mixed and incubated for 30 min at room temperature. 100 μL of reaction was used for measurement and absorbance was determined at a wavelength of 340 nm, glutamate concentration was determined using a standard curve of 10, 5, 2.5, 1.25, 0.625, and 0.0 mM glutamate, along with negative controls.

Analysis of glutamate and glutamine by RP-HPLC

Glutamate levels were analyzed by RP-HPLC using an Agilent 1200 liquid chromatograph and fluorescence detector as previously described [14] with a few

modifications. The experiments utilized 4.6 × 75 mm, 3.5 μm ZORBAX Eclipse AAA analytical columns (Agilent). A gradient elution program was optimized for glutamate measurement with a flow rate 0.75 ml/min.

Analyses of glutamate concentrations

The intracellular glutamate levels in whole brain lysates of mice and whole cell lysates were determined by Amplex Red Glutamic acid/Glutamate Oxidase Assay Kit (Invitrogen) based on the manufacturer's instruction. Brain tissue lysates and whole cell lysates were diluted to the same protein concentration before the assay.

Statistical analysis

Data are expressed as means ± SD unless otherwise specified. Statistical analysis was performed using ANOVA, followed by the Tukey-post-test for paired observations. Significance was determined by a p value < 0.05. All experiments were performed with cells from at least three donors to account for any donor-specific differences. Assays were performed at least three times in triplicate or quadruplicate within each assay.

4.4 Results

EV release in HIV-1-infected macrophages is dependent on glutamine.

Our previous work has demonstrated the role of GLS1 in the regulation of EV release. However, the mechanism of how GLS1 regulates the release remains unclear. To further study our hypothesis, different concentrations of glutamine were added to HIV-1-infected macrophages one day prior to harvest when media was changed into serum free DMEM. Three different concentrations were used, including 1 mM, 2 mM and 5 mM. EVs were isolated from the supernatants collected from HIV-1-infected macrophages and subjected to negative staining. TEM was used to capture images of EVs at magnification of 2700 X (Fig 4.1A-D) and 42,000 X (Fig 4.1E-H). Seven random fields were chosen by the instructor at the TEM core facility lab, who is blinded from the experiments and samples identifications. Quantification of EVs showed a significant increase of EVs at a concentration of 1 mM and high concentrations of glutamine-treated groups remain a high EV release but no significant dose-dependent effect (Fig 4.1A-I). The extracellular supernatants were then prepared for RP-HPLC. Glutamate generation was found to be increased with the increasing concentrations of glutamine in the supernatants (Fig 4.2A, B). We collected protein lysates from both the whole cells and EVs. The expression level of GAC under different concentrations of glutamine did not change compared to control group. GAC was also detected in the EVs as previously reported [178]. EV markers, Alix, flotillin-2 and CD9 were also detected using Western blot. The level of EV markers in the whole cell level is consistent. However, EV markers

were higher in HIV-1-infected macrophages with glutamine concentrations of 1 mM and 2 mM. Surprisingly, the 5 mM treatment group did not show a significant increase of EV markers as compared with the control. These results indicate that the presence of glutamine is important for the EV release in HIV-1-infected macrophages.

EV release in immune-activated microglia is dependent on glutamine.

To further investigate whether EV release is dependent on glutamine, BV2 cells were utilized to study the association of glutamine and the regulation of EV release. Different concentrations of glutamine were added six hours prior to LPS treatment. The presence of glutamine boosted the survival of BV2 cells, indicating the importance of glutamine (Fig 4.3A). The extracellular glutamate is increased significantly at the increasing level of glutamine added to the cell cultures. Nanoparticle tracking analysis showed that EV release was increased at the concentration of 2 mM or 5 mM (Fig 4.3B, C). Furthermore, the Western blot of whole cells showed increased GAC levels at 2 mM and 5 mM glutamine concentrations (Fig 4.3E, F). The Western blot of EVs showed an increase in the EV markers, Alix and flotillin-2, at increased glutamine concentrations (Fig 4.3E, G, H). Altogether, these results demonstrated that glutamine is involved in the EV release in immune-activated microglia cells.

EV release in immune-activated microglia is associated with the level of α-ketoglutarate.

Glutamine metabolism is an essential process to generate glutamate and thus α-ketoglutarate for energy production. To further study the potential pathway of GLS1-associated EV release, 1 mM of α-ketoglutarate (α-KG) was added with GLS1 inhibitors. Cell viability did not change upon treatment of GLS1 inhibitors and α-KG (Fig 4.4A). Whole cells lysates were collected and subjected to a GLS1 enzyme activity assay. GLS1 activity increased after LPS treatment and decreased after the treatment of GLS1 inhibitors in the presence of 1 mM α-KG (Fig 4.4C). EVs were then either isolated and resuspended using filtered PBS or lysed for Western blot. EVs were diluted for 100 times and subjected to nanoparticle tracking analysis. The decreased EV release after GLS1 inhibitors treatment was significantly reversed by the addition of α-KG (Fig 4.4B). Furthermore, EV lysates were subjected to Western blot. With the presence of α-KG, the level of EV markers, Alix and flotillin-2 were significantly increased even with the treatment of GLS1 inhibitors, BPTES or CB839 (Fig 4.4D-F). These results suggest that α-KG could be the downstream product of glutamate that is associated with the regulation of EV release.

EV release in immune-activated microglia is associated with sphingolipid metabolism.

Our previous report has shown that the release of EV can be blocked by the presence of the nSMase inhibitor, GW4869, which is an inhibitor of the production of ceramide [178]. Therefore, we hypothesized that adding ceramide to the LPS-treated BV2 with GLS1 inhibitors would help restore the release of

EVs. To test this hypothesis, we used two concentrations of ceramide, 50 μM or 100 μM with or without GLS1 inhibitors. LPS-treatment and GLS1 inhibitors treatment with or without ceramide didn't induce cell loss (Fig 4.5A). 50 μM of ceramide was utilized for following experiments. GLS1 activity increased after LPS treatment and decreased after the treatment of GLS1 inhibitors in the presence of ceramide (Fig 4.5B). Nanoparticle tracking analysis results showed that when 10 μM BPTES or CB839 was added, the release of EVs was decreased. Interestingly, when ceramide was added, the release of EVs increased (Fig 4.5C), indicating that the ceramide pathway of sphingolipid metabolism is involved in GLS1 regulated release of EVs.

4.5 Discussion

Our current study has focused on the identification of key pathogenic components for HAND. Our previous studies demonstrated a strong link between GLS and the pathogenesis of HAND via the overproduction of glutamate and related neuronal damage [49, 53, 71, 72, 108, 188]. Over the years, GLS1 has garnered more attention regarding the essential role it plays in normal and pathological human physiology. The knockout of GLS1 leads to lethal offspring one day after birth in mouse models, which indicates the critical role of GLS1 in the early development. We have also reported that GLS1 is essential for the proper functioning of neural progenitor cells including neuronal survival together with proliferation and differentiation [215]. During neuroinflammation, the activation of GLS1 and subsequently upregulated levels of GLS1 are associated with HIV-1 infection or immune activation and subsequent neurotoxicity [178].

In previous reports, it has been reported that GLS1 is involved in the regulation of EV release. However, the exact mechanism remains to be elucidated. In this study, we presented three major findings regarding the potential mechanism of EV release. First, the release of EVs is dependent on the presence of glutamine and its product glutamate. Second, the downstream product of glutamate, α–KG, can reverse the inhibition of EV release by GLS1 inhibitors, indicating that α–KG could be an effector for EV release. Third, the inhibition of EV release via GLS1 inhibitors could be mediated by the sphingolipid, ceramide pathway, as we have shown the addition of ceramide can rescue the reduced EV release. These observations suggest that GLS1 could

regulate EV release through the glutamine metabolism and sphingolipid metabolism.

To investigate our hypotheses on the mechanisms of GLS1's regulation of EV release, we tested the concentrations of isolated EVs from groups including glutamine-deprived, or 1 mM, 2 mM and 5 mM of glutamine. A wider range of glutamine concentration was utilized in order to study the effects of lower levels of glutamine on EV release. When 0.04 mM or 0.2 mM of glutamine was used to treat LPS-stimulated BV2 cells, the EV concentrations didn't show a significant increase compared with the control group. Changes in EV release were only observed till at a lowest glutamine level of 1 mM. The average sizes of the isolated EVs were consistent in all treatment groups, which were above 100 nm (data not shown). LPS treatment also did not alter the size of the released EVs. However, the increase of glutamine concentration from 1 mM to 5 mM did not show a significant or dose-dependent trend of increase of EV release, indicating the necessity of glutamine in the culture to release EVs. A potential rationale is that glutamine metabolism provides a possible energy resource for the EV budding. However, the detailed mechanism needs to be further elucidated.

When glutamine is involved in the EV release, the downstream product, α-KG, which is dependent on glutamine, could be an important regulator for EV release. Therefore, after the addition of GLS1 inhibitors, BPTES or CB839, to LPS-treated BV2 cells, 1 mM of α-KG was also added to the cultures prior to EV isolation. Interestingly, the presence of α-KG rescued the reduced EV release after treatment with GLS1 inhibitors. The inhibition of glutamate production from

GLS1 inhibitors leads to a reduced generation of α-KG. When α-KG was compensated, the level of EV release was rebooted, indicating that the EV release could be regulated through glutamine and α-KG. However, further study is warranted on whether the addition of α-KG boosts production of glutamate, or if this effect is due to the direct actions of α-KG. One possibility is that when α-KG enters the TCA cycle, energy production is increased. The increase production of ATP could activate the increased release of EV via P2X7 receptors, which could also be a further action of the mechanism.

Previously, we reported using GW4869 could effectively inhibit the release of EVs in HIV-1-infected macrophages and LPS-treated microglia [178]. Studies have also shown that GW4869 could inhibit EV release *in vitro* and *in vivo* in AD models and prion diseases [180, 214, 216-220]. It has also been reported that sphingolipid metabolism could be involved in EV release in microglia and neurological diseases [213, 221]. However, the role of sphingolipid metabolism in GLS1-associated EV release has never been reported. Therefore, ceramide was added to LPS-treated BV2 cells with GLS1 inhibitors. The NanoSight results demonstrated a rescue of EV release of ceramide to GLS1 inhibitors, which indicates ceramide could be involved in the pathway of GLS1-regulated EV release. The connection of ceramide pathway with glutamine metabolism has barely been investigated. Research has suggested a potential role of glutamine and glutamate in the essential supply of nitrogen bond to lipid biosynthesis including sphingolipids. Whether ceramide could be the downstream or upstream

product of this pathway remains unclear. The association between of ceramide and α-KG or energy production is also understudied.

Further investigation is needed for the relation between sphingolipids and GLS1 levels. After the treatment of GLS1 inhibitors, the activities and expression level of neutral sphingomyelinases needs to be measured. The level of ceramide would be assessed through mass spectrometry, which will provide further evidence for the association between ceramide, glutamine, and GLS1 in EV release. The other components in the sphingolipids family, including sphingomyelin, sphingosine and etc. should also be assessed to uncover the potential pathways to link these effectors to EV release. Furthermore, cholesterol has been reported to be associated with EV release [222, 223]. However, the involvement of cholesterol in GLS1-regulated EV release is unknown. These further investigations can shed light on the detail mechanisms of how GLS1 regulates EV.

4.6 Conclusion

In summary, the regulation of GLS1 in EV release is associated with glutamate, and its downstream product, α–KG and the sphingolipid, ceramide, which implicates the importance of glutamine metabolism and sphingolipid metabolism in EV release. This new mechanism will shed insight on the regulation of EVs and provide potential therapeutic targets for HAND and some types of neoplasms.

4.7 Tables and Figures

Figure 4.1

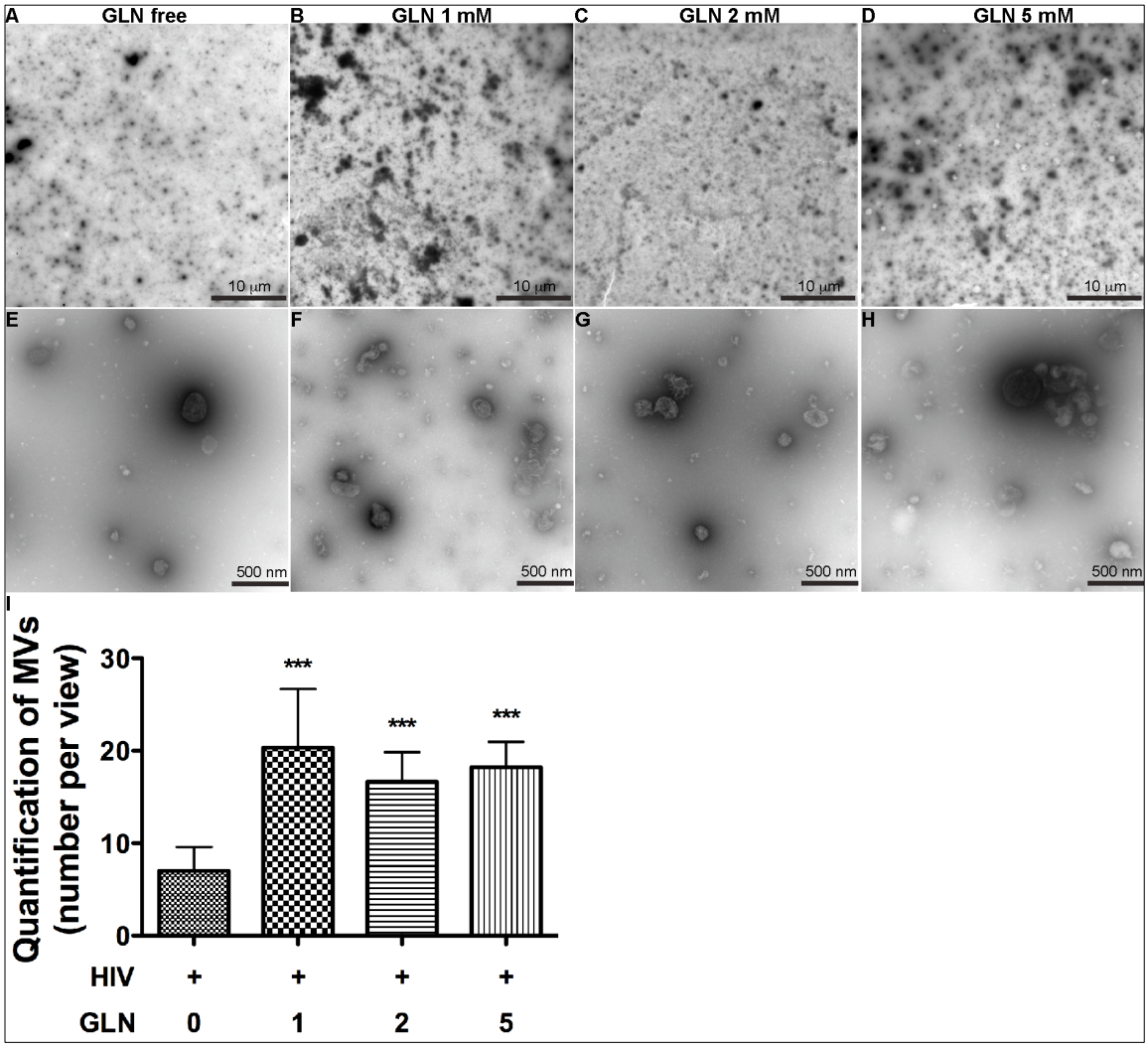

Figure 4.1. EV release in HIV-1-infected macrophages is dependent on glutamine.

(A-H) MDM was infected by HIV-1 virus for 6 days, and the medium was changed into serum free glutamine-free DMEM. Additional glutamine was added to the medium at the concentrations of 1 mM, 2 mM and 5 mM. EVs were isolated through differential centrifugation and resuspended upon the concentrations of whole cell lysates. EVs were fixed and subjected to negative staining using TEM under a magnification of 2700 X (A-D) and 42,000 X (E-H). **(I)** EVs numbers in E to H were quantified by manually counting from a total of 7 random vision fields. Results are representative of TEM images and quantification results are means ± SD of EV numbers from 7 fields of TEM images. *** denotes $p < 0.001$ in comparison to controls.

Figure 4.2

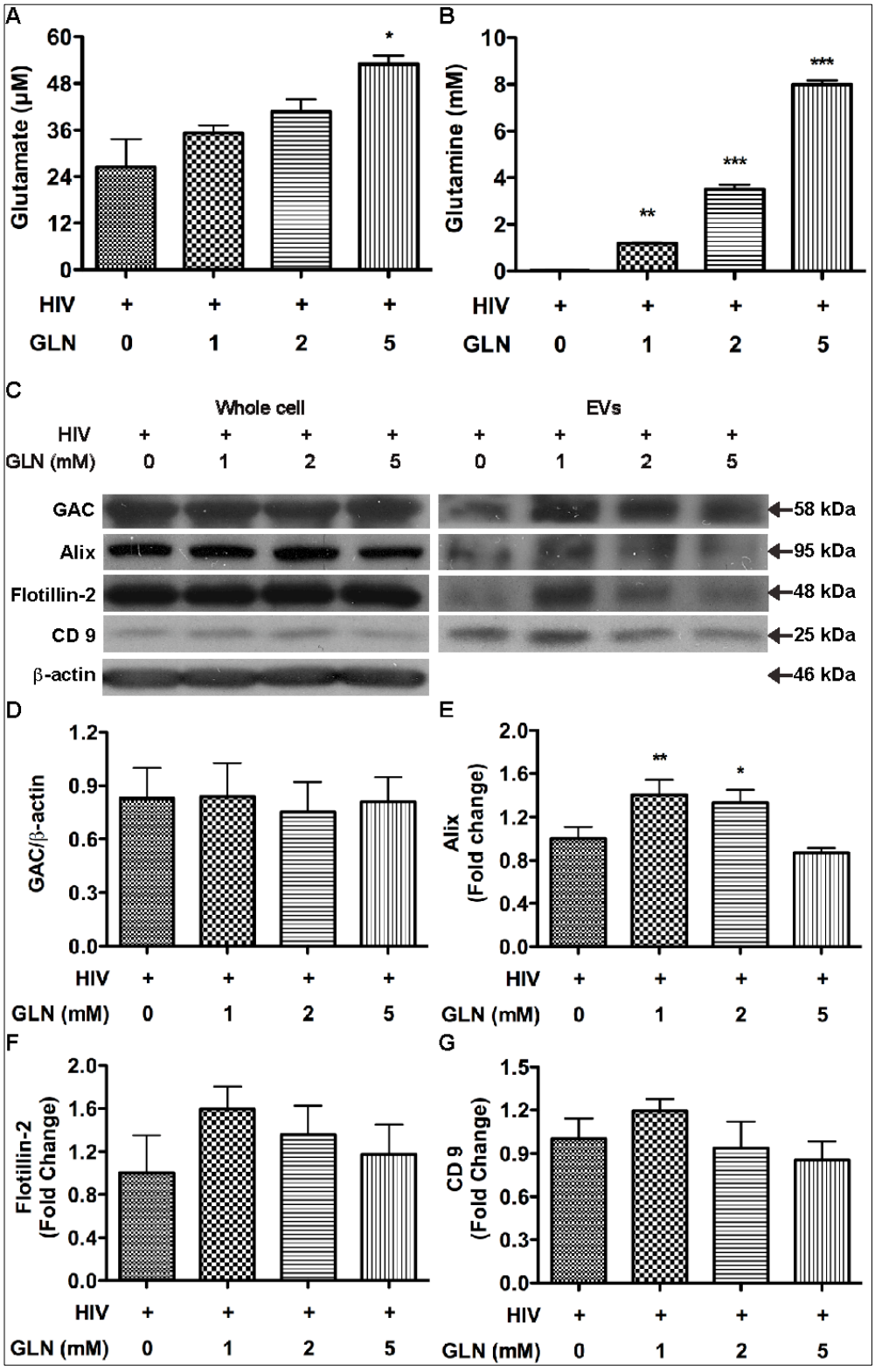
A
Glutamate (μM)
60
48
36
24
12
0
*
HIV + + + +
GLN 0 1 2 5
B
Glutamine (mM)
10
8
6
4
2
0
**
***
***
HIV + + + +
GLN 0 1 2 5
C
Whole cell
EVs
HIV + + + + + + + +
GLN (mM) 0 1 2 5 0 1 2 5
GAC
Alix
Flotillin-2
CD 9
β-actin
58 kDa
95 kDa
48 kDa
25 kDa
46 kDa
D
GAC/β-actin
1.2
0.9
0.6
0.3
0.0
HIV + + + +
GLN (mM) 0 1 2 5
E
Alix (Fold change)
2.0
1.6
1.2
0.8
0.4
0.0
**
*
HIV + + + +
GLN (mM) 0 1 2 5
F
Flotillin-2 (Fold Change)
2.0
1.6
1.2
0.8
0.4
0.0
HIV + + + +
GLN (mM) 0 1 2 5
G
CD 9 (Fold Change)
1.5
1.2
0.9
0.6
0.3
0.0
HIV + + + +
GLN (mM) 0 1 2 5

Figure 4.2. EV release in HIV-1-infected macrophages is dependent on glutamine.

MDM was infected by HIV-1 virus for 6 days, and the medium was changed into serum free glutamine-free DMEM. Additional glutamine was added to the medium at the concentrations of 1 mM, 2 mM and 5 mM. **(A, B)** Supernatants were collected and centrifuged at 1,500 rpm for 5 min to remove cells. Samples were prepared for RP-HPLC and the levels of glutamate and glutamine were determined. **(C)** Protein lysates were prepared from whole cell lysates and EVs pellets. The levels of GAC and EVs markers Alix, flotillin-2 and CD9 were analyzed by Western blot. EV protein loading was normalized with protein concentrations in whole cell lysates. **(D)** Densitometric quantification of the protein level of GAC in whole cell lysates was presented as fold change relative to β−actin. **(E-G)** Densitometric quantifications of the protein levels of EV markers were presented as fold changes relative to that in mock-infected control EV lysates. Western blot results shown are representative of three independent experiments. Quantification results shown are means ± SD of experiments performed in triplicate (n = 3 donors). *, ** and *** denotes $p < 0.05$, 0.01 and 0.001, compared with that of the control microglia cells.

Figure 4.3

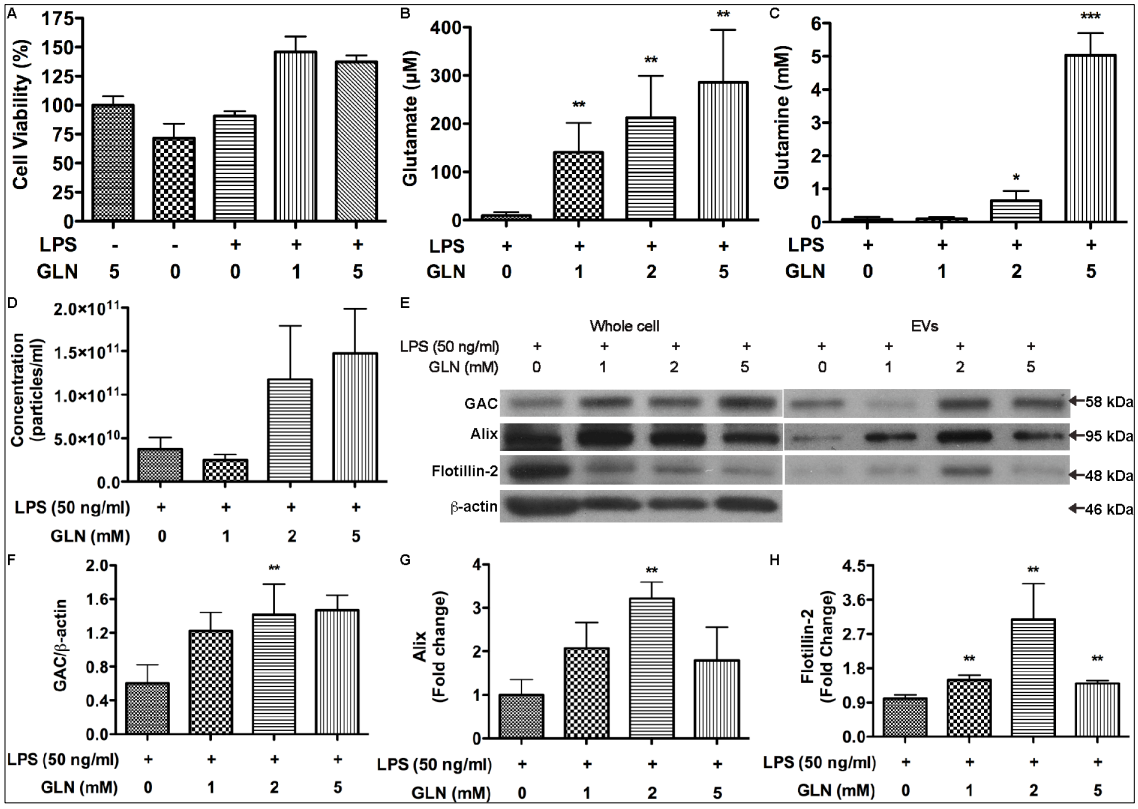
A
Cell Viability (%)
175
150
125
100
75
50
25
0
LPS - - + + +
GLN 5 0 0 1 5
B
Glutamate (μM)
400
300
200
100
0
**
**
**
LPS + + + +
GLN 0 1 2 5
C
Glutamine (mM)
6
5
4
3
2
1
0
*
***
LPS + + + +
GLN 0 1 2 5
D
Concentration (particles/ml)
2.0×10^11
1.5×10^11
1.0×10^11
5.0×10^10
0.0
LPS (50 ng/ml) + + + +
GLN (mM) 0 1 2 5
E
Whole cell
EVs
LPS (50 ng/ml) + + + + + + + +
GLN (mM) 0 1 2 5 0 1 2 5
GAC
Alix
Flotillin-2
β-actin
58 kDa
95 kDa
48 kDa
46 kDa
F
GAC/β-actin
2.0
1.6
1.2
0.8
0.4
0.0
**
LPS (50 ng/ml) + + + +
GLN (mM) 0 1 2 5
G
Alix (Fold change)
4
3
2
1
0
**
LPS (50 ng/ml) + + + +
GLN (mM) 0 1 2 5
H
Flotillin-2 (Fold Change)
4.5
3.6
2.7
1.8
0.9
0.0
**
**
LPS (50 ng/ml) + + + +
GLN (mM) 0 1 2 5

Figure 4.3. EV release in immune-activated microglia is dependent on glutamine.

When BV2 medium was changed into serum free glutamine-free DMEM, additional glutamine was added to the medium at concentrations of 1 mM, 2 mM and 5 mM 6 hours prior to LPS treatment. **(A)** Cell viability was measured after overnight treatment using MTS assay. **(B, C)** Supernatants were collected and centrifuged at 1,500 rpm for 5 min to remove cells. Samples were prepared for RP-HPLC and the levels of glutamate and glutamine were determined. **(D)** Quantifications of NanoSight NTA of vesicle concentration for samples from LPS-treated BV2 cell with different glutamine concentrations. **(E)** Protein lysates were prepared from the whole cell lysates and EVs pellets. The levels of GAC and EVs markers, Alix, flotillin-2 and CD9 were analyzed by Western blot. EVs protein loading was normalized with protein concentrations in whole cell lysates. **(F)** Densitometric quantification of the protein level of GAC in whole cell lysates was presented as fold changes relative to β−actin. **(G, H)** Densitometric quantifications of the protein levels in EV markers were presented as fold changes relative to that in mock-infected control EV lysates. Western blot results shown are representative of three independent experiments. Quantification results shown are means ± SD of experiments performed in triplicate (n = 3 donors). *, ** and *** denotes $p < 0.05$, 0.01 and 0.001, compared with that of control microglia cells.

Figure 4.4

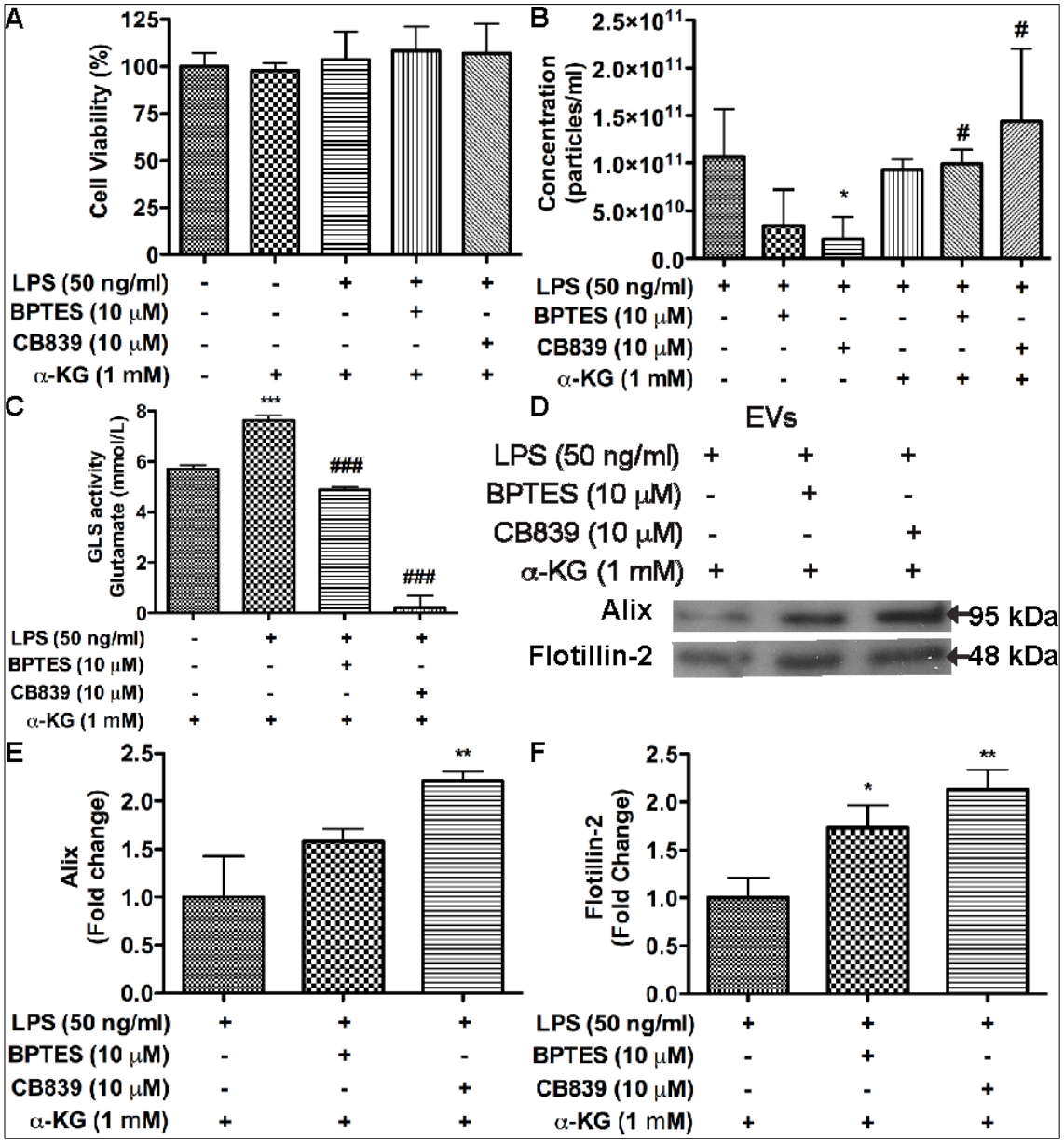
A
Cell Viability (%)
125
100
75
50
25
0
LPS (50 ng/ml) - - + + +
BPTES (10 μM) - - - + -
CB839 (10 μM) - - - - +
α-KG (1 mM) - + + + +
B
Concentration (particles/ml)
2.5×10^11
2.0×10^11
1.5×10^11
1.0×10^11
5.0×10^10
0.0
*
#
#
LPS (50 ng/ml) + + + + + +
BPTES (10 μM) - + - - + -
CB839 (10 μM) - - + - - +
α-KG (1 mM) - - - + + +
C
GLS activity Glutamate (mmol/L)
8
6
4
2
0
***
###
###
LPS (50 ng/ml) - + + +
BPTES (10 μM) - - + -
CB839 (10 μM) - - - +
α-KG (1 mM) + + + +
D
EVs
LPS (50 ng/ml) + + +
BPTES (10 μM) - + -
CB839 (10 μM) - - +
α-KG (1 mM) + + +
Alix
95 kDa
Flotillin-2
48 kDa
E
Alix (Fold change)
2.5
2.0
1.5
1.0
0.5
0.0
**
LPS (50 ng/ml) + + +
BPTES (10 μM) - + -
CB839 (10 μM) - - +
α-KG (1 mM) + + +
F
Flotillin-2 (Fold Change)
2.5
2.0
1.5
1.0
0.5
0.0
*
**
LPS (50 ng/ml) + + +
BPTES (10 μM) - + -
CB839 (10 μM) - - +
α-KG (1 mM) + + +

Figure 4.4. EV release in immune-activated microglia is associated with the level of α-ketoglutarate.

BV2 cells were treated with 10 μM BPTES or 10 μM CB839 4 hours prior to LPS treatment overnight. BV2 cell regular medium was changed to serum-free DMEM medium when GLS1 inhibitors were added. Two hours prior to LPS treatment, 1 mM of α-ketoglutarate was added to BV2 cells. **(A)** Cell viability was measured after overnight treatment using MTS assay. **(B)** After 1 mM of α-ketoglutarate treatment, Nanoparticle tracking analysis was conduct with 100 X dilution of collected EVs with filtered PBS. Quantifications of the NanoSight NTA of vesicle concentration for samples from LPS-treated BV2 cell with GLS1 inhibitors and α-ketoglutarate. **(C)** Protein lysates were collected from LPS-treated BV2 cells with or without GLS1 inhibitors or α-ketoglutarate. GLS1 activities were determined by the enzyme activity assay. **(D)** Protein lysates were prepared from EV pellets. The levels of GAC and EVs markers, Alix and flotillin-2 were analyzed by Western blot. EVs protein loading was normalized with protein concentrations in whole cell lysates. **(E, F)** Densitometric quantifications of the protein levels of in EV markers were presented as fold change relative to that in mock-infected control EV lysates. Western blot results shown are representative of three independent experiments. Quantification results shown are means ± SD of experiments performed in triplicate (n = 3 donors). *, ** and *** denotes $p < 0.05$, 0.01 and 0.001, compared with that of the control. $^{\#}$, and $^{\#\#\#}$ denotes $p < 0.05$ and 0.001 compared with that of the LPS-treated group.

Figure 4.5

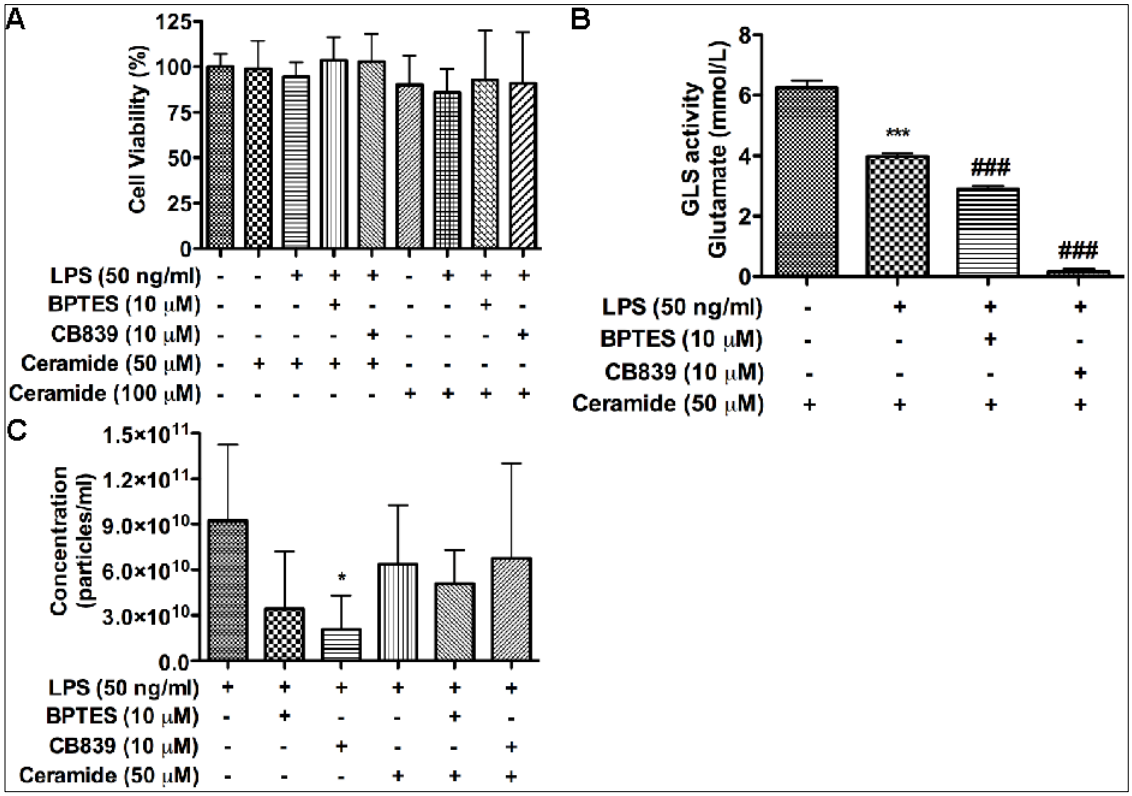
A
Cell Viability (%)
125
100
75
50
25
0
LPS (50 ng/ml) - - + + + - + + +
BPTES (10 μM) - - - + - - - + -
CB839 (10 μM) - - - - + - - - +
Ceramide (50 μM) - + + + + - - - -
Ceramide (100 μM) - - - - - + + + +
B
GLS activity
Glutamate (mmol/L)
8
6
4
2
0
***
###
###
LPS (50 ng/ml) - + + +
BPTES (10 μM) - - + -
CB839 (10 μM) - - - +
Ceramide (50 μM) + + + +
C
Concentration
(particles/ml)
1.5×10^11
1.2×10^11
9.0×10^10
6.0×10^10
3.0×10^10
0.0
*
LPS (50 ng/ml) + + + + + +
BPTES (10 μM) - + - - + -
CB839 (10 μM) - - + - - +
Ceramide (50 μM) - - - + + +

Figure 4.5. EV release in immune-activated microglia is associated with sphingolipid metabolism.

BV2 cells were treated with 10 μM BPTES or 10 μM CB839 4 hours prior to LPS treatment overnight. BV2 cell regular medium was changed to serum-free DMEM medium when GLS1 inhibitors were added. Two hours prior to LPS treatment, 50 μM or 100 μM ceramide was added to BV2 cells. **(A)** Cell viability was measured after overnight treatment using MTS assay. **(B)** Protein lysates were collected from LPS-treated BV2 cells with or without GLS1 inhibitors or ceramide. GLS1 activities were determined by the enzyme activity assay. **(C)** After 50 μM ceramide treatment, Nanoparticle tracking analysis was conduct with 100 X dilution of collected EVs with filtered PBS. Quantifications of the NanoSight NTA of vesicle concentration for samples from LPS-treated BV2 cell with GLS1 inhibitors and ceramide. * and *** denotes $p < 0.05$ and 0.001, compared with that of the control. ### denotes $p < 0.001$ compared with that of the LPS-treated group.

Chapter 5

General summary and future directions

5.1 Summary and General Discussion

Chronic neuroinflammation has been a hallmark of HAND, despite advances in HARRT. As such, a certain extent of cognitive impairment still exists and greatly affects patient quality of life. As the HIV-1 virus does not directly infect neurons, neuronal injury and synaptic damage are attributed to the HIV-1-infected macrophages and microglia, which are believed to be the reservoir of HIV-1 [42, 224, 225]. Among HIV-1-infected macrophages and microglia, the production and release of the soluble neurotoxic factor, glutamate, is known to contribute to the induction of extensive neuronal injury and brain inflammation [46, 50, 72, 74, 226, 227].

Over last decade, our lab has focused on the study of GLS1 in HAND. Significant evidence indicates that during HIV-1 infection GLS1 is upregulated and translocated from the inner membrane of mitochondria to cytosol [149]. GLS1 has also been detected in extracellular supernatants [188]. However, it was unknown how GLS1 is released from cytosol to extracellular space. Therefore, as discussed in chapter two, we investigated the role of EVs in carrying GLS1 as a cargo and as a facilitator of GLS1 release. We have shown that GLS1-containing EVs are able to acquire the GLS1 activity and generate more glutamate in the extracellular space or *ex vivo*. Using RP-HPLC to detect the level of glutamate in incubated EV supernatants, the production of glutamate was reversed by the addition of GLS1 inhibitors, which suggests GLS1 in EVs contributes to the generation of the excess levels of glutamate. The location of GLS1 in EVs remains undetermined. However, the detection of vGLUT1 in EVs

from macrophages and microglia suggests that during the budding of EVs from the plasma membrane, a transporter for glutamate is also translocated on the EVs. This facilitates the possible GLS1 activity in the EVs. The other contents in the EVs isolated from HIV-1-infected macrophages or immune-activated microglia have not been reported in the database for EVs, or exosomes online, which indicates the urgent need for detailed analysis of EV contents.

Interestingly, during the investigation of GLS1 release, we found that the presence of GLS1 inhibitors in the whole cell cultures not only affects the intracellular and extracellular glutamate level but also affect the level of EV secretion. A recent study reported that the production of EVs and their cargo could be interactively associated and regulated in retinal epithelial cells [228]. Therefore, we decided to investigate whether the EV cargo, GLS1 can also be involved in the regulation of EV release. An adenovirus construct was generated to overexpress both GLS1 isoforms, KGA and GAC in cells. The overexpression of GLS1 significantly increases the GLS1 activity and glutamate generation intracellularly and extracellularly. More importantly, the secretion of EVs was increased upon overexpression of GLS1, indicating the potential regulation of GLS1 in EV release. To further prove our hypothesis, we tested GLS1 inhibitors, BPTES, CB839, L-DON and CBX, a newly discovered blocker in HeLa cells, HIV-1-infected macrophages and immune-activated murine and human microglia. The inhibition of GLS1 significantly attenuates the release of EVs in all these types of cells, where GLS1 also is released in EV as cargos. This regulation

prompted us to further study what can be the potential mechanism of GLS1 regulating EV secretion.

The most direct link is the production of GLS, glutamate, which is affected instantly by the addition of GLS1 inhibitors. When different concentrations of glutamate were added, we did not observe a dose-dependent EV release. However, when glutamine was deprived, the EV level was significantly reduced, indicating the essential role of glutamine in the secretion of EVs. Glutamate is also known as a substrate that will be converted into α-ketoglutarate, which is a key intermediate of TCA cycle and Krebs cycle. Therefore, we added α-KG to LPS-treated BV2 cells with or without GLS1 inhibitors. The results showed that the α-KG along to control or LPS treated BV2 cells did not increase the level of EV release, where glutamine was present and glutamate production was not suppressed. However, when GLS1 inhibitors were added to LPS-stimulated BV2 cells, the GLS1 activity was significantly reduced and the release of EV was significantly decreased. When α-KG was added to the culture, the GLS1 activity was still reduced, indicating α-KG did not interrupt the function of GLS1 inhibitors. However, the release of EV was rescued from the inhibition of GLS1 blockers, which suggests α-KG as a downstream effector for the regulation of EVs. Further investigation is still needed to test the level of extracellular glutamate and intracellular glutamate level to determine whether α-KG rescues the EV release by reverse reproducing glutamate or a direct effector on further downstream pathways. Since both glutamine metabolism and α-KG have been know as

important energy sources, the role of energy production could be linked in this mechanism.

Previously, we have proven that the inhibition of ceramide production can prohibit the secretion of EVs to the extracellular space and thus rescue the GLS1-associated glutamate-induced neurotoxicity. Ceramide has been believed to be involved the formation of multivesicular bodies [134]. EVs have been reported to be secreted in a ceramide-dependent pathway. However, the association between GLS1-regulated EV release and ceramide has not been investigated. Therefore, 50 μM of ceramide was added to GLS1-inhibitors treated BV2 cells after LPS stimulation. The ceramide tended to rescue the reduced EV release after GLS1 inhibition. However, the effect is not as significant as α-KG. One possibility is that α-KG could be more direct downstream of EV release. More important questions are what the association between α-KG and ceramide is unclear and what the link between the glutamine metabolism and sphingolipid metabolism remains to be elucidated.

With the evidence of the important role of GLS1 in the regulation of EV secretion *in vitro*, we also testify its regulation *in vivo*. Over last 5 years, we have developed, generated and characterized a GLS1-overexpressing mice model to better study HAND pathogenesis. These Nestin-GAC mice showed a significant increase of GAC and intracellular glutamate specifically in brain areas, including the hippocampus, cortex, midbrain and cerebellum but not in kidney. The Nestin-GAC mice exhibited significant cognitive impairment in learning and memory. Increasing apoptosis and gliosis were also found in this model correlated with the

increasing amount of glutamate. More importantly, EV release in the brain was detected increased. This observation gives us a great inspiration that by inhibiting EV release and GLS1 release through GLS1 inhibitors, we can study the potential rescue effect from glutamate-associated neuronal injury. This *in vivo* study can truly provide an insight of the pathogenesis of HAND and further a therapeutic target and potential treatment for HAND.

Taken together, these results demonstrate a better understanding of the pathogenic role of GLS1 and EV in HIV-1-infected macrophages and microglia-related to HAND (Fig 5.1). The importance of glutamate-associated neurotoxicity and neuronal injury has merged to be an important target for HAND patients. EVs are no longer considered as a biomarker or degrading mechanism for unwanted cellular compartments but present as a critical pathogenic component during neuroinflammation and immune activation. The understanding of the mechanism of EV release, GLS1, glutamine metabolism and sphingolipid metabolism definitely sheds light on to a potential pathway not only in neuroscience but also in cancer research and other broader aspects.

5.2 Future directions

5.2.1 The role of EVs in macrophage/microglia-specific GLS1-overexpressing mice

For this study, we focused on the regulation of EV release in macrophages and microglia *in vitro*. When studying this phenomenon *in vivo*, due to the limitation of our mouse model, we utilized the Nestin-GAC and Thy1-GAC mouse to assess the effect of GLS1 on EV release. These two models majorly overexpress GLS1 in most of the regions of the brain. However, to further investigate the regulation of EV release in macrophages and microglia, we are in the process of generating the macrophage-specific and microglia-specific GAC-overexpressing mice to better study the specific role of GLS1 in the release of EVs *in vivo*. We will compare the behavioral impairment of the macrophage-specific and microglia-specific GAC-overexpressing mice with that of the Nestin-GAC mouse model. We will also examine the expression of GLS1 and intracellular glutamate levels in different regions of the mouse brain. Furthermore, the level of EV release will be assessed and compared using TEM, nanoparticle analysis and Western blot. GW4869, an inhibitor of neutral sphingomyelinase and EV release will be injected intraperitoneally into the mice immediately after the induction of GLS1 overexpression to evaluate the change in neuroinflammation and EV release in the brain. Furthermore, the GLS1 inhibitors, including CBX, BPTES and CB839, will also be injected to further assess the role in the regulation of EV release. The levels of sphingolipids in the brain from different treatments will also be determined and compared using mass

spectrometry. These future experiments will further expand our knowledge of GLS1 regulating EV release *in vivo*.

5.2.2 The role of EVs in GLS1 cKO mice

The previous generation of GLS1 KO mice was not successful due to the lethal developmental deficiencies in the respiratory system. This has caused additional challenge for further investigations into GLS1 functions and its mechanisms. Therefore, we are in the process of generating GLS1 conditional KO mice by crossing the GLS1-floxed mice with Csf1R-CreER mice. In this new Csf1R-GLS1$^{-/-}$ mouse model, GLS1 will be knocked out specifically from macrophages and microglia with temporal control of tamoxifen. The level of EV release from the mice brain will be assessed. Furthermore, we will cross the Csf1R-GLS1$^{-/-}$ mouse with HIV-Tat transgenic mice to investigate the effects of deletion of GLS1 in macrophages and microglia. Specifically we will be looking at reversing the destructive effects of the HIV-Tat mouse by assessing the behavioral parameters, brain inflammation levels, and electrophysiological functions. The release of EVs will also be examined to further confirm the role of GLS1 in the regulation of EV release. If our hypothesis is proven to be true, the newly developed GLS1 inhibitors from our lab could be a novel therapeutic method for HAND patients.

5.2.3 The role of extracellular vesicles in astrocytes

In the general microenvironment of the brain, astrocytes are abundant and play a crucial role during inflammation and neurodegenerative disease. In HAND, reports show that astrocytes contribute to CNS damage through the toxic and pro-apoptotic signaling to neighboring cells. During HIV infection, the glutamate metabolism and transportation is impaired in astrocytes, which further leads to access extracellular levels of glutamate. Additionally, astrocytes release EVs that contains ATP, lipid droplets, and miRNA that induces neurotoxicity. Our preliminary data has shown that the treatment of TNF-α and IL-1β on astrocytes alters the level of GLS1 and consequently the release of EVs. Interestingly, the GLS1 inhibitors, BPTES and CBX reversed the elevated EV release, which further indicating the regulation of EV release via GLS1.

5.2.4 The role of extracellular vesicles in stem cell biology

GLS1 has also gained significant attention in cancer research as a therapeutic target [204, 229, 230]. Aberrant glutamine metabolism has been found in many neoplastic cells, and has been noted to promote the proliferation, transformation, invasion and metastasis of said neoplastic cells [174, 231-234]. Interestingly, EVs released from neoplasms have been reported to modify the cancer stem cells (CSCs) niche via the promotion of angiogenesis, tumor cell proliferation and metastasis [235-239]. EVs isolated from body fluids of cancer patients, including blood, ascites fluid, urine, and CSF, can modulate the metastatic niche through various growth factors and cytokines. EVs have also been utilized in the study of neurogenesis and stem cell therapy. However, the

direct role of EVs in the neurogenic niches has not yet been addressed. Potential roles include cellular and molecular mechanisms of exosomal regulation

A casual relationship between neurogenesis and neurodegenerative diseases has been revealed. In this case, the strong association of EVs and various neurodegenerative disorders, such as AD, PD, Prion disease and HAND provides the evidence that EVs may also play an important role in the neurogenic role in the brain microenvironment as powerful regulators, biomarkers, and therapeutic targets. Furthermore, our lab has reported that GLS1 is essential for the differentiation, survival and proliferation of human neural progenitor cells. This indicates the potential correlation between EVs, GLS1 and neural stem cell biology, which would be a novel future project.

5.3 Tables and Figures

Figure 5.1

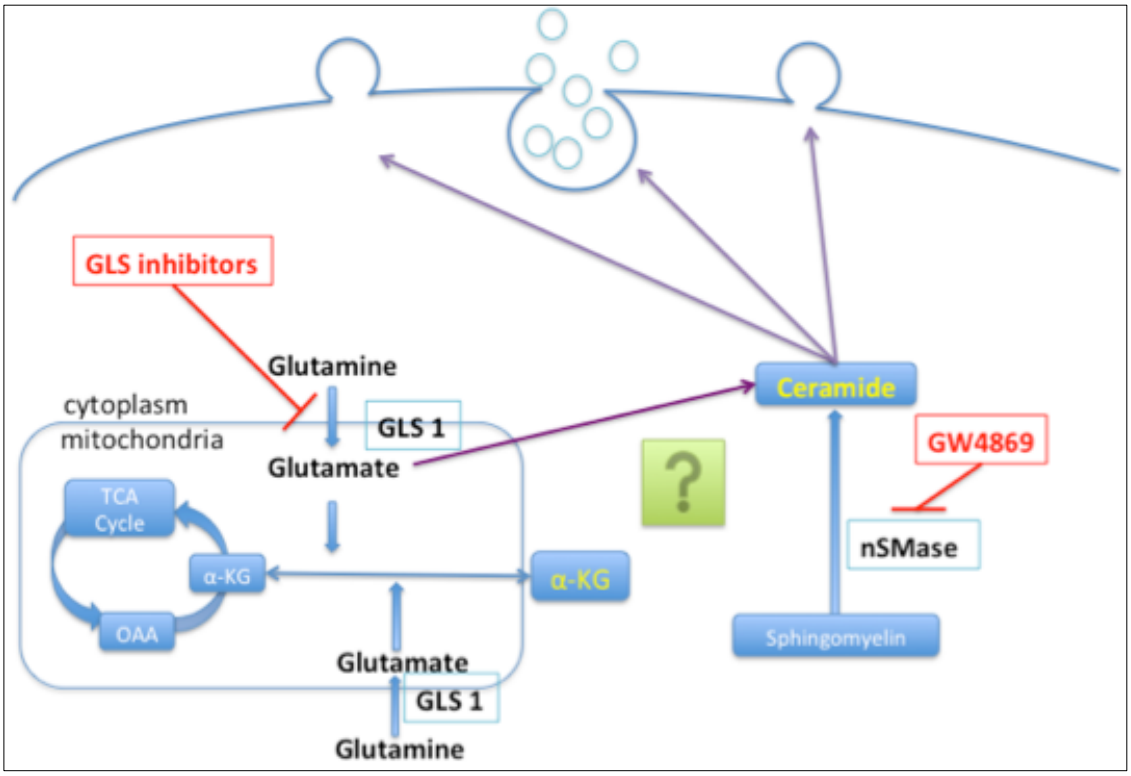

Figure 5.1 Scheme of EV release associated with GLS1, glutamine and sphingolipid metabolism.

Acknowledgments

First, I would like to express my most sincere gratitude to my advisor Dr. Jialin Zheng for his mentoring over the last five years of PhD study. Without his encouragement and support, I would not be able to complete my study and reach my goals. He has helped me to solve a lot of puzzles and problems during the process of my research in academic aspects and in extracurricular aspects. His enthusiasm and devotion to science has inspired me to be more diligent and look up to him. Second, I would like to thank my instructor/direct supervisor, Dr. Yunlong Huang. He has been patiently working with from the very first day of my rotation in the lab. He has spent substantial amount of time working with me and brainstorm for my projects. He taught me how to do procedures, how to design experiments, how to analyze data and how to trouble shoot. Third, I can't express how much I appreciate my extremely supportive committee members, Dr. Andrew Dudley, Dr. Daniel Monaghan, Dr. Dong Wang and Dr. Shelly Smith. They have given me so much valuable suggestions and continuous support in my research, career development, and future plan.

I would like to extend my special thanks to our collaborators, Dr. Norman Curthoys, Dr. Kurt Hauser and Dr. Yong Zhao. They have provided us so much great advice and critical research tools. Aside from that, I have many thanks to our current and former lab members of Zheng laboratory, and also Dr. Alexander Braun and Dr. Myron Toews for their great supports. Furthermore, I would like to thank the UNMC Comparative Medicine, NanoSight Core and EM core facilities for providing fantastic technical support. Further gratitude is towards the Chinese

Scholarship Council, the Department of Pharmacology and Experimental Neuroscience, and the Asia Pacific Rim Development Program. Without their support, I would not be able to complete my PhD study in UNMC. Finally, I would not achieve what I am without my beloved family in China and US.

Reference:

1. **Mediouni S, Marcondes MC, Miller C, McLaughlin JP, Valente ST: The cross-talk of HIV-1 Tat and methamphetamine in HIV-associated neurocognitive disorders. *Frontiers in microbiology* 2015, 6:1164.**
2. **Tan IL, Smith BR, von Geldern G, Mateen FJ, McArthur JC: HIV-associated opportunistic infections of the CNS. *The Lancet Neurology* 2012, 11:605-617.**
3. **Nightingale S, Winston A, Letendre S, Michael BD, McArthur JC, Khoo S, Solomon T: Controversies in HIV-associated neurocognitive disorders. *The Lancet Neurology* 2014, 13:1139-1151.**
4. **Elbirt D, Mahlab-Guri K, Bezalel-Rosenberg S, Gill H, Attali M, Asher I: HIV-associated neurocognitive disorders (HAND). *The Israel Medical Association journal : IMAJ* 2015, 17:54-59.**
5. **McArthur JC, Haughey N, Gartner S, Conant K, Pardo C, Nath A, Sacktor N: Human immunodeficiency virus-associated dementia: an evolving disease. *Journal of neurovirology* 2003, 9:205-221.**
6. **Antinori A, Arendt G, Becker JT, Brew BJ, Byrd DA, Cherner M, Clifford DB, Cinque P, Epstein LG, Goodkin K, et al: Updated research nosology for HIV-associated neurocognitive disorders. *Neurology* 2007, 69:1789-1799.**
7. **McArthur JC, Steiner J, Sacktor N, Nath A: Human immunodeficiency virus-associated neurocognitive disorders: Mind the gap. *Annals of neurology* 2010, 67:699-714.**

8. **Letendre S, Ances B, Gibson S, Ellis RJ: Neurologic complications of HIV disease and their treatment. *Topics in HIV medicine : a publication of the International AIDS Society, USA* 2007, 15:32-39.**

9. **Boisse L, Gill MJ, Power C: HIV infection of the central nervous system: clinical features and neuropathogenesis. *Neurologic clinics* 2008, 26:799-819, x.**

10. **Michaud V, Bar-Magen T, Turgeon J, Flockhart D, Desta Z, Wainberg MA: The dual role of pharmacogenetics in HIV treatment: mutations and polymorphisms regulating antiretroviral drug resistance and disposition. *Pharmacological reviews* 2012, 64:803-833.**

11. **Roquebert B, Malet I, Wirden M, Tubiana R, Valantin MA, Simon A, Katlama C, Peytavin G, Calvez V, Marcelin AG: Role of HIV-1 minority populations on resistance mutational pattern evolution and susceptibility to protease inhibitors. *AIDS* 2006, 20:287-289.**

12. **Varatharajan L, Thomas SA: The transport of anti-HIV drugs across blood-CNS interfaces: summary of current knowledge and recommendations for further research. *Antiviral research* 2009, 82:A99-109.**

13. **Persidsky Y, Poluektova L: Immune privilege and HIV-1 persistence in the CNS. *Immunological reviews* 2006, 213:180-194.**

14. **Burdo TH, Lackner A, Williams KC: Monocyte/macrophages and their role in HIV neuropathogenesis. *Immunological reviews* 2013, 254:102-113.**

15. **Letendre SL, Ellis RJ, Ances BM, McCutchan JA: Neurologic complications of HIV disease and their treatment. *Topics in HIV medicine : a publication of the International AIDS Society, USA* 2010, 18:45-55.**

16. **Pardo CA, McArthur JC, Griffin JW: HIV neuropathy: insights in the pathology of HIV peripheral nerve disease. *Journal of the peripheral nervous system : JPNS* 2001, 6:21-27.**

17. **Lv Z, Chu Y, Wang Y: HIV protease inhibitors: a review of molecular selectivity and toxicity. *HIV AIDS (Auckl)* 2015, 7:95-104.**

18. **Underwood J, Robertson KR, Winston A: Could antiretroviral neurotoxicity play a role in the pathogenesis of cognitive impairment in treated HIV disease? *AIDS* 2015, 29:253-261.**

19. **Sacktor N, Lyles RH, Skolasky R, Kleeberger C, Selnes OA, Miller EN, Becker JT, Cohen B, McArthur JC: HIV-associated neurologic disease incidence changes:: Multicenter AIDS Cohort Study, 1990-1998. *Neurology* 2001, 56:257-260.**

20. **Haase AT: The AIDS lentivirus connection. *Microbial pathogenesis* 1986, 1:1-4.**

21. **Masliah E, Achim CL, Ge N, DeTeresa R, Terry RD, Wiley CA: Spectrum of human immunodeficiency virus-associated neocortical damage. *Annals of neurology* 1992, 32:321-329.**

22. **Persidsky Y, Buttini M, Limoges J, Bock P, Gendelman HE: An analysis of HIV-1-associated inflammatory products in brain tissue of**

humans and SCID mice with HIV-1 encephalitis. *Journal of neurovirology* 1997, 3:401-416.

23. Zink WE, Anderson E, Boyle J, Hock L, Rodriguez-Sierra J, Xiong H, Gendelman HE, Persidsky Y: Impaired spatial cognition and synaptic potentiation in a murine model of human immunodeficiency virus type 1 encephalitis. *The Journal of neuroscience : the official journal of the Society for Neuroscience* 2002, 22:2096-2105.

24. Gelman BB: Neuropathology of HAND With Suppressive Antiretroviral Therapy: Encephalitis and Neurodegeneration Reconsidered. *Current HIV/AIDS reports* 2015, 12:272-279.

25. Williams K, Alvarez X, Lackner AA: Central nervous system perivascular cells are immunoregulatory cells that connect the CNS with the peripheral immune system. *Glia* 2001, 36:156-164.

26. Sharer LR, Cho ES, Epstein LG: Multinucleated giant cells and HTLV-III in AIDS encephalopathy. *Human pathology* 1985, 16:760.

27. Budka H: Multinucleated giant cells in brain: a hallmark of the acquired immune deficiency syndrome (AIDS). *Acta neuropathologica* 1986, 69:253-258.

28. Navia BA, Cho ES, Petito CK, Price RW: The AIDS dementia complex: II. Neuropathology. *Annals of neurology* 1986, 19:525-535.

29. Ketzler S, Weis S, Haug H, Budka H: Loss of neurons in the frontal cortex in AIDS brains. *Acta neuropathologica* 1990, 80:92-94.

30. Masliah E, Ge N, Achim CL, Hansen LA, Wiley CA: Selective neuronal vulnerability in HIV encephalitis. *Journal of neuropathology and experimental neurology* 1992, 51:585-593.

31. Manji H, Jager HR, Winston A: HIV, dementia and antiretroviral drugs: 30 years of an epidemic. *Journal of neurology, neurosurgery, and psychiatry* 2013, 84:1126-1137.

32. Price RW, Spudich SS, Peterson J, Joseph S, Fuchs D, Zetterberg H, Gisslen M, Swanstrom R: Evolving character of chronic central nervous system HIV infection. *Seminars in neurology* 2014, 34:7-13.

33. Canizares S, Cherner M, Ellis RJ: HIV and aging: effects on the central nervous system. *Seminars in neurology* 2014, 34:27-34.

34. Gray F, Adle-Biassette H, Brion F, Ereau T, le Maner I, Levy V, Corcket G: Neuronal apoptosis in human immunodeficiency virus infection. *Journal of neurovirology* 2000, 6 Suppl 1:S38-43.

35. Takahashi K, Wesselingh SL, Griffin DE, McArthur JC, Johnson RT, Glass JD: Localization of HIV-1 in human brain using polymerase chain reaction/in situ hybridization and immunocytochemistry. *Annals of neurology* 1996, 39:705-711.

36. Thompson KA, Churchill MJ, Gorry PR, Sterjovski J, Oelrichs RB, Wesselingh SL, McLean CA: Astrocyte specific viral strains in HIV dementia. *Annals of neurology* 2004, 56:873-877.

37. Ma M, Geiger JD, Nath A: Characterization of a novel binding site for the human immunodeficiency virus type 1 envelope protein gp120 on human fetal astrocytes. *Journal of virology* 1994, 68:6824-6828.

38. Di Rienzo AM, Aloisi F, Santarcangelo AC, Palladino C, Olivetta E, Genovese D, Verani P, Levi G: Virological and molecular parameters of HIV-1 infection of human embryonic astrocytes. *Archives of virology* 1998, 143:1599-1615.

39. Tornatore C, Chandra R, Berger JR, Major EO: HIV-1 infection of subcortical astrocytes in the pediatric central nervous system. *Neurology* 1994, 44:481-487.

40. Conant K, Tornatore C, Atwood W, Meyers K, Traub R, Major EO: In vivo and in vitro infection of the astrocyte by HIV-1. *Advances in neuroimmunology* 1994, 4:287-289.

41. Koenig S, Gendelman HE, Orenstein JM, Dal Canto MC, Pezeshkpour GH, Yungbluth M, Janotta F, Aksamit A, Martin MA, Fauci AS: Detection of AIDS virus in macrophages in brain tissue from AIDS patients with encephalopathy. *Science* 1986, 233:1089-1093.

42. Gendelman HE, Persidsky Y, Ghorpade A, Limoges J, Stins M, Fiala M, Morrisett R: The neuropathogenesis of the AIDS dementia complex. *AIDS* 1997, 11 Suppl A:S35-45.

43. Nath A, Geiger J: Neurobiological aspects of human immunodeficiency virus infection: neurotoxic mechanisms. *Progress in neurobiology* 1998, 54:19-33.

44. Zheng J, Gendelman HE: The HIV-1 associated dementia complex: a metabolic encephalopathy fueled by viral replication in mononuclear phagocytes. *Current opinion in neurology* 1997, 10:319-325.

45. Conant K, Garzino-Demo A, Nath A, McArthur JC, Halliday W, Power C, Gallo RC, Major EO: Induction of monocyte chemoattractant protein-1 in HIV-1 Tat-stimulated astrocytes and elevation in AIDS dementia. *Proceedings of the National Academy of Sciences of the United States of America* 1998, 95:3117-3121.

46. Giulian D, Wendt E, Vaca K, Noonan CA: The envelope glycoprotein of human immunodeficiency virus type 1 stimulates release of neurotoxins from monocytes. *Proceedings of the National Academy of Sciences of the United States of America* 1993, 90:2769-2773.

47. Takikita S, Takano T, Narita T, Takikita M, Ohno M, Shimada M: Neuronal apoptosis mediated by IL-1 beta expression in viral encephalitis caused by a neuroadapted strain of the mumps virus (Kilham Strain) in hamsters. *Experimental neurology* 2001, 172:47-59.

48. Viviani B, Bartesaghi S, Corsini E, Galli CL, Marinovich M: Cytokines role in neurodegenerative events. *Toxicology letters* 2004, 149:85-89.

49. Huang Y, Erdmann N, Peng H, Zhao Y, Zheng J: The role of TNF related apoptosis-inducing ligand in neurodegenerative diseases. *Cellular & molecular immunology* 2005, 2:113-122.

50. Sui Z, Sniderhan LF, Schifitto G, Phipps RP, Gelbard HA, Dewhurst S, Maggirwar SB: Functional synergy between CD40 ligand and HIV-1

Tat contributes to inflammation: implications in HIV type 1 dementia. *J Immunol* 2007, 178:3226-3236.

51. Smith JA, Das A, Ray SK, Banik NL: Role of pro-inflammatory cytokines released from microglia in neurodegenerative diseases. *Brain research bulletin* 2012, 87:10-20.

52. Glass JD, Johnson RT: Human immunodeficiency virus and the brain. *Annual review of neuroscience* 1996, 19:1-26.

53. Huang Y, Zhao L, Jia B, Wu L, Li Y, Curthoys N, Zheng JC: Glutaminase dysregulation in HIV-1-infected human microglia mediates neurotoxicity: relevant to HIV-1-associated neurocognitive disorders. *The Journal of neuroscience : the official journal of the Society for Neuroscience* 2011, 31:15195-15204.

54. Batchelor PE, Liberatore GT, Wong JY, Porritt MJ, Frerichs F, Donnan GA, Howells DW: Activated macrophages and microglia induce dopaminergic sprouting in the injured striatum and express brain-derived neurotrophic factor and glial cell line-derived neurotrophic factor. *The Journal of neuroscience : the official journal of the Society for Neuroscience* 1999, 19:1708-1716.

55. Soontornniyomkij V, Wang G, Pittman CA, Wiley CA, Achim CL: Expression of brain-derived neurotrophic factor protein in activated microglia of human immunodeficiency virus type 1 encephalitis. *Neuropathology and applied neurobiology* 1998, 24:453-460.

56. Peng H, Erdmann N, Whitney N, Dou H, Gorantla S, Gendelman HE, Ghorpade A, Zheng J: HIV-1-infected and/or immune activated macrophages regulate astrocyte SDF-1 production through IL-1beta. *Glia* 2006, 54:619-629.

57. Tornatore C, Nath A, Amemiya K, Major EO: Persistent human immunodeficiency virus type 1 infection in human fetal glial cells reactivated by T-cell factor(s) or by the cytokines tumor necrosis factor alpha and interleukin-1 beta. *Journal of virology* 1991, 65:6094-6100.

58. Moses AV, Bloom FE, Pauza CD, Nelson JA: Human immunodeficiency virus infection of human brain capillary endothelial cells occurs via a CD4/galactosylceramide-independent mechanism. *Proceedings of the National Academy of Sciences of the United States of America* 1993, 90:10474-10478.

59. Wiley CA, Schrier RD, Nelson JA, Lampert PW, Oldstone MB: Cellular localization of human immunodeficiency virus infection within the brains of acquired immune deficiency syndrome patients. *Proceedings of the National Academy of Sciences of the United States of America* 1986, 83:7089-7093.

60. Strizki JM, Albright AV, Sheng H, O'Connor M, Perrin L, Gonzalez-Scarano F: Infection of primary human microglia and monocyte-derived macrophages with human immunodeficiency virus type 1

isolates: evidence of differential tropism. *Journal of virology* 1996, 70:7654-7662.

61. Perno CF, Crowe SM, Kornbluth RS: A continuing enigma: the role of cells of macrophage lineage in the development of HIV disease. *Journal of leukocyte biology* 1997, 62:1-3.

62. Aquaro S, Panti S, Caroleo MC, Balestra E, Cenci A, Forbici F, Ippolito G, Mastino A, Testi R, Mollace V, et al: Primary macrophages infected by human immunodeficiency virus trigger CD95-mediated apoptosis of uninfected astrocytes. *Journal of leukocyte biology* 2000, 68:429-435.

63. Gelbard HA, Nottet HS, Swindells S, Jett M, Dzenko KA, Genis P, White R, Wang L, Choi YB, Zhang D, et al.: Platelet-activating factor: a candidate human immunodeficiency virus type 1-induced neurotoxin. *Journal of virology* 1994, 68:4628-4635.

64. Perry SW, Hamilton JA, Tjoelker LW, Dbaibo G, Dzenko KA, Epstein LG, Hannun Y, Whittaker JS, Dewhurst S, Gelbard HA: Platelet-activating factor receptor activation. An initiator step in HIV-1 neuropathogenesis. *The Journal of biological chemistry* 1998, 273:17660-17664.

65. Nishida K, Markey SP, Kustova Y, Morse HC, 3rd, Skolnick P, Basile AS, Sei Y: Increased brain levels of platelet-activating factor in a murine acquired immune deficiency syndrome are NMDA receptor-mediated. *Journal of neurochemistry* 1996, 66:433-435.

66. **Nottet HS, Jett M, Flanagan CR, Zhai QH, Persidsky Y, Rizzino A, Bernton EW, Genis P, Baldwin T, Schwartz J, et al.: A regulatory role for astrocytes in HIV-1 encephalitis. An overexpression of eicosanoids, platelet-activating factor, and tumor necrosis factor-alpha by activated HIV-1-infected monocytes is attenuated by primary human astrocytes. *J Immunol* 1995, 154:3567-3581.**

67. **Gelbard HA, Dzenko KA, DiLoreto D, del Cerro C, del Cerro M, Epstein LG: Neurotoxic effects of tumor necrosis factor alpha in primary human neuronal cultures are mediated by activation of the glutamate AMPA receptor subtype: implications for AIDS neuropathogenesis. *Developmental neuroscience* 1993, 15:417-422.**

68. **Heyes MP, Saito K, Lackner A, Wiley CA, Achim CL, Markey SP: Sources of the neurotoxin quinolinic acid in the brain of HIV-1-infected patients and retrovirus-infected macaques. *FASEB journal : official publication of the Federation of American Societies for Experimental Biology* 1998, 12:881-896.**

69. **Kerr SJ, Armati PJ, Brew BJ: Neurocytotoxity of quinolinic acid in human brain cultures. *Journal of neurovirology* 1995, 1:375-380.**

70. **Adamson DC, Wildemann B, Sasaki M, Glass JD, McArthur JC, Christov VI, Dawson TM, Dawson VL: Immunologic NO synthase: elevation in severe AIDS dementia and induction by HIV-1 gp41. *Science* 1996, 274:1917-1921.**

71. Jiang Z, Piggee C, Heyes MP, Murphy C, Quearry B, Bauer M, Zheng J, Gendelman HE, Markey SP: Glutamate is a mediator of neurotoxicity in secretions of activated HIV- 1-infected macrophages. *Journal of neuroimmunology* 2001, 117:97-107.

72. Zhao J, Lopez AL, Erichsen D, Herek S, Cotter RL, Curthoys NP, Zheng J: Mitochondrial glutaminase enhances extracellular glutamate production in HIV-1-infected macrophages: linkage to HIV-1 associated dementia. *Journal of neurochemistry* 2004, 88:169-180.

73. Boutin H, LeFeuvre RA, Horai R, Asano M, Iwakura Y, Rothwell NJ: Role of IL-1alpha and IL-1beta in ischemic brain damage. *The Journal of neuroscience : the official journal of the Society for Neuroscience* 2001, 21:5528-5534.

74. Kaul M, Garden GA, Lipton SA: Pathways to neuronal injury and apoptosis in HIV-associated dementia. *Nature* 2001, 410:988-994.

75. Matusevicius D, Navikas V, Soderstrom M, Xiao BG, Haglund M, Fredrikson S, Link H: Multiple sclerosis: the proinflammatory cytokines lymphotoxin-alpha and tumour necrosis factor-alpha are upregulated in cerebrospinal fluid mononuclear cells. *Journal of neuroimmunology* 1996, 66:115-123.

76. Navikas V, Matusevicius D, Soderstrom M, Fredrikson S, Kivisakk P, Ljungdahl A, Hojeberg B, Link H: Increased interleukin-6 mRNA expression in blood and cerebrospinal fluid mononuclear cells in multiple sclerosis. *Journal of neuroimmunology* 1996, 64:63-69.

77. **Meda L, Baron P, Prat E, Scarpini E, Scarlato G, Cassatella MA, Rossi F: Proinflammatory profile of cytokine production by human monocytes and murine microglia stimulated with beta-amyloid[25-35].** ***Journal of neuroimmunology*** **1999, 93:45-52.**

78. **Ye L, Huang Y, Zhao L, Li Y, Sun L, Zhou Y, Qian G, Zheng JC: IL-1beta and TNF-alpha induce neurotoxicity through glutamate production: a potential role for neuronal glutaminase.** ***Journal of neurochemistry*** **2013, 125:897-908.**

79. **Erecinska M, Silver IA: Metabolism and role of glutamate in mammalian brain.** ***Progress in neurobiology*** **1990, 35:245-296.**

80. **Komuro H, Rakic P: Intracellular Ca2+ fluctuations modulate the rate of neuronal migration.** ***Neuron*** **1996, 17:275-285.**

81. **LoTurco JJ, Blanton MG, Kriegstein AR: Initial expression and endogenous activation of NMDA channels in early neocortical development.** ***The Journal of neuroscience : the official journal of the Society for Neuroscience*** **1991, 11:792-799.**

82. **McEntee WJ, Crook TH: Glutamate: its role in learning, memory, and the aging brain.** ***Psychopharmacology*** **1993, 111:391-401.**

83. **Chua JJ, Kindler S, Boyken J, Jahn R: The architecture of an excitatory synapse.** ***Journal of cell science*** **2010, 123:819-823.**

84. **Boyken J, Gronborg M, Riedel D, Urlaub H, Jahn R, Chua JJ: Molecular profiling of synaptic vesicle docking sites reveals novel**

proteins but few differences between glutamatergic and GABAergic synapses. *Neuron* 2013, 78:285-297.

85. Karakas E, Regan MC, Furukawa H: Emerging structural insights into the function of ionotropic glutamate receptors. *Trends in biochemical sciences* 2015, 40:328-337.

86. Golubeva AV, Moloney RD, O'Connor RM, Dinan TG, Cryan JF: Metabotropic Glutamate Receptors in Central Nervous System Diseases. *Current drug targets* 2015.

87. Gegelashvili G, Schousboe A: Cellular distribution and kinetic properties of high-affinity glutamate transporters. *Brain research bulletin* 1998, 45:233-238.

88. Rose CF, Verkhratsky A, Parpura V: Astrocyte glutamine synthetase: pivotal in health and disease. *Biochemical Society transactions* 2013, 41:1518-1524.

89. Chaudhry FA, Schmitz D, Reimer RJ, Larsson P, Gray AT, Nicoll R, Kavanaugh M, Edwards RH: Glutamine uptake by neurons: interaction of protons with system a transporters. *The Journal of neuroscience : the official journal of the Society for Neuroscience* 2002, 22:62-72.

90. Didier M, Xu M, Berman SA, Saido TC, Bursztajn S: Involvement of three glutamate receptor epsilon subunits in the formation of N-methyl-D-aspartate receptors mediating excitotoxicity in primary

cultures of mouse cerebellar granule cells. *Neuroscience* 1997, 78:1129-1146.

91. Lipton SA, Yeh M, Dreyer EB: Update on current models of HIV-related neuronal injury: platelet-activating factor, arachidonic acid and nitric oxide. *Advances in neuroimmunology* 1994, 4:181-188.

92. Clifford DB, Ances BM: HIV-associated neurocognitive disorder. *The Lancet Infectious diseases* 2013, 13:976-986.

93. Haughey NJ, Mattson MP: Calcium dysregulation and neuronal apoptosis by the HIV-1 proteins Tat and gp120. *J Acquir Immune Defic Syndr* 2002, 31 Suppl 2:S55-61.

94. Foga IO, Nath A, Hasinoff BB, Geiger JD: Antioxidants and dipyridamole inhibit HIV-1 gp120-induced free radical-based oxidative damage to human monocytoid cells. *Journal of acquired immune deficiency syndromes and human retrovirology : official publication of the International Retrovirology Association* 1997, 16:223-229.

95. Lipton SA: Memantine prevents HIV coat protein-induced neuronal injury in vitro. *Neurology* 1992, 42:1403-1405.

96. Nath A, Haughey NJ, Jones M, Anderson C, Bell JE, Geiger JD: Synergistic neurotoxicity by human immunodeficiency virus proteins Tat and gp120: protection by memantine. *Annals of neurology* 2000, 47:186-194.

97. Fernandes SP, Edwards TM, Ng KT, Robinson SR: HIV-1 protein gp120 rapidly impairs memory in chicks by interrupting the glutamate-glutamine cycle. *Neurobiology of learning and memory* 2007, 87:1-8.

98. Zhou BY, Liu Y, Kim B, Xiao Y, He JJ: Astrocyte activation and dysfunction and neuron death by HIV-1 Tat expression in astrocytes. *Molecular and cellular neurosciences* 2004, 27:296-305.

99. Wang Z, Pekarskaya O, Bencheikh M, Chao W, Gelbard HA, Ghorpade A, Rothstein JD, Volsky DJ: Reduced expression of glutamate transporter EAAT2 and impaired glutamate transport in human primary astrocytes exposed to HIV-1 or gp120. *Virology* 2003, 312:60-73.

100. Su ZZ, Leszczyniecka M, Kang DC, Sarkar D, Chao W, Volsky DJ, Fisher PB: Insights into glutamate transport regulation in human astrocytes: cloning of the promoter for excitatory amino acid transporter 2 (EAAT2). *Proceedings of the National Academy of Sciences of the United States of America* 2003, 100:1955-1960.

101. Patton HK, Zhou ZH, Bubien JK, Benveniste EN, Benos DJ: gp120-induced alterations of human astrocyte function: Na(+)/H(+) exchange, K(+) conductance, and glutamate flux. *American journal of physiology Cell physiology* 2000, 279:C700-708.

102. Rao VL, Baskaya MK, Dogan A, Rothstein JD, Dempsey RJ: Traumatic brain injury down-regulates glial glutamate transporter

(GLT-1 and GLAST) proteins in rat brain. *Journal of neurochemistry* 1998, 70:2020-2027.

103. Killestein J, Kalkers NF, Polman CH: Glutamate inhibition in MS: the neuroprotective properties of riluzole. *Journal of the neurological sciences* 2005, 233:113-115.

104. Benveniste H: Glutamate, microdialysis, and cerebral ischemia: lost in translation? *Anesthesiology* 2009, 110:422-425.

105. Holcomb T, Taylor L, Trohkimoinen J, Curthoys NP: Isolation, characterization and expression of a human brain mitochondrial glutaminase cDNA. *Brain research Molecular brain research* 2000, 76:56-63.

106. Marquez J, Cardona C, Campos-Sandoval JA, Penalver A, Tosina M, Mates JM, Martin-Rufian M: Mammalian glutaminase isozymes in brain. *Metabolic brain disease* 2013, 28:133-137.

107. Mock B, Kozak C, Seldin MF, Ruff N, D'Hoostelaere L, Szpirer C, Levan G, Seuanez H, O'Brien S, Banner C: A glutaminase (gis) gene maps to mouse chromosome 1, rat chromosome 9, and human chromosome 2. *Genomics* 1989, 5:291-297.

108. Erdmann NB, Whitney NP, Zheng J: Potentiation of Excitotoxicity in HIV-1 Associated Dementia and the Significance of Glutaminase. *Clinical neuroscience research* 2006, 6:315-328.

109. Elgadi KM, Meguid RA, Qian M, Souba WW, Abcouwer SF: Cloning and analysis of unique human glutaminase isoforms generated by

tissue-specific alternative splicing. *Physiological genomics* 1999, 1:51-62.

110. Brosnan JT, Ewart HS, Squires SA: Hormonal control of hepatic glutaminase. *Advances in enzyme regulation* 1995, 35:131-146.

111. Tian C, Sun L, Jia B, Ma K, Curthoys N, Ding J, Zheng J: Mitochondrial glutaminase release contributes to glutamate-mediated neurotoxicity during human immunodeficiency virus-1 infection. *Journal of neuroimmune pharmacology : the official journal of the Society on NeuroImmune Pharmacology* 2012, 7:619-628.

112. Erdmann N, Tian C, Huang Y, Zhao J, Herek S, Curthoys N, Zheng J: In vitro glutaminase regulation and mechanisms of glutamate generation in HIV-1-infected macrophage. *Journal of neurochemistry* 2009, 109:551-561.

113. Zhao L, Huang Y, Tian C, Taylor L, Curthoys N, Wang Y, Vernon H, Zheng J: Interferon-alpha regulates glutaminase 1 promoter through STAT1 phosphorylation: relevance to HIV-1 associated neurocognitive disorders. *PloS one* 2012, 7:e32995.

114. Gould GW, Lippincott-Schwartz J: New roles for endosomes: from vesicular carriers to multi-purpose platforms. *Nature reviews Molecular cell biology* 2009, 10:287-292.

115. Klumperman J, Raposo G: The complex ultrastructure of the endolysosomal system. *Cold Spring Harbor perspectives in biology* 2014, 6:a016857.

116. Raposo G, Nijman HW, Stoorvogel W, Liejendekker R, Harding CV, Melief CJ, Geuze HJ: B lymphocytes secrete antigen-presenting vesicles. *The Journal of experimental medicine* 1996, 183:1161-1172.

117. Jaiswal JK, Andrews NW, Simon SM: Membrane proximal lysosomes are the major vesicles responsible for calcium-dependent exocytosis in nonsecretory cells. *The Journal of cell biology* 2002, 159:625-635.

118. Edgar BA, Zielke N, Gutierrez C: Endocycles: a recurrent evolutionary innovation for post-mitotic cell growth. *Nature reviews Molecular cell biology* 2014, 15:197-210.

119. Mathivanan S, Fahner CJ, Reid GE, Simpson RJ: ExoCarta 2012: database of exosomal proteins, RNA and lipids. *Nucleic acids research* 2012, 40:D1241-1244.

120. Batiz LF, Castro MA, Burgos PV, Velasquez ZD, Munoz RI, Lafourcade CA, Troncoso-Escudero P, Wyneken U: Exosomes as Novel Regulators of Adult Neurogenic Niches. *Frontiers in cellular neuroscience* 2015, 9:501.

121. Kim DK, Lee J, Kim SR, Choi DS, Yoon YJ, Kim JH, Go G, Nhung D, Hong K, Jang SC, et al: EVpedia: a community web portal for extracellular vesicles research. *Bioinformatics* 2015, 31:933-939.

122. Chaput N, Thery C: Exosomes: immune properties and potential clinical implementations. *Seminars in immunopathology* 2011, 33:419-440.

123. Thery C, Boussac M, Veron P, Ricciardi-Castagnoli P, Raposo G, Garin J, Amigorena S: Proteomic analysis of dendritic cell-derived exosomes: a secreted subcellular compartment distinct from apoptotic vesicles. *J Immunol* 2001, 166:7309-7318.

124. Nogueira E, Gomes AC, Preto A, Cavaco-Paulo A: Design of liposomal formulations for cell targeting. *Colloids and surfaces B, Biointerfaces* 2015, 136:514-526.

125. Cocucci E, Meldolesi J: Ectosomes and exosomes: shedding the confusion between extracellular vesicles. *Trends in cell biology* 2015, 25:364-372.

126. Moreno-Gonzalo O, Villarroya-Beltri C, Sanchez-Madrid F: Post-translational modifications of exosomal proteins. *Frontiers in immunology* 2014, 5:383.

127. Villarroya-Beltri C, Baixauli F, Gutierrez-Vazquez C, Sanchez-Madrid F, Mittelbrunn M: Sorting it out: regulation of exosome loading. *Seminars in cancer biology* 2014, 28:3-13.

128. Bobrie A, Colombo M, Raposo G, Thery C: Exosome secretion: molecular mechanisms and roles in immune responses. *Traffic* 2011, 12:1659-1668.

129. Thery C, Ostrowski M, Segura E: Membrane vesicles as conveyors of immune responses. *Nature reviews Immunology* 2009, 9:581-593.

130. Street JM, Barran PE, Mackay CL, Weidt S, Balmforth C, Walsh TS, Chalmers RT, Webb DJ, Dear JW: Identification and proteomic profiling of exosomes in human cerebrospinal fluid. *Journal of translational medicine* 2012, 10:5.

131. Grapp M, Wrede A, Schweizer M, Huwel S, Galla HJ, Snaidero N, Simons M, Buckers J, Low PS, Urlaub H, et al: Choroid plexus transcytosis and exosome shuttling deliver folate into brain parenchyma. *Nature communications* 2013, 4:2123.

132. Chiasserini D, van Weering JR, Piersma SR, Pham TV, Malekzadeh A, Teunissen CE, de Wit H, Jimenez CR: Proteomic analysis of cerebrospinal fluid extracellular vesicles: a comprehensive dataset. *Journal of proteomics* 2014, 106:191-204.

133. Hanson PI, Cashikar A: Multivesicular body morphogenesis. *Annual review of cell and developmental biology* 2012, 28:337-362.

134. Trajkovic K, Hsu C, Chiantia S, Rajendran L, Wenzel D, Wieland F, Schwille P, Brugger B, Simons M: Ceramide triggers budding of exosome vesicles into multivesicular endosomes. *Science* 2008, 319:1244-1247.

135. Santana SM, Antonyak MA, Cerione RA, Kirby BJ: Cancerous epithelial cell lines shed extracellular vesicles with a bimodal size

distribution that is sensitive to glutamine inhibition. *Physical biology* 2014, 11:065001.

136. Schuenke K, Gelman BB: Human microglial cell isolation from adult autopsy brain: brain pH, regional variation, and infection with human immunodeficiency virus type 1. *Journal of neurovirology* 2003, 9:346-357.

137. Ryan LA, Cotter RL, Zink WE, 2nd, Gendelman HE, Zheng J: Macrophages, chemokines and neuronal injury in HIV-1-associated dementia. *Cell Mol Biol (Noisy-le-grand)* 2002, 48:137-150.

138. Whitney NP, Eidem TM, Peng H, Huang Y, Zheng JC: Inflammation mediates varying effects in neurogenesis: relevance to the pathogenesis of brain injury and neurodegenerative disorders. *Journal of neurochemistry* 2009, 108:1343-1359.

139. Yamamoto C: [Memory, learning and glutamate receptor]. *Rinsho shinkeigaku = Clinical neurology* 1989, 29:1526-1528.

140. Schousboe A, Larsson OM, Frandsen A, Belhage B, Pasantes-Morales H, Krogsgaard-Larsen P: Neuromodulatory actions of glutamate, GABA and taurine: regulatory role of astrocytes. *Advances in experimental medicine and biology* 1991, 296:165-180.

141. Ghijsen WE, Leenders AG, Lopes da Silva FH: Regulation of vesicle traffic and neurotransmitter release in isolated nerve terminals. *Neurochemical research* 2003, 28:1443-1452.

142. Ollenschlager G, Jansen S, Schindler J, Rasokat H, Schrappe-Bacher M, Roth E: Plasma amino acid pattern of patients with HIV infection. *Clin Chem* 1988, 34:1787-1789.

143. Droge W, Eck HP, Betzler M, Naher H: Elevated plasma glutamate levels in colorectal carcinoma patients and in patients with acquired immunodeficiency syndrome (AIDS). *Immunobiology* 1987, 174:473-479.

144. Ferrarese C, Aliprandi A, Tremolizzo L, Stanzani L, De Micheli A, Dolara A, Frattola L: Increased glutamate in CSF and plasma of patients with HIV dementia. *Neurology* 2001, 57:671-675.

145. Ellis RJ, Moore DJ, Childers ME, Letendre S, McCutchan JA, Wolfson T, Spector SA, Hsia K, Heaton RK, Grant I: Progression to neuropsychological impairment in human immunodeficiency virus infection predicted by elevated cerebrospinal fluid levels of human immunodeficiency virus RNA. *Arch Neurol* 2002, 59:923-928.

146. Newcomb R, Sun X, Taylor L, Curthoys N, Giffard RG: Increased production of extracellular glutamate by the mitochondrial glutaminase following neuronal death. *The Journal of biological chemistry* 1997, 272:11276-11282.

147. McCall A, Glaeser BS, Millington W, Wurtman RJ: Monosodium glutamate neurotoxicity, hyperosmolarity, and blood-brain barrier dysfunction. *Neurobehavioral toxicology* 1979, 1:279-283.

148. Epstein LG, Gelbard HA: HIV-1-induced neuronal injury in the developing brain. *Journal of leukocyte biology* 1999, 65:453-457.

149. Tian C, Erdmann N, Zhao J, Cao Z, Peng H, Zheng J: HIV-infected macrophages mediate neuronal apoptosis through mitochondrial glutaminase. *Journal of neurochemistry* 2008, 105:994-1005.

150. Nicklas WJ, Zeevalk G, Hyndman A: Interactions between neurons and glia in glutamate/glutamine compartmentation. *Biochemical Society transactions* 1987, 15:208-210.

151. Ward HK, Thanki CM, Bradford HF: Glutamine and glucose as precursors of transmitter amino acids: ex vivo studies. *Journal of neurochemistry* 1983, 40:855-860.

152. Curthoys NP, Watford M: Regulation of glutaminase activity and glutamine metabolism. *Annu Rev Nutr* 1995, 15:133-159.

153. Thangavelu K, Pan CQ, Karlberg T, Balaji G, Uttamchandani M, Suresh V, Schuler H, Low BC, Sivaraman J: Structural basis for the allosteric inhibitory mechanism of human kidney-type glutaminase (KGA) and its regulation by Raf-Mek-Erk signaling in cancer cell metabolism. *Proceedings of the National Academy of Sciences of the United States of America* 2012, 109:7705-7710.

154. Cassago A, Ferreira AP, Ferreira IM, Fornezari C, Gomes ER, Greene KS, Pereira HM, Garratt RC, Dias SM, Ambrosio AL: Mitochondrial localization and structure-based phosphate activation mechanism of Glutaminase C with implications for cancer metabolism. *Proceedings*

of the National Academy of Sciences of the United States of America **2012, 109:1092-1097.**

155. Kadiu I, Narayanasamy P, Dash PK, Zhang W, Gendelman HE: Biochemical and biologic characterization of exosomes and microvesicles as facilitators of HIV-1 infection in macrophages. *J Immunol* 2012, 189:744-754.

156. Cocucci E, Racchetti G, Meldolesi J: Shedding microvesicles: artefacts no more. *Trends in cell biology* 2009, 19:43-51.

157. Darios F, Wasser C, Shakirzyanova A, Giniatullin A, Goodman K, Munoz-Bravo JL, Raingo J, Jorgacevski J, Kreft M, Zorec R, et al: Sphingosine facilitates SNARE complex assembly and activates synaptic vesicle exocytosis. *Neuron* 2009, 62:683-694.

158. Li B, Antonyak MA, Zhang J, Cerione RA: RhoA triggers a specific signaling pathway that generates transforming microvesicles in cancer cells. *Oncogene* 2012, 31:4740-4749.

159. van der Vos KE, Balaj L, Skog J, Breakefield XO: Brain tumor microvesicles: insights into intercellular communication in the nervous system. *Cellular and molecular neurobiology* 2011, 31:949-959.

160. Tetta C, Ghigo E, Silengo L, Deregibus MC, Camussi G: Extracellular vesicles as an emerging mechanism of cell-to-cell communication. *Endocrine* 2013, 44:11-19.

161. Fais S, Logozzi M, Lugini L, Federici C, Azzarito T, Zarovni N, Chiesi A: Exosomes: the ideal nanovectors for biodelivery. *Biological chemistry* 2013, 394:1-15.

162. Fruhbeis C, Frohlich D, Kuo WP, Kramer-Albers EM: Extracellular vesicles as mediators of neuron-glia communication. *Frontiers in cellular neuroscience* 2013, 7:182.

163. Joshi P, Turola E, Ruiz A, Bergami A, Libera DD, Benussi L, Giussani P, Magnani G, Comi G, Legname G, et al: Microglia convert aggregated amyloid-beta into neurotoxic forms through the shedding of microvesicles. *Cell death and differentiation* 2014, 21:582-593.

164. Saman S, Kim W, Raya M, Visnick Y, Miro S, Saman S, Jackson B, McKee AC, Alvarez VE, Lee NC, Hall GF: Exosome-associated tau is secreted in tauopathy models and is selectively phosphorylated in cerebrospinal fluid in early Alzheimer disease. *The Journal of biological chemistry* 2012, 287:3842-3849.

165. Jayachandran M, Litwiller RD, Lahr BD, Bailey KR, Owen WG, Mulvagh SL, Heit JA, Hodis HN, Harman SM, Miller VM: Alterations in platelet function and cell-derived microvesicles in recently menopausal women: relationship to metabolic syndrome and atherogenic risk. *Journal of cardiovascular translational research* 2011, 4:811-822.

166. Raymond AD, Campbell-Sims TC, Khan M, Lang M, Huang MB, Bond VC, Powell MD: HIV Type 1 Nef is released from infected cells in

CD45(+) microvesicles and is present in the plasma of HIV-infected individuals. *AIDS research and human retroviruses* 2011, 27:167-178.

167. Verderio C, Muzio L, Turola E, Bergami A, Novellino L, Ruffini F, Riganti L, Corradini I, Francolini M, Garzetti L, et al: Myeloid microvesicles are a marker and therapeutic target for neuroinflammation. *Annals of neurology* 2012, 72:610-624.

168. Gendelman HE, Orenstein JM, Martin MA, Ferrua C, Mitra R, Phipps T, Wahl LA, Lane HC, Fauci AS, Burke DS, et al.: Efficient isolation and propagation of human immunodeficiency virus on recombinant colony-stimulating factor 1-treated monocytes. *The Journal of experimental medicine* 1988, 167:1428-1441.

169. Constantino AA, Huang Y, Zhang H, Wood C, Zheng JC: HIV-1 clade B and C isolates exhibit differential replication: relevance to macrophage-mediated neurotoxicity. *Neurotoxicity research* 2011, 20:277-288.

170. Frleta D, Ochoa CE, Kramer HB, Khan SA, Stacey AR, Borrow P, Kessler BM, Haynes BF, Bhardwaj N: HIV-1 infection-induced apoptotic microparticles inhibit human DCs via CD44. *The Journal of clinical investigation* 2012, 122:4685-4697.

171. Kosaka N, Iguchi H, Yoshioka Y, Takeshita F, Matsuki Y, Ochiya T: Secretory mechanisms and intercellular transfer of microRNAs in living cells. *The Journal of biological chemistry* 2010, 285:17442-17452.

172. Brenchley JM, Price DA, Schacker TW, Asher TE, Silvestri G, Rao S, Kazzaz Z, Bornstein E, Lambotte O, Altmann D, et al: Microbial translocation is a cause of systemic immune activation in chronic HIV infection. *Nature medicine* 2006, 12:1365-1371.

173. Erickson JW, Cerione RA: Glutaminase: a hot spot for regulation of cancer cell metabolism? *Oncotarget* 2010, 1:734-740.

174. Wang JB, Erickson JW, Fuji R, Ramachandran S, Gao P, Dinavahi R, Wilson KF, Ambrosio AL, Dias SM, Dang CV, Cerione RA: Targeting mitochondrial glutaminase activity inhibits oncogenic transformation. *Cancer cell* 2010, 18:207-219.

175. Baglietto-Vargas D, Lopez-Tellez JF, Moreno-Gonzalez I, Gutierrez A, Aledo JC: Segregation of two glutaminase isoforms in islets of Langerhans. *The Biochemical journal* 2004, 381:483-487.

176. Kanellopoulos GK, Xu XM, Hsu CY, Lu X, Sundt TM, Kouchoukos NT: White matter injury in spinal cord ischemia: protection by AMPA/kainate glutamate receptor antagonism. *Stroke; a journal of cerebral circulation* 2000, 31:1945-1952.

177. Zoia CP, Tagliabue E, Isella V, Begni B, Fumagalli L, Brighina L, Appollonio I, Racchi M, Ferrarese C: Fibroblast glutamate transport in aging and in AD: correlations with disease severity. *Neurobiology of aging* 2005, 26:825-832.

178. Wu B, Huang Y, Braun AL, Tong Z, Zhao R, Li Y, Liu F, Zheng JC: Glutaminase-containing microvesicles from HIV-1-infected

macrophages and immune-activated microglia induce neurotoxicity. *Molecular neurodegeneration* 2015, 10:61.

179. Coleman BM, Hill AF: Extracellular vesicles--Their role in the packaging and spread of misfolded proteins associated with neurodegenerative diseases. *Seminars in cell & developmental biology* 2015, 40:89-96.

180. Asai H, Ikezu S, Tsunoda S, Medalla M, Luebke J, Haydar T, Wolozin B, Butovsky O, Kugler S, Ikezu T: Depletion of microglia and inhibition of exosome synthesis halt tau propagation. *Nature neuroscience* 2015, 18:1584-1593.

181. Arainga M, Su H, Poluektova LY, Gorantla S, Gendelman HE: HIV-1 cellular and tissue replication patterns in infected humanized mice. *Scientific reports* 2016, 6:23513.

182. Jaeger LB, Nath A: Modeling HIV-associated neurocognitive disorders in mice: new approaches in the changing face of HIV neuropathogenesis. *Disease models & mechanisms* 2012, 5:313-322.

183. Dash PK, Gorantla S, Gendelman HE, Knibbe J, Casale GP, Makarov E, Epstein AA, Gelbard HA, Boska MD, Poluektova LY: Loss of neuronal integrity during progressive HIV-1 infection of humanized mice. *The Journal of neuroscience : the official journal of the Society for Neuroscience* 2011, 31:3148-3157.

184. Gorantla S, Gendelman HE, Poluektova LY: Can humanized mice reflect the complex pathobiology of HIV-associated neurocognitive

disorders? ***Journal of neuroimmune pharmacology : the official journal of the Society on NeuroImmune Pharmacology*** **2012, 7:352-362.**

185. Chao CC, Gekker G, Sheng WS, Hu S, Tsang M, Peterson PK: Priming effect of morphine on the production of tumor necrosis factor-alpha by microglia: implications in respiratory burst activity and human immunodeficiency virus-1 expression. ***The Journal of pharmacology and experimental therapeutics*** **1994, 269:198-203.**

186. Perez-Gonzalez R, Gauthier SA, Kumar A, Levy E: The exosome secretory pathway transports amyloid precursor protein carboxyl-terminal fragments from the cell into the brain extracellular space. ***The Journal of biological chemistry*** **2012, 287:43108-43115.**

187. Curthoys NP, Weiss RF: Regulation of renal ammoniagenesis. Subcellular localization of rat kidney glutaminase isoenzymes. ***The Journal of biological chemistry*** **1974, 249:3261-3266.**

188. Erdmann N, Zhao J, Lopez AL, Herek S, Curthoys N, Hexum TD, Tsukamoto T, Ferraris D, Zheng J: Glutamate production by HIV-1 infected human macrophage is blocked by the inhibition of glutaminase. ***Journal of neurochemistry*** **2007, 102:539-549.**

189. Antonyak MA, Li B, Boroughs LK, Johnson JL, Druso JE, Bryant KL, Holowka DA, Cerione RA: Cancer cell-derived microvesicles induce transformation by transferring tissue transglutaminase and

fibronectin to recipient cells. *Proceedings of the National Academy of Sciences of the United States of America* 2011, 108:4852-4857.

190. Giulian D, Vaca K, Noonan CA: Secretion of neurotoxins by mononuclear phagocytes infected with HIV-1. *Science* 1990, 250:1593-1596.

191. Yeckel MF, Berger TW: Spatial distribution of potentiated synapses in hippocampus: dependence on cellular mechanisms and network properties. *The Journal of neuroscience : the official journal of the Society for Neuroscience* 1998, 18:438-450.

192. Naie K, Manahan-Vaughan D: Regulation by metabotropic glutamate receptor 5 of LTP in the dentate gyrus of freely moving rats: relevance for learning and memory formation. *Cereb Cortex* 2004, 14:189-198.

193. Manahan-Vaughan D, Braunewell KH: The metabotropic glutamate receptor, mGluR5, is a key determinant of good and bad spatial learning performance and hippocampal synaptic plasticity. *Cereb Cortex* 2005, 15:1703-1713.

194. Magnusson KR, Scruggs B, Zhao X, Hammersmark R: Age-related declines in a two-day reference memory task are associated with changes in NMDA receptor subunits in mice. *BMC neuroscience* 2007, 8:43.

195. Brim BL, Haskell R, Awedikian R, Ellinwood NM, Jin L, Kumar A, Foster TC, Magnusson KR: Memory in aged mice is rescued by

enhanced expression of the GluN2B subunit of the NMDA receptor. *Behavioural brain research* 2013, 238:211-226.

196. Delint-Ramirez I, Salcedo-Tello P, Bermudez-Rattoni F: Spatial memory formation induces recruitment of NMDA receptor and PSD-95 to synaptic lipid rafts. *Journal of neurochemistry* 2008, 106:1658-1668.

197. De Toro J, Herschlik L, Waldner C, Mongini C: Emerging roles of exosomes in normal and pathological conditions: new insights for diagnosis and therapeutic applications. *Frontiers in immunology* 2015, 6:203.

198. Rajendran L, Annaert W: Membrane trafficking pathways in Alzheimer's disease. *Traffic* 2012, 13:759-770.

199. Candelario KM, Steindler DA: The role of extracellular vesicles in the progression of neurodegenerative disease and cancer. *Trends in molecular medicine* 2014, 20:368-374.

200. Budnik V, Ruiz-Canada C, Wendler F: Extracellular vesicles round off communication in the nervous system. *Nature reviews Neuroscience* 2016, 17:160-172.

201. Rajendran L, Honsho M, Zahn TR, Keller P, Geiger KD, Verkade P, Simons K: Alzheimer's disease beta-amyloid peptides are released in association with exosomes. *Proceedings of the National Academy of Sciences of the United States of America* 2006, 103:11172-11177.

202. Colombo E, Borgiani B, Verderio C, Furlan R: Microvesicles: novel biomarkers for neurological disorders. *Frontiers in physiology* 2012, 3:63.

203. Shanware NP, Bray K, Eng CH, Wang F, Follettie M, Myers J, Fantin VR, Abraham RT: Glutamine deprivation stimulates mTOR-JNK-dependent chemokine secretion. *Nature communications* 2014, 5:4900.

204. DeBerardinis RJ, Cheng T: Q's next: the diverse functions of glutamine in metabolism, cell biology and cancer. *Oncogene* 2010, 29:313-324.

205. Shanware NP, Mullen AR, DeBerardinis RJ, Abraham RT: Glutamine: pleiotropic roles in tumor growth and stress resistance. *J Mol Med (Berl)* 2011, 89:229-236.

206. Kenny J, Bao Y, Hamm B, Taylor L, Toth A, Wagers B, Curthoys NP: Bacterial expression, purification, and characterization of rat kidney-type mitochondrial glutaminase. *Protein expression and purification* 2003, 31:140-148.

207. Klysz D, Tai X, Robert PA, Craveiro M, Cretenet G, Oburoglu L, Mongellaz C, Floess S, Fritz V, Matias MI, et al: Glutamine-dependent alpha-ketoglutarate production regulates the balance between T helper 1 cell and regulatory T cell generation. *Science signaling* 2015, 8:ra97.

208. Wellen KE, Lu C, Mancuso A, Lemons JM, Ryczko M, Dennis JW, Rabinowitz JD, Coller HA, Thompson CB: The hexosamine biosynthetic pathway couples growth factor-induced glutamine uptake to glucose metabolism. *Genes & development* 2010, 24:2784-2799.

209. Cooper AJ, Jeitner TM: Central Role of Glutamate Metabolism in the Maintenance of Nitrogen Homeostasis in Normal and Hyperammonemic Brain. *Biomolecules* 2016, 6.

210. Butterworth RF: Pathophysiology of brain dysfunction in hyperammonemic syndromes: The many faces of glutamine. *Molecular genetics and metabolism* 2014, 113:113-117.

211. Sidoryk-Wegrzynowicz M, Aschner M: Manganese toxicity in the central nervous system: the glutamine/glutamate-gamma-aminobutyric acid cycle. *Journal of internal medicine* 2013, 273:466-477.

212. Clarke CJ, Hannun YA: Neutral sphingomyelinases and nSMase2: bridging the gaps. *Biochimica et biophysica acta* 2006, 1758:1893-1901.

213. van Echten-Deckert G, Walter J: Sphingolipids: critical players in Alzheimer's disease. *Progress in lipid research* 2012, 51:378-393.

214. Guo BB, Bellingham SA, Hill AF: The neutral sphingomyelinase pathway regulates packaging of the prion protein into exosomes. *The Journal of biological chemistry* 2015, 290:3455-3467.

215. Wang Y, Huang Y, Zhao L, Li Y, Zheng J: Glutaminase 1 is essential for the differentiation, proliferation, and survival of human neural progenitor cells. *Stem cells and development* 2014, 23:2782-2790.

216. Dinkins MB, Dasgupta S, Wang G, Zhu G, Bieberich E: Exosome reduction in vivo is associated with lower amyloid plaque load in the 5XFAD mouse model of Alzheimer's disease. *Neurobiology of aging* 2014, 35:1792-1800.

217. Fedele E, Rivera D, Marengo B, Pronzato MA, Ricciarelli R: Amyloid beta: Walking on the dark side of the moon. *Mechanisms of ageing and development* 2015, 152:1-4.

218. Joshi P, Benussi L, Furlan R, Ghidoni R, Verderio C: Extracellular vesicles in Alzheimer's disease: friends or foes? Focus on abeta-vesicle interaction. *International journal of molecular sciences* 2015, 16:4800-4813.

219. Yuyama K, Sun H, Mitsutake S, Igarashi Y: Sphingolipid-modulated exosome secretion promotes clearance of amyloid-beta by microglia. *The Journal of biological chemistry* 2012, 287:10977-10989.

220. Wang G, Dinkins M, He Q, Zhu G, Poirier C, Campbell A, Mayer-Proschel M, Bieberich E: Astrocytes secrete exosomes enriched with proapoptotic ceramide and prostate apoptosis response 4 (PAR-4): potential mechanism of apoptosis induction in Alzheimer disease (AD). *The Journal of biological chemistry* 2012, 287:21384-21395.

221. Antonucci F, Turola E, Riganti L, Caleo M, Gabrielli M, Perrotta C, Novellino L, Clementi E, Giussani P, Viani P, et al: Microvesicles released from microglia stimulate synaptic activity via enhanced sphingolipid metabolism. *The EMBO journal* 2012, 31:1231-1240.

222. Tamboli IY, Barth E, Christian L, Siepmann M, Kumar S, Singh S, Tolksdorf K, Heneka MT, Lutjohann D, Wunderlich P, Walter J: Statins promote the degradation of extracellular amyloid {beta}-peptide by microglia via stimulation of exosome-associated insulin-degrading enzyme (IDE) secretion. *The Journal of biological chemistry* 2010, 285:37405-37414.

223. Parlo RA, Coleman PS: Enhanced rate of citrate export from cholesterol-rich hepatoma mitochondria. The truncated Krebs cycle and other metabolic ramifications of mitochondrial membrane cholesterol. *The Journal of biological chemistry* 1984, 259:9997-10003.

224. Bredesen DE: Neural apoptosis. *Annals of neurology* 1995, 38:839-851.

225. Yuan J, Yankner BA: Apoptosis in the nervous system. *Nature* 2000, 407:802-809.

226. Li W, Huang Y, Reid R, Steiner J, Malpica-Llanos T, Darden TA, Shankar SK, Mahadevan A, Satishchandra P, Nath A: NMDA receptor activation by HIV-Tat protein is clade dependent. *The Journal of*

neuroscience : the official journal of the Society for Neuroscience **2008, 28:12190-12198.**

227. Eggert D, Dash PK, Serradji N, Dong CZ, Clayette P, Heymans F, Dou H, Gorantla S, Gelbard HA, Poluektova L, Gendelman HE: Development of a platelet-activating factor antagonist for HIV-1 associated neurocognitive disorders. *Journal of neuroimmunology* 2009, 213:47-59.

228. Gangalum RK, Bhat AM, Kohan SA, Bhat SP: Inhibition of the Expression of the Small Heat Shock Protein alphaB-crystallin Inhibits Exosome Secretion in Human Retinal Pigment Epithelial Cells in Culture. *The Journal of biological chemistry* 2016.

229. Wise DR, Thompson CB: Glutamine addiction: a new therapeutic target in cancer. *Trends in biochemical sciences* 2010, 35:427-433.

230. Hensley CT, Wasti AT, DeBerardinis RJ: Glutamine and cancer: cell biology, physiology, and clinical opportunities. *The Journal of clinical investigation* 2013, 123:3678-3684.

231. Le A, Lane AN, Hamaker M, Bose S, Gouw A, Barbi J, Tsukamoto T, Rojas CJ, Slusher BS, Zhang H, et al: Glucose-independent glutamine metabolism via TCA cycling for proliferation and survival in B cells. *Cell metabolism* 2012, 15:110-121.

232. Seltzer MJ, Bennett BD, Joshi AD, Gao P, Thomas AG, Ferraris DV, Tsukamoto T, Rojas CJ, Slusher BS, Rabinowitz JD, et al: Inhibition

of glutaminase preferentially slows growth of glioma cells with mutant IDH1. *Cancer research* 2010, 70:8981-8987.

233. Son J, Lyssiotis CA, Ying H, Wang X, Hua S, Ligorio M, Perera RM, Ferrone CR, Mullarky E, Shyh-Chang N, et al: Glutamine supports pancreatic cancer growth through a KRAS-regulated metabolic pathway. *Nature* 2013, 496:101-105.

234. van den Heuvel AP, Jing J, Wooster RF, Bachman KE: Analysis of glutamine dependency in non-small cell lung cancer: GLS1 splice variant GAC is essential for cancer cell growth. *Cancer biology & therapy* 2012, 13:1185-1194.

235. Tickner JA, Urquhart AJ, Stephenson SA, Richard DJ, O'Byrne KJ: Functions and therapeutic roles of exosomes in cancer. *Frontiers in oncology* 2014, 4:127.

236. Kuhlmann JD, Hein L, Kurth I, Wimberger P, Dubrovska A: Targeting Cancer Stem Cells: Promises and Challenges. *Anti-cancer agents in medicinal chemistry* 2015, 16:38-58.

237. Plaks V, Kong N, Werb Z: The cancer stem cell niche: how essential is the niche in regulating stemness of tumor cells? *Cell stem cell* 2015, 16:225-238.

238. Chen G, Huang JB, Mi J, He YF, Wu XH, Luo CL, Liang SM, Li JB, Tang YX, Li J: Characterization of acute renal allograft rejection by proteomic analysis of renal tissue in rat. *Molecular biology reports* 2012, 39:1315-1322.

239. Santana SM, Antonyak MA, Cerione RA, Kirby BJ: Microfluidic isolation of cancer-cell-derived microvesicles from hetergeneous extracellular shed vesicle populations. *Biomedical microdevices* 2014, 16:869-877.